

The Synthesis and Coordination Chemistry of Amino-
substituted Bisphosphines

by

Andrew John Phillips
BSc., University of East Anglia, 1986.

A THESIS SUBMITTED IN PARTIAL FULFILLMENT

OF THE REQUIREMENTS FOR THE DEGREE OF

MASTER OF SCIENCE

in the Department

of

Chemistry

ACCEPTED
FACULTY OF GRADUATE STUDIES

[Redacted]

DATE Sept 13, 1988 DEAN

We accept this thesis as conforming
to the required standard

[Redacted]

Dr. K. R. Dixon

[Redacted]

Dr. R. H. Mitchell

[Redacted]

Dr. D. A. Vandenberg

[Redacted]

Dr. A. Watton

© Andrew John Phillips, 1988

University of Victoria

All rights reserved. This thesis may not be reproduced
in whole or in part, by mimeograph or other means,
without the permission of the author

Permission has been granted to the National Library of Canada to microfilm this thesis and to lend or sell copies of the film.

The author (copyright owner) has reserved other publication rights, and neither the thesis nor extensive extracts from it may be printed or otherwise reproduced without his/her written permission.

L'autorisation a été accordée à la Bibliothèque nationale du Canada de microfilmer cette thèse et de prêter ou de vendre des exemplaires du film.

L'auteur (titulaire du droit d'auteur) se réserve les autres droits de publication; ni la thèse ni de longs extraits de celle-ci ne doivent être imprimés ou autrement reproduits sans son autorisation écrite.

ISBN 0-315-46540-9

Supervisor: Professor Keith R. Dixon

ABSTRACT

The ligands $[\text{Ph}_2\text{PCH}_2\text{P}(\text{NR}_2)_2]$, $[\text{Ph}_2\text{P}(\text{S})\text{CH}_2\text{P}(\text{NET}_2)_2]$, $[\text{Ph}_2\text{P}(\text{S})\text{CH}_2\text{P}(\text{S})(\text{NET}_2)_2]$ and $[\text{Ph}_2\text{P}(\text{S})\text{CHP}(\text{S})(\text{NET}_2)_2]\text{Li}$ were synthesized and their coordination chemistry with the metals Rh, Ir, Pd and Pt investigated. Coordination reactions generally involved the cleavage of one equivalent of neutral chloro-bridged metal dimer ($[\text{M}_2\text{Cl}_2(\mu\text{-Cl})_2(\text{PET}_3)_2]$ M = Pt or Pd and $[\text{M}_2(\mu\text{-Cl})_2(\text{cod})_2]$ M = Ir or Rh) with two equivalents of ligand and two equivalents of NaBF_4 .

Reaction of the palladium and platinum neutral dimers with $[\text{Ph}_2\text{PCH}_2\text{P}(\text{NET}_2)_2]$ generated both *cis* and *trans* four-membered ring P,P' bonded complexes. The crystal structure of *cis*- $[\text{PtCl}(\text{PET}_3)\{\text{Ph}_2\text{PCH}_2\text{P}(\text{NET}_2)_2\text{-P,P'}\}]\text{BF}_4$ was solved. Extensive $p_\pi\text{-}d_\pi$ interaction between nitrogen lone pair of electrons and low lying $3d_{x^2-y^2}$ and $3d_{z^2}$ orbitals on the phosphorus caused shorter than calculated P-N bonding distances (found 1.58 Å, calculated 1.80 Å) and rationalized the apparent inability of the nitrogen atoms to coordinate.

The reaction of $[\text{Ph}_2\text{P}(\text{S})\text{CH}_2\text{P}(\text{NET}_2)_2]$ with rhodium, platinum and palladium dimers formed monomeric five-membered ring S,P coordinated complexes.

The reaction of $[\text{Ph}_2\text{P}(\text{S})\text{CH}_2\text{P}(\text{S})(\text{NEt}_2)_2]$ and $[\text{Ph}_2\text{P}(\text{S})\text{CH}-\text{P}(\text{S})(\text{NEt}_2)_2]\text{Li}$ with metal dimers formed six-membered S,S' bonded chelate complexes. The crystal structure of *cis*- $[\text{PdCl}(\text{PEt}_3)(\text{Ph}_2\text{P}(\text{S})\text{CH}_2\text{P}(\text{S})(\text{NEt}_2)_2-S,S')]\text{BF}_4$ again showed extensive $p_\pi-d_\pi$ bonding between the amine nitrogen atoms and the phosphorus atom.

The $^{31}\text{P}\{^1\text{H}\}$ NMR of the reaction between $[\text{Ph}_2\text{P}(\text{S})\text{CH}-\text{P}(\text{S})(\text{NEt}_2)_2]\text{Li}$ and $[\text{Pd}_2\text{Cl}_2(\mu-\text{Cl})_2(\text{PEt}_3)_2]$ also showed the collapse of the S,S' bonded chelate complex to a C,S bonded chelate complex with the $(\text{NEt}_2)_2\text{P}(\text{S})-$ group *trans* to the chloride ligand. This complex then isomerized to complexes with the phosphinesulphides *trans* to the triethylphosphine such that the *trans*-labilizing effect of the triethylphosphine caused the dynamic, intramolecular interchange of the coordinated and non-coordinated phosphinesulphides. Variable-temperature $^{31}\text{P}\{^1\text{H}\}$ NMR confirmed the process and band shape analysis of the results provided thermodynamic parameters for the process.

Nitrogen-metal coordination was forced by first chelating the bisphosphine to a metal $[\text{PtCl}_2\{\text{Ph}_2\text{PCH}_2\text{P}(\text{NEt}_2)_2-P,P'\}]$ then reacting the complex with $[\text{Rh}(\text{cod})(\text{CH}_3\text{CN})_2]\text{BF}_4$ to form $[\text{PtCl}_2\{\text{Ph}_2\text{PCH}_2\text{P}(\text{NEt}_2)_2-P,P'\}\{N,N-\text{Rh}(\text{cod})\}]\text{BF}_4$. The product was interesting in that quarternized phosphorus-bound nitrogen atoms are rare.

$^{31}\text{P}\{^1\text{H}\}$ NMR was used extensively for structural assignments. Natural abundance nitrogen-15 NMR was recorded for $[\text{Ph}_2\text{PCH}_2\text{P}(\text{NEt}_2)_2]$ although it was found impossible to record that of the complexes due to solubility problems.

Examiners:


Dr. K. R. Dixon


Dr. R. H. Mitchell


Dr. D. A. Vandenberg


Dr. A. Watton

TABLE OF CONTENTS

	PAGE
Title Page	i
Abstract	ii
Table of Contents	v
List of Tables	viii
List of Figures	xi
Abbreviations	xiv
Acknowledgments	xv
Chapter 1: Introduction	1
Chapter 2: Syntheses of Amino-Substituted Bisphosphine Ligands	17
2.1. Introduction	18
2.1.1. Possible Coordination Modes	18
2.1.2. Reactivity of the Phosphorus- Nitrogen Bond	20
2.2. Ligand Syntheses	22
2.2.1. Syntheses of $[\text{Ph}_2\text{PCH}_2\text{PRR}']$ Ligands	23
2.2.2. Synthesis of $[\text{Ph}_2\text{P}(\text{S})\text{CH}_2\text{P}(\text{NEt}_2)_2]$ and $[\text{Ph}_2\text{PCH}_2\text{P}(\text{O})(\text{NEt}_2)_2]$	24
2.2.3. Synthesis of $[\text{Ph}_2\text{P}(\text{S})\text{CH}_2\text{P}(\text{S})(\text{NEt}_2)_2]$ and $[\text{Ph}_2\text{P}(\text{S})\text{CHP}(\text{S})(\text{NEt}_2)_2]\text{Li}$	26
2.3. Discussion of NMR Parameters	27
Chapter 3: Coordination Chemistry and Reactivity of the Ligands $[\text{Ph}_2\text{PCH}_2\text{P}(\text{NEt}_2)_2]$ and $[\text{Ph}_2\text{PCH}_2\text{P}(\text{NEt}_2)\text{Ph}]$	38
3.1. Introduction	39

3.2.1. Reaction of $[\text{Pt}_2(\mu\text{-Cl})_2\text{Cl}_2(\text{PEt}_3)_2]$ With $[\text{Ph}_2\text{PCH}_2\text{P}(\text{NEt}_2)_2]$	40
3.2.2 Discussion on the Platinum-195 NMR of $[\text{PtCl}(\text{PEt}_3)\{\text{Ph}_2\text{PCH}_2\text{P}(\text{NEt}_2)_2\text{-P,P'}\}]\text{BF}_4$	49
3.3. Reaction of $[\text{Ph}_2\text{PCH}_2\text{P}(\text{NEt}_2)_2]$ and $[\text{Ph}_2\text{PCH}_2\text{P}(\text{N}(\text{CH}_2\text{CH}_2)_2\text{CH})_2]$ with $[\text{Pd}_2(\mu\text{-Cl})_2\text{Cl}_2(\text{PEt}_3)_2]$	53
3.4. Rhodium-Bisphosphine Complexes of $[\text{Ph}_2\text{PCH}_2\text{P}(\text{NEt}_2)_2]$	54
3.5. Discussion on the Crystal Structure of <i>cis</i> - $[\text{PtCl}(\text{PEt}_3)\{\text{Ph}_2\text{PCH}_2\text{P}(\text{NEt}_2)_2\text{-P,P'}\}]\text{BF}_4$	56
3.6. Phosphorus-Nitrogen Bond Cleavage of Coordinated $[\text{Ph}_2\text{PCH}_2\text{P}(\text{NEt}_2)_2]$ and $[\text{Ph}_2\text{PCH}_2\text{P}(\text{NEt}_2)\text{Ph}]$	62
3.6.1. Reaction of $[\text{PtCl}_2(\text{Ph}_2\text{PCH}_2\text{P}(\text{NEt}_2)_2\text{-P,P'})]$ with Hydrogen Chloride	62
3.6.2. Reaction of $[\text{PtCl}_2(\text{Ph}_2\text{PCH}_2\text{P}(\text{NEt}_2)\text{Ph-P,P'})]$ with Hydrogen Chloride	64
3.7. Attempts at Promoting Nitrogen Coordination on the Complex $[\text{PtCl}_2(\text{Ph}_2\text{PCH}_2\text{P}(\text{NEt}_2)_2\text{-P,P'})]$	69
Chapter 4: Coordination Chemistry of $[\text{Ph}_2\text{P}(\text{S})\text{CH}_2\text{P}(\text{NEt}_2)_2]$, $[\text{Ph}_2\text{P}(\text{S})\text{CH}_2\text{P}(\text{S})(\text{NEt}_2)_2]$ and $[\text{Ph}_2\text{P}(\text{S})\text{CHP}(\text{S})(\text{NEt}_2)_2]\text{Li}$ with some of the Platinum Group Metals	91
4.1. The Coordination Chemistry of	

[Ph ₂ P(S)CH ₂ P(NEt ₂) ₂] with Platinum, Palladium and Rhodium.	92
4.2.1. The Coordination Chemistry of [Ph ₂ P(S)CH ₂ P(S)(NEt ₂) ₂] with Palladium, Platinum, Rhodium and Iridium.	99
4.2.2. Discussion on the X-ray Crystal Structure of <i>cis</i> -[PdCl(PEt ₃)(Ph ₂ P(S)CH ₂ - P(S)(NEt ₂) ₂ - <i>S,S'</i>)]BF ₄	105
4.3. The Coordination Chemistry of [Ph ₂ P(S)CHP(S)(NEt ₂) ₂]Li with Palladium, Platinum and Rhodium	109
4.3.1. The Coordination Chemistry of [Ph ₂ P(S)CHP(S)(NEt ₂) ₂]Li with Rhodium	112
4.3.2 The Coordination Chemistry of [Ph ₂ P(S)CHP(S)(NEt ₂) ₂]Li with Palladium	118
4.3.3. The Coordination Chemistry of [Ph ₂ P(S)CHP(S)(NEt ₂) ₂]Li with Platinum	130
Chapter 5: Experimental Section	150
References	174

List of Tables

Table	PAGE
2.1. $^{31}\text{P}\{^1\text{H}\}$ NMR data for phosphine compounds used in chemical shift assignments of the ligands $[\text{Ph}_2\text{P}(\text{X})\text{CH}(\text{Q})\text{P}(\text{Y})\text{RR}']$.	35
2.2. $^{31}\text{P}\{^1\text{H}\}$ NMR data for $[\text{Ph}_2\text{P}(\text{X})\text{CH}(\text{Q})\text{P}(\text{Y})\text{RR}']$ ligands.	36
2.3. $^{13}\text{C}\{^1\text{H}\}$ NMR data for $[\text{Ph}_2\text{PCH}(\text{Q})\text{P}(\text{Y})\text{RR}']$ ligands.	37
3.1. $^{31}\text{P}\{^1\text{H}\}$ NMR data for cationic complexes of the bisphosphine $[\text{Ph}_2\text{PCH}_2\text{P}(\text{NR}_2)_2]$.	77
3.2. $^{31}\text{P}\{^1\text{H}\}$ NMR data for neutral complexes of the bisphosphine $[\text{Ph}_2\text{PCH}_2\text{PRR}']$ and the HCl reaction products.	78
3.3. Platinum-195 NMR data for $[\text{Ph}_2\text{PCH}_2\text{P}(\text{NEt}_2)_2]$, $[\text{Ph}_2\text{PCH}_2\text{P}(\text{NEt}_2)\text{Ph}]$ and $[\text{Ph}_2\text{P}(\text{S})\text{CH}_2\text{P}(\text{S})(\text{NEt}_2)_2]$.	79
3.4. Some platinum-phosphorus single-bond coupling constants for $[\text{P}(\text{NR}_2)_3]$ and $[\text{P}(\text{Cl})(\text{NR}_2)_2]$ phosphines.	80
3.5. $^{13}\text{C}\{^1\text{H}\}$ NMR data for complexes containing $[\text{Ph}_2\text{PCH}_2\text{P}(\text{NEt}_2)_2]$ and $[\text{Ph}_2\text{PCH}_2\text{P}(\text{NEt}_2)\text{Ph}]$.	81
3.6. ^1H NMR data for complexes containing $[\text{Ph}_2\text{PCH}_2\text{P}(\text{NEt}_2)_2]$ and $[\text{Ph}_2\text{PCH}_2\text{P}(\text{NEt}_2)\text{Ph}]$.	82
3.7. Crystallographic parameters for <i>cis</i> - $[\text{PtCl}(\text{PEt}_3)\{\text{Ph}_2\text{PCH}_2\text{P}(\text{NEt}_2)_2\text{-P,P}'\}]\text{BF}_4$.	83
3.8. Fractional atomic coordinates and temperature parameters for	

- [PtCl(PET₃)(Ph₂P-CH₂P(NEt₂)₂-P,P')]BF₄. 84
- 3.9. Anisotropic temperature parameters (Å²) for
[PtCl(PET₃)(Ph₂PCH₂P(NEt₂)₂-P,P')]BF₄. 86
- 3.10. Interatomic distances (Å) for
[PtCl(PET₃)(Ph₂PCH₂P(NEt₂)₂-P,P')]BF₄. 88
- 3.11. Bond angles (°) for
[PtCl(PET₃)(Ph₂PCH₂P(NEt₂)₂-P,P')]BF₄. 89
- 3.12. Selected intermolecular distances (Å) for
[PtCl(PET₃)(Ph₂PCH₂P(NEt₂)₂-P,P')]BF₄. 90
- 4.1. ³¹P{¹H} NMR data for complexes containing
the ligand [Ph₂P(S)CH₂P(NEt₂)₂]. 134
- 4.2. ³¹P{¹H} NMR data for the cationic complexes
of the disulphide ligand;
[LL'M(Ph₂P(S)CH₂P(S)R₂-S,S')]anion. 135
- 4.3. ¹³C{¹H} NMR data for the cationic complexes
of the disulphide ligand;
[LL'M(Ph₂P(S)CH₂P(S)R₂-S,S')]BF₄. 136
- 4.4. ¹H NMR data for the cationic complexes
of the disulphide ligand;
[LL'M(Ph₂P(S)CHP(S)R₂-S,S')]BF₄. 137
- 4.5. ³¹P{¹H} NMR data for
[MCl(PET₃)(Ph₂P(S)CHP(S)(NEt₂)₂-C,S)]. 138
- 4.6. ³¹P{¹H} NMR data for
[MLL'(Ph₂P(S)CHP(S)R₂-S,S')]. 139
- 4.7. Rate data for the dynamic sulphur exchange in
trans-[PdCl(PET₃)(Ph₂P(S)CHP(S)(NEt₂)₂-C,S)]
derived from the parameters used in the band

- shape analysis simulation of the variable
temperature $^{31}\text{P}\{^1\text{H}\}$ NMR. 140
- 4.8. Rate plot and thermodynamic parameters for
sulphur interchange in *trans*-
[PdCl(PEt₃){Ph₂P(S)CHP(S)(NEt₂)₂-C,S}]. 141
- 4.9. Crystallographic parameters for
[PdCl(PEt₃){Ph₂P(S)CH₂P(S)(NEt₂)₂-S,S'}]BF₄. 142
- 4.10. Interatomic distances (Å) for
[PdCl(PEt₃){Ph₂P(S)CH₂P(S)(NEt₂)₂-S,S'}]BF₄. 143
- 4.11. Bond angles (°) for
[PdCl(PEt₃){Ph₂P(S)CH₂P(S)(NEt₂)₂-S,S'}]BF₄. 144
- 4.12. Fractional atomic coordinates and temperature
parameters for
[PdCl(PEt₃){Ph₂P(S)CH₂P(S)(NEt₂)₂-S,S'}]BF₄. 145
- 4.13. Anisotropic temperature parameters (Å²) for
[PdCl(PEt₃){Ph₂P(S)CH₂P(S)(NEt₂)₂-S,S'}]BF₄. 147
- 4.14. Selected intermolecular distances (Å) for
[PdCl(PEt₃){Ph₂P(S)CH₂P(S)(NEt₂)₂-S,S'}]BF₄. 149

List of Figures

Figure	Page
1.1. Diagram showing the π back donation of electron density from metal M to the phosphorus atom P.	12
1.2. Diagram showing the orbitals used in a square-planar complex with respect to the <i>trans</i> -influence.	14
2.1. Possible Coordination modes of $[\text{Ph}_2\text{PCH}_2\text{P}(\text{NR}_2)_2]$ with transition-metals.	19
3.1. $^{31}\text{P}\{^1\text{H}\}$ NMR of <i>trans</i> - $[\text{PtCl}(\text{PET}_3)(\text{Ph}_2\text{PCH}_2\text{-P}(\text{NEt}_2)_2\text{-P,P'})]\text{BF}_4$; a) actual, b) simulated	43
3.2. $^{31}\text{P}\{^1\text{H}\}$ NMR of <i>cis</i> - $[\text{PtCl}(\text{PET}_3)(\text{Ph}_2\text{PCH}_2\text{-P}(\text{NEt}_2)_2\text{-P,P'})]\text{BF}_4$; a) actual, b) simulated.	44
3.3. A series of simulated spectra showing the gradual transformation of an ABX spin-system to a deceptively simple A_2X spin-system by increasing the ratio of $J/\Delta\delta$. a) $J/\Delta\delta = 0.6$; b) $J/\Delta\delta = 5.0$; $J/\Delta\delta = 60.0$.	48
3.4. $^{195}\text{Pt}\{^1\text{H}\}$ NMR of a mixture of <i>cis</i> and <i>trans</i> $[\text{PtCl}(\text{PET}_3)(\text{Ph}_2\text{PCH}_2\text{P}(\text{NEt}_2)_2\text{-P,P'})]\text{BF}_4$.	50
3.5. A diagrammatical representation of a $d_\pi\text{-p}_\pi$ bonding interaction between phosphorus and nitrogen atoms.	56
3.6. ORTEP diagram of <i>cis</i> - $[\text{PtCl}(\text{PET}_3)(\text{Ph}_2\text{PCH}_2\text{-P}(\text{NEt}_2)_2\text{-P,P'})]\text{BF}_4$.	58
3.7. A selected ORTEP view of the bis(diethylamino)-phosphino group in <i>cis</i> - $[\text{PtCl}(\text{PET}_3)(\text{Ph}_2\text{PCH}_2\text{-$	

- $P(\text{NEt}_2)_2\text{-P,P'}$] BF_4 showing the planar arrangement of substituents around the nitrogen atoms. 60
- 3.8. A diagram showing the orbitals used in the $d_\pi\text{-p}_\pi$ interaction present in the $P(\text{NEt}_2)_2$ group. 61
- 3.9. ^1H NMR of $[\text{PtCl}_2\{\text{Ph}_2\text{PCH}_2\text{P}(\text{NEt}_2)\text{Ph-P,P'}\}]$. 68
- 3.10. $[\text{PtCl}_2\{\text{Ph}_2\text{PCH}_2\text{P}(\text{NEt}_2)\text{Ph-P,P'}\}]$ showing the two chemically different environments that the $\text{P-CH}_2\text{-P}$ hydrogens reside. 69
- 3.11. $[\text{PtCl}_2\{\text{Ph}_2\text{PCH}_2\text{P}(\text{NEt}_2)_2\text{-P,P'}\}\{\text{N,N-Rh}(\text{cod})\}]\text{BF}_4$. 69
- 3.12. ^1H NMR of the reaction mixture $[\text{PtCl}_2\{\text{Ph}_2\text{PCH}_2\text{P}(\text{NEt}_2)_2\text{-P,P'}\}] + [\text{Rh}(\text{cod})(\text{NCCH}_3)_2]\text{BF}_4$. 70
- 3.13. Natural abundance $^{15}\text{N}\{^1\text{H}\}$ NMR of $[\text{Ph}_2\text{PCH}_2\text{P}(\text{NEt}_2)_2]$. 74
- 4.1. $^{31}\text{P}\{^1\text{H}\}$ NMR of $[\text{Rh}(\text{cod})\{\text{Ph}_2\text{P}(\text{S})\text{CH}_2\text{-P}(\text{NEt}_2)_2\text{-S,P}\}]\text{BF}_4$. 94
- 4.2. $^{31}\text{P}\{^1\text{H}\}$ NMR of $[\text{PtCl}(\text{PEt}_3)\{\text{Ph}_2\text{P}(\text{S})\text{CH}_2\text{-P}(\text{S})(\text{NEt}_2)_2\text{-S,S'}\}]\text{BF}_4$. 102
- 4.3. ^1H NMR of $[\text{PtCl}(\text{PEt}_3)\{\text{Ph}_2\text{P}(\text{S})\text{CH}_2\text{-P}(\text{S})(\text{NEt}_2)_2\text{-S,S'}\}]\text{BF}_4$. 104
- 4.4. ORTEP diagram of *cis*- $[\text{PdCl}(\text{PEt}_3)\{\text{Ph}_2\text{P}(\text{S})\text{CH}_2\text{-P}(\text{S})(\text{NEt}_2)_2\text{-S,S'}\}]\text{BF}_4$. 106
- 4.5. $^{31}\text{P}\{^1\text{H}\}$ NMR of $[\text{Rh}(\text{cod})\{\text{Ph}_2\text{P}(\text{S})\text{CH-P}(\text{S})(\text{NEt}_2)_2\text{-S,S'}\}]$. 114
- 4.6. $^{13}\text{C}\{^1\text{H}\}$ NMR of $[\text{Rh}(\text{cod})\{\text{Ph}_2\text{P}(\text{S})\text{CH-}$

- $P(S)(NEt_2)_2-S,S'$]. 116
- 4.7. $^{31}P\{^1H\}$ NMR ($-80^\circ C$) of an isomeric mixture of S,S' bonded (-) and C,S bonded $[PdCl(PET_3)-\{Ph_2P(S)CHP(S)(NEt_2)_2\}]$ with the carbon *trans* to the chloride and $P(S)(NEt_2)_2$ coordinated (+) and $Ph_2P(S)$ coordinated (#). 120
- 4.8. Variable-temperature $^{31}P\{^1H\}$ NMR of *trans*- $[PdCl(PET_3)\{Ph_2P(S)CHP(S)(NEt_2)_2-C,S\}]$. Both actual and simulated shown. 126
- 4.9. Plot of $\ln(k/T)$ vs. $1/T$ with the line of best fit for the dynamic phosphorus interchange in *trans*- $[PdCl(PET_3)\{Ph_2P(S)CHP(S)(NEt_2)_2\}]$. 128

List of Abbreviations

bipy	bipyridyl
cod	1,5-cyclooctadiene
Bu ^t	tertiary butyl
d	doublet
δ	chemical shift
Et	ethyl
h	hour(s)
J	coupling constant
IR	infrared
LP	lone pair
M	metal
m	multiplet
Me	methyl
min	minute(s)
Ph	phenyl
ppm	parts per million
q	quartet
R	alkyl, aryl
s	singlet
THF	tetrahydrofuran
TMP	trimethylphosphite
TMS	tetramethylsilane
t	triplet

Acknowledgements

I would like to thank my supervisor Prof. K. R. Dixon for his encouragement and guidance throughout the work for this thesis. I would also like to express my gratitude to Dr. J. Browning for the crystallographic work, Mrs. C. Greenwood for help with the recording of NMR spectra and Dr. D. E. Berry for his time and consideration both in and out of the laboratory. Thanks also to all those who made my stay in Victoria an enjoyable one.

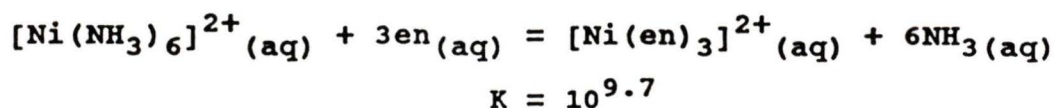
CHAPTER 1: Introduction

The use of ligands is essential to the control and enhancement of transition-metal chemistry. An understanding of the properties a ligand can impart to a metal once a metal-ligand complex has been formed is important if the design of ligands for specific goals is to be possible.

Countless varieties of ligands are known. Many ligands, including those to be discussed in this thesis, are Lewis-base donor types. That is, the coordinating atoms (N, O, S, P etc.) possess lone-pairs of electrons that can bind to transition-metals to form dative-covalent bonds. These Lewis-base ligands are divided into classes depending on how many atoms in that ligand are coordinated to the metal (unidentate, bidentate, multidentate). Multidentate ligands usually form chelate rings, with five-membered rings being the most stable.¹ Multidentate complexes that may form 5- or 6-membered chelate rings are generally more stable (i.e. higher formation constants) than analogous unidentate complexes. For example, $[\text{Ni}(\text{NH}_3)_6]^{+2}$ and $[\text{Ni}(\text{en})_3]^{+2}$ (en = ethylenediamine) have formation constants of $10^{8.6}$ and $10^{18.3}$ respectively. The enthalpic contribution to the formation of chelates may or may not be favorable and is always small, whereas the entropic contribution is always favorable and large. Thus the chelate effect is mainly an entropic effect. That is, the important process at work is the liberation of molecules upon forming chelate complexes. For example, the reaction shown in Scheme 1.1 has more mol-

ecules on the right-hand side of the equation than on the left (higher disorder).²

Scheme 1.1



The chelate effect is particularly important in inorganic chemistry and will be used throughout this thesis to explain the results obtained.

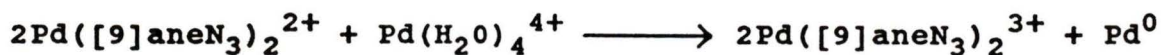
The binding ability of a coordinating atom follows the Hard-Soft-Acid-Base theory (HSAB). Hard Lewis-bases (weakly polarizable) such as oxygen do not bind efficiently with soft-metals (i.e. platinum group metals such as rhodium and platinum) compared to the relatively soft (polarizable) atoms like phosphorus.

The number and type of donor atoms in a ligand, and the substituents around the donor atoms, will impart different properties to the metal-complexes formed. A list of some of the desired properties often looked for in transition-metal-ligands is given below.

1) **Stabilization of Unusual Oxidation States.** Macrocyclic ligands (cyclic compounds with nine or more members and at

least three ligating atoms)³ enable some transition-metals to exist in oxidation states normally considered unstable. The macrocycle is thought to work by imparting both thermodynamic stability via entropic considerations (much like the chelate effect) and kinetic stability by the immobilization of the macrocycle. As an example, palladium(III) is considered an unstable oxidation state (stable states are normally 0, II and sometimes IV). It can, however, be stabilized by the macrocyclic ligand nonane ([9]aneN₃); a cyclic nine-membered organic ligand containing three nitrogen atoms; Scheme 1.2.

Scheme 1.2⁴



2) Enhancement of Metal Reactivity Through Strained Geometries. Some ligands can enhance metal reactivity by forcing the metal into a geometry not typical for its oxidation state. Such ligands are usually found in biological systems (proteins) because of the complexity and mass necessary to absorb the strain. The stereochemical requirements of the protein molecule result in abnormal site symmetry for the metal. For redox metalloenzymes this is often associated with unusual redox potentials and difficulties in defining metal oxidation states. It has been suggested that the

active site of the enzyme is in a geometry approaching that of the transition-state of the reaction and as such is uniquely fitted for catalytic action. The energy difference between the ground-state and the excited-state is reduced by raising the energy of the ground-state complex. The energetic ground-state has been termed an entatic-state.⁵

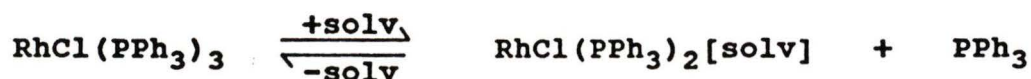
An example is found with carbonic anhydrase. The molecular weight of the protein-ligand is about 30,000 with zinc at its reactive centre. Carbonic anhydrase is able to catalyze the dehydration of the bicarbonate anion and the hydration of carbon dioxide in red blood cells, where the uncatalyzed reaction would be too slow for physiological processes. The turnover rate of CO₂ hydration at 10⁶ moles per second (per 1 mole of carbonic anhydrase at 37°C) is about 10⁹ times faster than the uncatalyzed rate at 7x10⁻⁴ s⁻¹.

3) Increasing Metal Reactivity by Production of Coordination Unsaturation. This method of metal reactivity enhancement can be considered as the synthetic approach to obtaining the conditions mentioned in point two above. The ligands around the metal are chosen and arranged such that at least one of them is labile. Under suitable conditions the labile ligand detaches itself from the metal centre generating a site of coordination unsaturation (i.e. an unusual coordination number for the metal's oxidation state is attained). Incoming ligands may then attack the complex

at the vacant coordination site. Examples of such complexes typically contain at least one relatively strong *trans*-influencing ligand.

Homogeneous catalytic systems employing metal complexes always have as part of their reaction sequence the generation of a reactive site of the type discussed above. For example, a key step in hydrogenation reactions catalyzed by rhodium-phosphine complexes is dissociation of a phosphine ligand to generate a coordinatively unsaturated (or solvent-associated) species, as has been shown by the extensively studied Wilkinson's catalyst, $[\text{RhCl}(\text{PPh}_3)_3]$; Scheme 1.3.

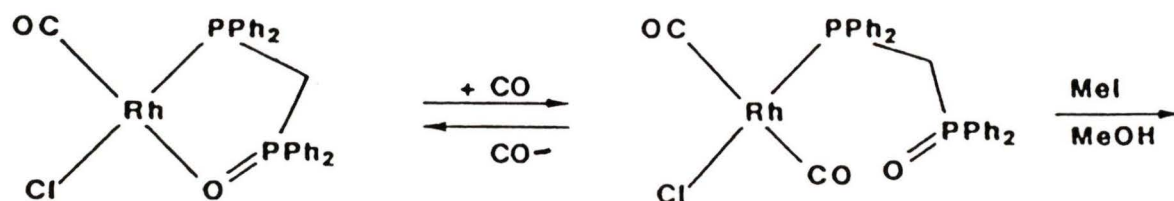
Scheme 1.3



The instability of these solvent-associated complexes has led many researchers to synthesize more stable analogues which may be formed using unsymmetrical, bidentate ligands.⁶ In an attempt to mimic the solvent-associated complex one end of the ligand is designed to be weakly coordinating (i.e. for a platinum group metal such as rhodium a hard Lewis-base is employed). The other end is strongly coordinating in order to "anchor" the ligand to the complex and confer additional stability to the complex through the chelate effect. For example, the complex *cis*- $[\text{RhCl}(\text{CO})(\text{Ph}_2\text{P}$ -

$(\text{CH}_2)_2\text{P}(\text{O})\text{Ph}_2\text{-P, O}]$ is an extremely active methanol carbonylation catalyst under very mild reaction conditions (80°C , 50 psig CO at a turn over rate of 400 h^{-1}). The reaction is believed to go via displacement of the phosphine oxide with CO as shown in Scheme 1.4. Here the labile ligand is the P=O group.⁶

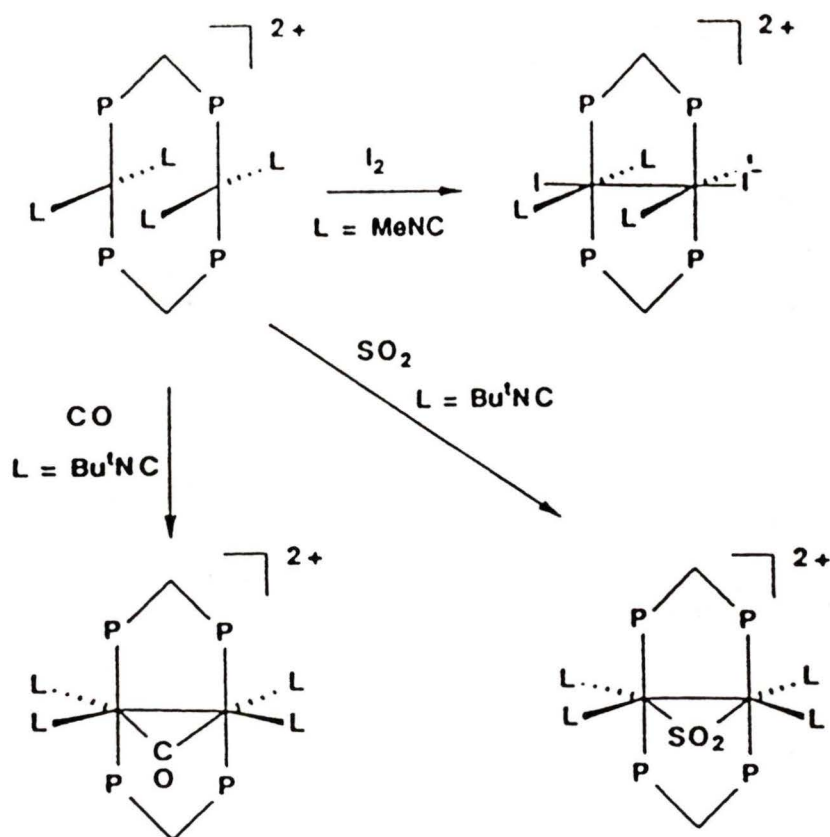
Scheme 1.4



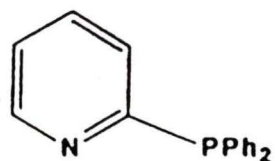
4) Maintaining the Integrity of Multimetal Complexes.

Ligands may be used to maintain the integrity of multimetal complexes such as dimers and trimers by forming strong bonds to two or more of the metals present. For example, dppm (bis(diphenylphosphino)methane) has the ability to form bridged dinuclear complexes. Because metal-phosphorus bonds are often very strong, the bridging bisphosphine ligand can lock together two metal centres in close proximity and promote organometallic reactions without fragmentation; Scheme 1.5.⁷ The strength and flexibility of the bridging bisphosphine-ligand can allow for both metal-metal interaction and non-interaction distances.

Scheme 1.5

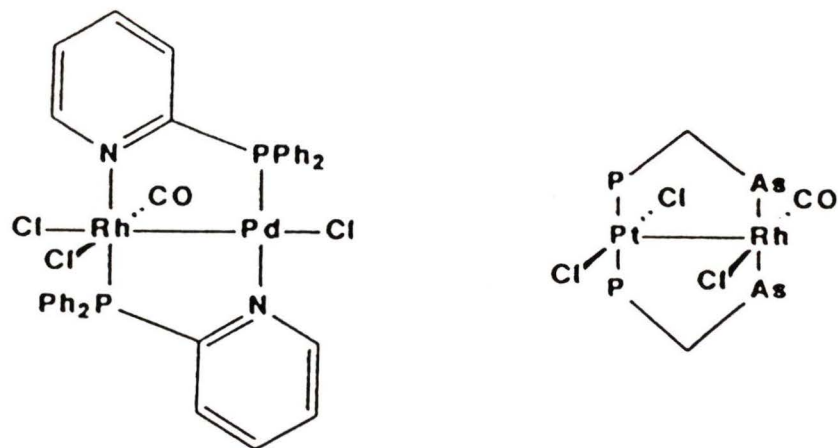


Unsymmetrical bidentate ligands such as 2-(diphenylphosphino)pyridine,

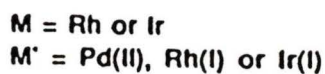
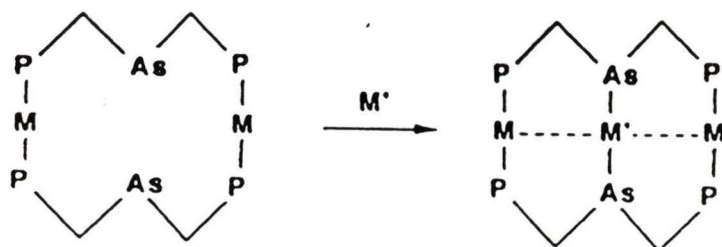


and (diphenylarsino)(diphenylphosphino)methane, $[Ph_2PCH_2-AsPh_2]$, also form binuclear complexes. They are

particularly useful for bridging between unlike metal atoms.^{8,9}



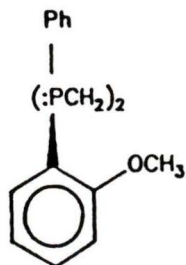
Unsymmetrical multidentate ligands have also been used to build up multi-metallic clusters where the selective binding of one donor atom over another towards a particular metal is employed.^{10,11}



5) Controlling the approach of Substrates about to React at the Metal Centre and/or Rearrangement of those Substrates.

The approach and subsequent rearrangement of substrates about a metal centre may be controlled by the careful design of the surrounding ligands. For example, the catalytic asymmetric addition of hydrogen to unsaturated prochiral

substrates has become increasingly important over past years. These asymmetric syntheses are achieved by homogeneous catalysts bearing chiral ligands. The ligands have typically been phosphines such as chiral monophosphines, although the more rigid chelating ligands have appeared to be superior. For example, (-)DIPAMP.



The rhodium complex of (-)DIPAMP, $[\text{Rh}((-)\text{DIPAMP})\text{S}_2]^+$, asymmetrically hydrogenates α -acetylaminocinnamic acid to the S configuration in 96% enantiomeric excess.¹²

The above list of some of the desired properties of complex ligands included, whenever appropriate, examples employing bisphosphine ligands. Thus bisphosphine compounds and related compounds, such as the oxidized forms as seen with *cis*- $[\text{RhCl}(\text{CO})(\text{Ph}_2\text{P}(\text{CH}_2)_2\text{P}(\text{O})\text{Ph}_2\text{-P,O})]$, are found to be an extremely important class of compounds. Indeed, many other bidentate ligands could show similar and sometimes better properties than the bisphosphines, but they rarely show the same versatility as a class of ligands.

Phosphines are also extremely versatile compounds with respect to their synthetic chemistry. There is an enormous

amount of phosphorus chemistry known. Many of the synthetic routes lend themselves to asymmetric synthesis and hence the obviously important application with respect to point five above. Much of the synthetic versatility of phosphorus chemistry lies in phosphorus being able to exist in various oxidation states (typically III and V). Unlike nitrogen, and other first row elements, phosphorus can adopt what is termed an expanded valence shell. That is, low lying virtual (empty) $3d$ orbitals on the phosphorus can also take part in its chemistry along with the $3s$ and $3p$ orbitals. This enables phosphorus to adopt a variety of coordination numbers, which range from one up to six (e.g. PR_2^- , PR_2^- , PR_3 , $\text{PR}_3=\text{O}$, PF_5 and PF_6^- respectively).

Organophosphines typically form stable coordination complexes with transition-metals. The stability is owed to both the strong σ dative bond formed and the sometimes appreciable π back donation of electron density from the metal into low lying $3d$ orbitals on the phosphorus, Figure 1.1.

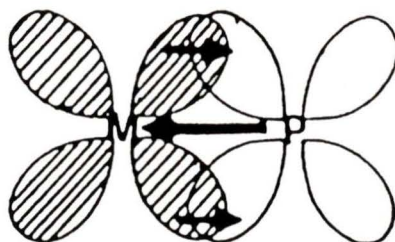


Figure 1.1. The π back donation of electron density from metal M to the phosphorus atom P.

Phosphorus-31 NMR is a particularly useful spectroscopic technique and was used extensively throughout the research for this thesis. Phosphorus exists naturally as 100% spin-active phosphorus-31. Since the advent of fast computers enabling the feasibility of Fourier transform techniques, and the improvement in NMR sensitivity, through the development of superconductors and larger magnetic fields, the routine use of phosphorus-31 NMR has become possible.

Many useful trends have been observed in the steady accumulation of phosphorus-31 NMR data (from the early 1960's to the present) making it a powerful structural probe. The large range of values possible for both the chemical shifts and coupling constants make phosphorus-31 NMR very sensitive to complex geometry and phosphorus oxidation state. As will be seen in the rest of this thesis phosphorus-31 NMR can, in many cases, be used to assign complex conformations. An understanding of the trends observed for phosphorus-31 NMR has been attempted many times, although few have got past

the qualitative discussion stage.

A particularly important observation with respect to the identification of the platinum-phosphorus complexes generated in the research for this thesis is the relationship between the *trans*-influence and phosphorus-platinum coupling constants. Platinum exists naturally as a combination of 33.8% spin-active ^{195}Pt ($I = 1/2$) and 66.2% non-spin-active platinum ($I = 0$). Therefore any single resonance of a nucleus bound to a platinum centre will have associated with it, satellites one-quarter the intensity of the central resonance. These are symmetrically disposed either side with the distance between them (in Hertz) representing the coupling to platinum. The magnitude of a phosphorus-platinum coupling constant is a powerful indicator of the type of ligand *trans* to that phosphorus (i.e. the *trans* ligands *trans*-influence relative to that phosphine).

Many theories concerning the "*trans*-influence" have been advanced. Grinberg's "polarization theory", which is essentially an electrostatic approach, fails in the respect that metals for which the *trans*-influence is most pronounced are those that form metal-ligand bonds containing a large degree of covalency.

A more popular theory, of which there are many similar spin-offs, is Syrkin's hybridization approach. In a square pla-

nar complex, a metal-ion is considered to use the $5d_{x^2-y^2}$, $6s$, $6p_x p_y$ hybrid orbitals for σ bonding (i.e. those pointing in the direction of the ligands, Figure 1.2). When ligand L forms a strong covalent bond with metal M, the orbitals involved will be mainly $5d$ and $6s$ in character, as they are lower and similar in energy. The ligand trans to L, L', has to use the same s and d hybrid orbitals such that if the L-M bond contains a large amount of s and d character, the M-L' bond will weaken: the *trans*-influence.

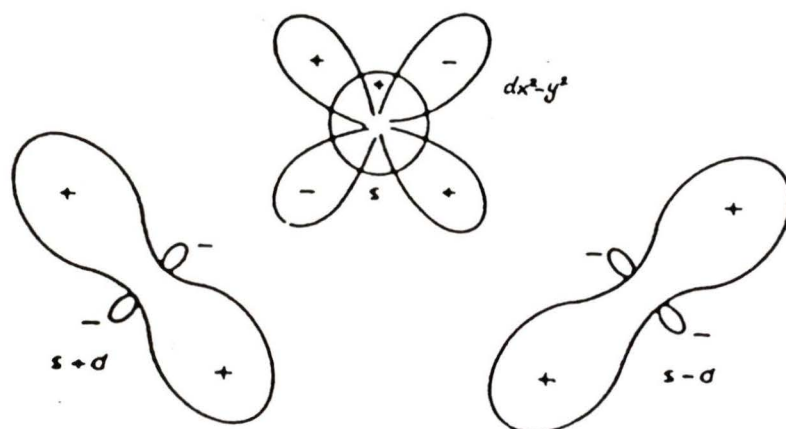


Figure 1.2. The orbitals used in a square-planar complex with respect to the *trans*-influence.

The *trans*-influence has been used to account for variations in $^1J(\text{Pt-P})$ values found in platinum-phosphine complexes by considering the most important contributor to $^1J(\text{Pt-P})$ to be the Fermi contact interaction,¹³ equation 1.1.

$$J_{AB} \propto \gamma_A \gamma_B \alpha_A^2 \alpha_B^2 |\psi_{A(ns)}(0)|^2 |\psi_{B(ns)}(0)|^2 ({}^3\Delta E)^{-1} \quad \text{Equation 1.1}$$

γ_A = gyromagnetic ratio for nucleus A

α_A^2 = s-character of the bond hybrid orbital used by A in the A-B bond

$|\psi_{A(ns)}(0)|^2$ = electron density of the ns orbital at nucleus A

${}^3\Delta E$ = mean singlet-triplet excitation energy. An approximation sometimes used instead of the mutual polarizability term π_{AB}

The only term considered a variable, with respect to the *trans*-influence for square-planar platinum complexes, is α_{Pt}^2 .^{14,15} If a phosphorus atom is *trans* to a ligand with a weaker *trans*-influence than itself, it will have a large amount of s-character in its Pt-P bond (α_{Pt}^2), hence ${}^1J(\text{Pt-P})$ will be higher than when it is *trans* to a ligand with a stronger *trans*-influence. ${}^1J(\text{Pt-P})$ couplings can range from 2200 to 2400 Hz when the phosphorus atom is *trans* to a phosphine or 3100 to 3800 when the phosphorus atom is *trans* to a halide such as a chloride. Many correlations have been presented which illustrate these effects¹⁶ and similar arguments will be used throughout this thesis.

The research summarized in this thesis is an extension of

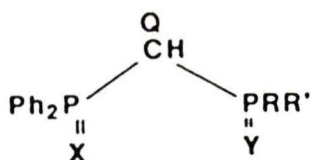
two areas of research which have been of interest to our group for some years: aminophosphine coordination chemistry and bisphosphine chalcogenide chemistry. It also has possible extensions into the third area of research interest, that of multimetallic complexes.

Much of the introductory chemistry is given at the beginning of each chapter. An outline of the ligand syntheses is given in Chapter 2 and the coordination chemistry of the ligands synthesized is given in Chapters 3 and 4. All information regarding general synthetic and spectroscopic procedures together with the description of individual experiments has been collected in Chapter 5.

**Chapter 2: Syntheses of Amino-substituted Bisphosphine
Ligands**

2.1. Introduction

Aminophosphines show interesting structural and stereochemical features, which have been extensively investigated by NMR spectroscopy (typically ^1H and to a lesser extent ^{13}C (^1H) NMR) and X-ray crystallography.¹⁷ However, little research has gone into the study of aminophosphines as sources of unusual coordination chemistry. This deficiency in the literature prompted interest in the synthesis of the following ligand systems, their coordination chemistry with group 8 transition-metals, and the reactivity of the complexes formed.



X and Y = O, S, Lone pair

R = R' = NMe₂, NEt₂, N(CH₂CH₂)₂CH₂

R' = NEt₂ and R' = Ph

Q = H or Li

2.1.1. Possible Coordination Modes.

(Bis(dialkylamino)phosphino)(diphenylphosphino)methane [Ph₂PCH₂P(NR₂)₂] may coordinate in a variety of ways with transition-metals. A few possible modes of coordination are outlined in Figure 2.1.

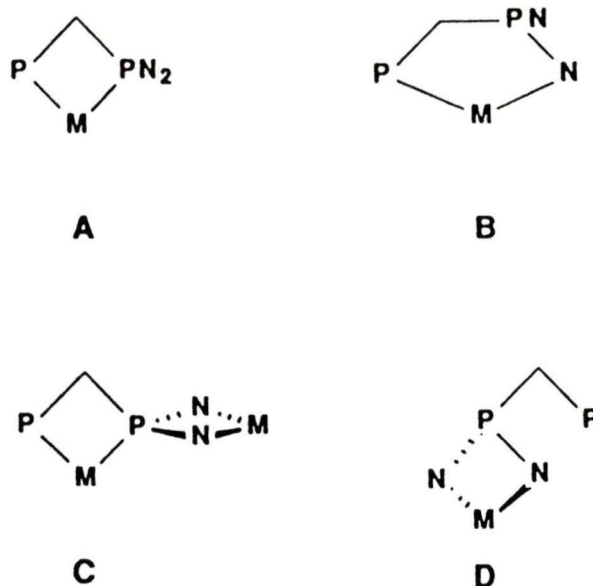
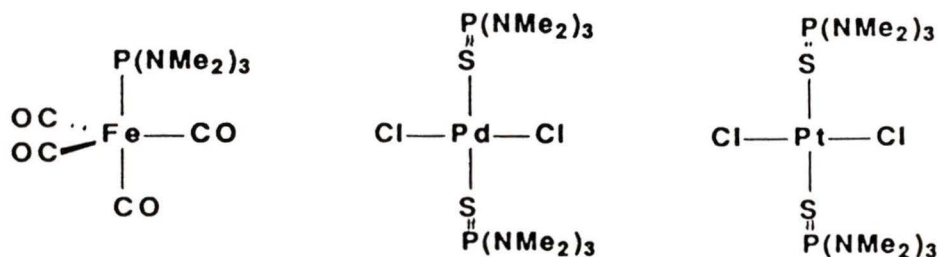
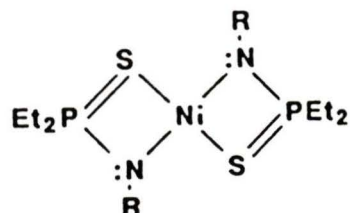


Figure 2.1. Possible coordination modes of $[\text{Ph}_2\text{PCH}_2\text{P}(\text{NR}_2)_2]$ with transition-metals.

Mode B may possibly be preferred over mode A since five-membered rings are more stable than the strained four-membered rings.^{1,7} The possibility of coordination modes C and D depends on the availability of the nitrogen lone pair of electrons, and the N-P-N "bite angle". To-date, however, aminophosphine transition-metal complexes have not shown nitrogen coordination. Coordination has always been through the phosphorus, or through the attached chalcogenide.



The only example of a nitrogen bound aminophosphinothioyl complex, although it does not have a dative nitrogen bond of the type being discussed (i.e. a nitrogen lone-pair donation), is shown below.¹⁸

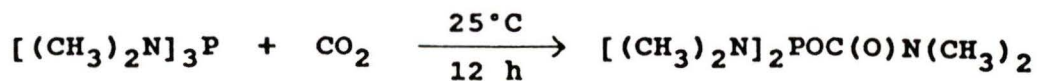


It was therefore of interest to see if the stability of chelation could promote nitrogen coordination.

2.1.2. Reactivity of the Phosphorus-Nitrogen Bond

There are numerous phosphorus-nitrogen (P-N) bond reactions known, many of which are unique to certain aminophosphines. A class of P-N reactions that has been of interest to the coordination chemist is phosphorus-nitrogen bond cleavage. For example, small molecules such as CO_2 and CS_2 can insert themselves into P-N bonds; Scheme 2.1.¹⁹

Scheme 2.1



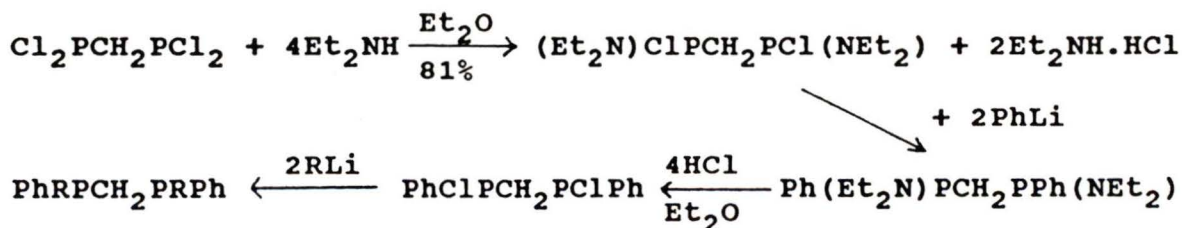
Phosphorus-nitrogen bonds can also be cleaved by halo-acids to form the phosphorus-halide and the corresponding amine hydrogenchloride as shown in Scheme 2.2.²⁰

Scheme 2.2



The possibility of cleaving off one, two or all three amine groups in $\text{P}(\text{NR}_2)_3$ and the unreactivity of the P-NR_2 group towards alkyllithium reagents makes aminophosphines particularly well suited as precursors for chiral phosphine syntheses. This was demonstrated recently by Schmidbaur with the synthesis of $\text{RR}'\text{PCH}_2\text{PRR}'$;²¹ Scheme 2.3.

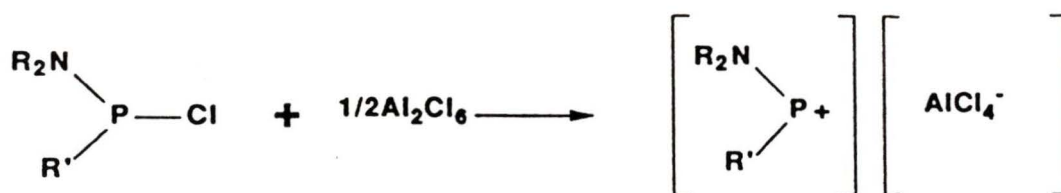
Scheme 2.3



Chiral phosphines have been widely used to prepare low-valent transition-metal complex catalysts for enantioselective organic transformations. Therefore access to, and knowledge of, the reactivity of aminophosphines as either free or coordinated ligands is extremely valuable if they are to be used as precursors in chiral phosphine syntheses.

Chlorophosphines are also important precursors to the formation of other potentially reactive phosphines. For example, the generation of the phosphonium ion, (PR_2^+) , Scheme 2.4. The phosphonium ion may then be used to generate phosphido bridged complexes.²²

Scheme 2.4



2.2. Ligand Syntheses

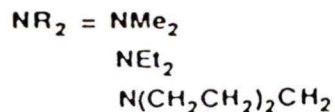
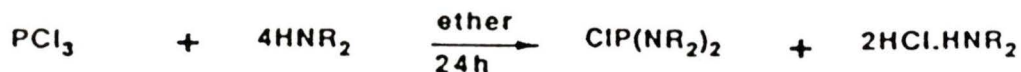
The synthetic basis of many of the following bidentate phosphines involves the linking together of a phosphorus-alkyl-lithium with a chlorophosphine, Scheme 2.5.

Scheme 2.5

2.2.1. Syntheses of $[Ph_2PCH_2P(NR_2)_2]$ Ligands

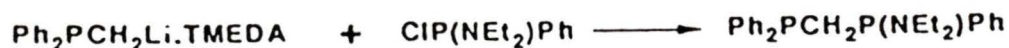
The title bisphosphines (with $NR_2 = NMe_2, NEt_2, N(CH_2CH_2)_2CH_2$) were synthesized by a procedure similar to that described by Grim et al, Scheme 2.6.²³ It was found necessary to generate the chlorophosphine as pure as possible, as even 2-3% impurity (usually $[PCl_2(NR_2)]$) appreciably lowered the purity and bench lifetime of the product, even under an inert atmosphere.

Scheme 2.6



$[Ph_2PCH_2P(NEt_2)Ph]$ was also synthesized, Scheme 2.7, in order to elucidate P-N cleavage products (which will be discussed later in chapter 3).

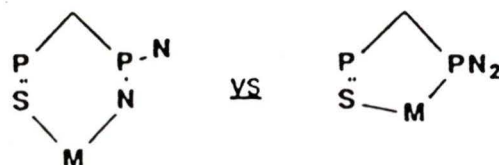
Scheme 2.7



A majority of the chemistry discussed in this thesis concerns the bisphosphine $[\text{Ph}_2\text{PCH}_2\text{P(NEt}_2)_2]$, because the methyl derivative was particularly unstable towards oxidation and hydrolysis, and the piperidine derivative would have had complex ^1H and $^{13}\text{C}\{^1\text{H}\}$ NMR spectra.

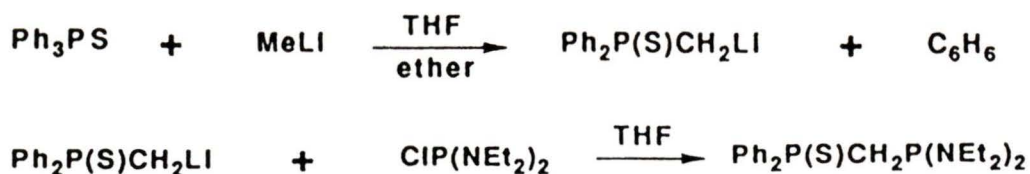
2.2.2. Synthesis of $[\text{Ph}_2\text{P(S)CH}_2\text{P(NEt}_2)_2]$ and $[\text{Ph}_2\text{PCH}_2\text{P(O)(NEt}_2)_2]$

The monochalcogenide derivatives of $[\text{Ph}_2\text{PCH}_2\text{P(NEt}_2)_2]$ were synthesized in an attempt to generate six-membered versus five-membered ring chelates.



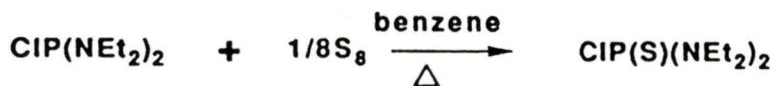
$[\text{Ph}_2\text{P(S)CH}_2\text{P(NEt}_2)_2]$ was prepared by a similar procedure to that described by Grim et al.²⁴, Scheme 2.8

Scheme 2.8



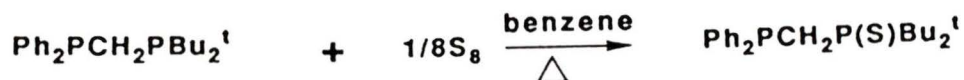
Attempts to generate $[\text{Ph}_2\text{PCH}_2\text{P(S)(NEt}_2)_2]$, with the sulphur on the aminophosphine end, were unsuccessful. Scheme 2.9 outlines the routes attempted.

Scheme 2.9



In retrospect, routes utilizing the basicity of the aminophosphine should have been tried. Possible methods, Scheme 2.10²⁵ and 2.11,²⁴ involve the preferential coordination of sulphur to the more basic phosphine.

Scheme 2.10



Scheme 2.11



However, the sulphur exchange reaction, Scheme 2.11, may not have worked for $[\text{Ph}_2\text{P}(\text{S})\text{CH}_2\text{P}(\text{NET}_2)_2]$ because of the harsh reaction conditions involved: 160°C in diglyme. Ligands containing a three-coordinate aminophosphine ($[\text{R}_2\text{N}]_2\text{P}-$) were found to be less stable than anticipated. As a neat oil, $[\text{Ph}_2\text{PCH}_2\text{P}(\text{NET}_2)_2]$ decomposed in 48 hours; as a dichloromethane solution, in less than 24 hours.

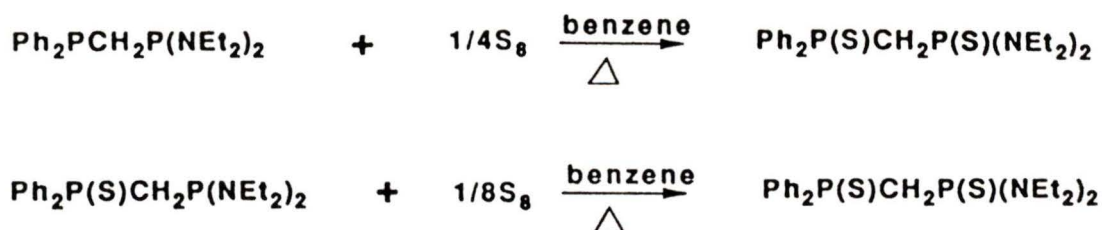
The enhanced basicity of the bis(dialkylamino)phosphino group over the diphenylphosphino group was shown by the reaction of $[\text{Ph}_2\text{PCH}_2\text{P}(\text{NET}_2)_2]$ with air; the mono-oxide $[\text{Ph}_2\text{PCH}_2\text{P}(\text{O})(\text{NET}_2)_2]$ formed exclusively (prolonged exposure led to decomposition).

2.2.3. Synthesis of $[\text{Ph}_2\text{P}(\text{S})\text{CH}_2\text{P}(\text{S})(\text{NET}_2)_2]$ and

$[\text{Ph}_2\text{P}(\text{S})\text{CHP}(\text{S})(\text{NET}_2)_2]\text{Li}$

$[\text{Ph}_2\text{P}(\text{S})\text{CH}_2\text{P}(\text{S})(\text{NET}_2)_2]$ was readily synthesized by two methods; reaction of two equivalents of sulphur with $[\text{Ph}_2\text{PCH}_2\text{P}(\text{NET}_2)_2]$, or one equivalent with $[\text{Ph}_2\text{P}(\text{S})\text{CH}_2\text{P}(\text{NET}_2)_2]$, Scheme 2.12.

Scheme 2.12



$[\text{Ph}_2\text{P}(\text{S})\text{CH}_2\text{P}(\text{S})(\text{NEt}_2)_2]\text{Li}$ was synthesized in an attempt to generate metal-carbon bonded complexes. The anion was readily generated following a procedure outlined by Davison and Reger,²⁶ Scheme 2.13.

Scheme 2.13



2.3. Discussion of NMR Parameters

Normal electron density arguments, as used for ^1H and to a lesser extent ^{13}C NMR chemical shifts, fail for heavy nuclei such as phosphorus, due to the increased importance of local paramagnetic shift effects (where local effects are those that arise on the atom that is undergoing the NMR transition). The contribution is difficult if not impossible to calculate with any accuracy as it involves knowing the wavefunctions and energies of all excited states, including those in the continuum. Energies of virtual orbitals are difficult to calculate, and in consequence rigorous chemical shift calculations are impossible.

Phosphorus NMR assignments were therefore made possible by comparing the chemical shifts of the bisphosphine ligands with the chemical shifts of related monophosphines, as the contributions from electrons in valence orbitals should be similar. For example; $[\text{Ph}_2\text{PCH}_2\text{P}(\text{NEt}_2)_2]$ can be compared to $[\text{Ph}_2\text{PCH}_3]$ and $[\text{CH}_3\text{P}(\text{NEt}_2)_2]$ fragments, which resonate at 169 and -66 ppm respectively (Table 2.2). Therefore the resonances at -163.37 and -59.96 ppm of the bisphosphine (Table 2.2) are assigned to those of the diphenylphosphino and bis(diethylamino)phosphino group respectively.

Phosphorus-phosphorus coupling constants typically provide more chemical information than proton-proton coupling constants. This is due to the dependence of the coupling constant on the *s*-electron density at the nucleus, the *s*-orbital character of the molecular orbitals involved in the chemical bond and the increased importance of the mutual polarizability term (π_{AB}) in the Fermi contact expression for elements other than those in the first row. Thus, both hybridization and effective electronic charge are important. Therefore, $J(\text{P-P})$ values are structurally more sensitive than $J(\text{H-H})$, and fall over a wider range of frequencies. For example, $^1J(\text{P-P})$ can range from -451 Hz in $\text{P}_2\text{Bu}_4^{\text{t}}$ ²⁷ to +766 Hz in $\text{P}_2\text{F}_4\text{O}_4^{2-}$.²⁸

There has been much effort in the literature²⁹ (particularly

by Grim and co-workers^{24,30,31}) to explain the coupling constant trends observed in the series: P-CH₂-P, P(X)-CH₂-P, P(X)-CH₂-P(X), where X = O, S or Se. However, the explanations have only been empirical, owing to the lack of molecular orbital data necessary to describe the molecules exactly. The values of two-bond phosphorus-phosphorus couplings of the type P-E-P where E is a non-metal such as C, N, O, S etc. are believed to vary in a similar fashion to those of single bond phosphorus-phosphorus couplings. That is, the oxidation state, substituent electronegativity and substituent bulk are thought to be important.²⁹ π bonding possibilities (not applicable for E = CH₂) and interbond angles have also been considered important.¹⁷

In the present work, on going from P(III)-P(III) through P(III)-P(V) to P(V)-P(V), via successive oxidation of the phosphorus atoms, $^2J(\text{P-P})$ is seen to decrease in magnitude; >130, 65 - 102, 3 Hz respectively (Table 2.2). A similar observation was reported for the oxidation of $[\text{X}^1\text{X}^2\text{PN}(\text{R})\text{-PX}^3\text{X}^4]$. The bisphospine couplings at about 300 Hz³² are larger than the monochalcogenide at 50 - 150 Hz³³ and the bischalcogenide at 11 - 43 Hz.³⁴ Variations in $^2J(\text{P-P})$ observed in the P^{III}-N-P^{III} system are thought to be a consequence of the relative populations of the eclipsed and staggered conformers (with reference to the lone pairs of electrons). This was seen in a study of the series $[\text{Ph}_2\text{P-N}(\text{R})\text{PPhCl}]$.³⁵ The results showed a dramatic dependence of

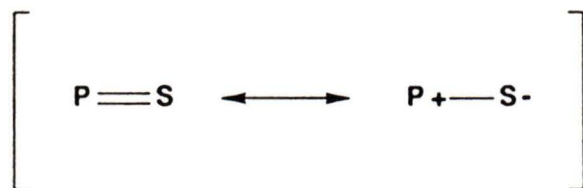
$^2J(\text{P-P})$ on the bulk of R: R = Me (+333.5 Hz); Et (+158 Hz); n-Pr (+145 Hz); i-Pr (-29 Hz); t-Bu (-35 Hz). Therefore the reduction in $^2J(\text{P-P})$ upon oxidation of $[\text{Ph}_2\text{PCH}_2\text{P}(\text{NEt}_2)_2]$ could be a result of the change in oxidation state of the phosphorus and the electron withdrawing properties of the chalcogenide or of a change in the relative conformer populations which is seen to affect $^2J(\text{P-P})$ quite dramatically in the $\text{P}^{\text{III}}\text{-N-P}^{\text{III}}$ system. An electron withdrawing argument, however, would appear to oppose the observed trends. In the series of substituted cyclophosphazenes $\text{P}_3\text{N}_3\text{X}_6$, $^2J(\text{P-P})$ increases with increasing electronegativity of X: X = F (199.2 Hz); Cl (42.8 Hz); Br (4.8 Hz).³⁶

Further evidence supporting the conformational argument over the oxidation(rehybridization)/substituent-effect argument is observed with the series $[\text{Ph}_2\text{PCH}_2\text{PR}_2]$ and $[\text{Ph}_2\text{P}(\text{S})\text{-CH}_2\text{PR}_2]$.³¹ In both cases increasing the bulk of R (R = Me < i-Pr < t-Bu) increases the magnitude of $^2J(\text{P-P})$: $[\text{Ph}_2\text{P-CH}_2\text{PR}_2]$ (108, 119, 138 Hz); $[\text{Ph}_2\text{P}(\text{S})\text{CH}_2\text{PR}_2]$ (56, 77, 87 Hz). It is considered doubtful that the size of the change observed for $^2J(\text{P-P})$ is a consequence of substituent electronegativity and bulk-causing rehybridization of the phosphorus atom. That is, for the series of complexes $[(\text{Ph}_2\text{P-CH}_2\text{PR}_2)\text{W}(\text{CO})_5]$ the coupling $^1J(^{31}\text{P-}^{183}\text{W})$ is relatively insensitive to the bulk of R. McFarlane and co-workers have also shown that with the trisphosphine system $[(\text{Ph}_3\text{P})_3\text{CH}]$ and related oxidized forms, $[(\text{Ph}_3\text{P})_2\{\text{Ph}_3\text{P}(\text{S})\}\text{CH}]$,

$[(\text{Ph}_3\text{P})(\text{Ph}_3\text{P}(\text{S}))_2\text{CH}]$ and $[(\text{Ph}_3\text{P}(\text{S}))_3\text{CH}]$, the presence of sulphur atoms on phosphorus leads to greater steric interactions than do lone pairs of electrons.³⁷ Therefore the dependence of $^2J(\text{P-P})$ on the oxidation state of the bisphosphine is due to lone-pair/lone-pair, lone-pair/P=S, and P=S/P=S steric interactions causing small changes in the relative populations of the conformers.

The only useful $^{13}\text{C}\{^1\text{H}\}$ NMR data (Table 2.3) is that for the bridging methylene unit. There is a general deshielding of the methylene resonance in the series $\text{P}(\text{:})\text{CH}_2\text{P}(\text{:}) < \text{P}(\text{S})\text{CH}_2\text{P}(\text{:}) < \text{P}(\text{S})\text{CH}_2\text{P}(\text{S})$. Grim observed a similar trend for the methylene proton resonances in analogous compounds and ascribed this to the partial positive charge build up on the phosphorus atom caused by attachment of a chalcogenide atom,³⁰ Scheme 2.14.

Scheme 2.14



Single-bond phosphorus-carbon couplings, in contrast to two-bond phosphorus-phosphorus couplings, increase on going from P(III) to P(V). A similar trend has been reported for the series of ligands $[\text{Ph}_2\text{P}(\text{X})\text{CH}_2\text{P}(\text{Y})\text{PPh}_2]$ where X and Y are S, O

or electron-pairs: ${}^1J(\text{P}(\text{:})-\text{C}) < {}^1J(\text{P}(\text{Se})-\text{C}) < {}^1J(\text{P}(\text{S})-\text{C}) < {}^1J(\text{P}(\text{O})-\text{C})$.^{30,38} No explanation for this observation has ever been forwarded. It might, however, be expected to have a similar explanation to that for ${}^2J(\text{P}-\text{P})$ as changes only occur at the phosphorus atom. It is unlikely that the observed trend is a consequence of changes in the relative conformer populations, as oxidation of $[\text{Ph}_2\text{PCH}_2\text{P}(\text{NEt}_2)_2]$ to $[\text{Ph}_2\text{PCH}_2\text{P}(\text{S})(\text{NEt}_2)_2]$ causes an increase in ${}^1J(\text{P}-\text{C})$ but further oxidation to $[\text{Ph}_2\text{P}(\text{S})\text{CH}_2\text{P}(\text{S})(\text{NEt}_2)_2]$ changes ${}^1J(\text{P}-\text{C})$ very little.

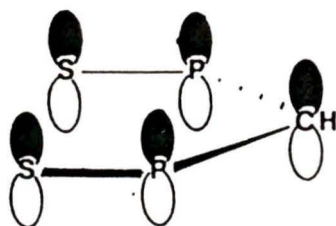
Unlike ${}^2J(\text{P}-\text{P})$, ${}^1J(\text{P}-\text{C})$ is usually negative for tertiary phosphines³⁹ ($\text{PMe}_3 = -13.6 \text{ Hz}$).⁴⁰ However the sign changes when the phosphorus atom is quarternized ($\text{PMe}_4^+ = +55 \text{ Hz}$).⁴¹ The sign changes in the reduced coupling constants for the series Me_3P , $\text{Me}_3\text{P}=\text{S}$ and $\text{Me}_3\text{P}=\text{O}$ which exhibit one-bond ${}^{13}\text{C}-{}^{31}\text{P}$ couplings of -13.6 , $+56.1$ and $+68.3 \text{ Hz}$ respectively, have been explained by an increase in the phosphorus *s*-character as for the Fermi-contact relationship.⁴⁰ Similar effects are seen with ${}^1J(\text{P}-\text{P})$ couplings in P_2R_4 compounds.³⁶ Sign changes, however, are usually considered to arise from the polarizability term in the Fermi-contact expression. That is, when the mean excitation energy expression (${}^{-1}\Delta E$) breaks down the polarizability term becomes negative. Thus arguments solely presented in terms of *s*-orbital character are incorrect. Many of the attempts at predicting single-bond couplings have only found success with the first row

elements, as many of the approximations involved cannot be made for heavier elements.⁴²⁻⁴⁵

In the present work, only the magnitude of $^1J(P-C)$ is measured and as such, arguments relating to the trends observed are precluded.

Changing the hybridization at the central carbon atom from sp^3 to sp^2 , by deprotonation of the disulphide $[Ph_2P(S)-CH_2P(S)(NEt_2)_2]$ with butyllithium to form the anion $[Ph_2P(S)CHP(S)(NEt_2)_2]^-$, caused an increase in both $^1J(P-C)$ and $^2J(P-P)$: $\Delta^1J(Ph_2P-C)$, +66 Hz; $\Delta^1J((Et_2N)_2P-C)$, +70 Hz; $^2J(P-P)$, 41 Hz. The increase in $^1J(P-C)$ could be due to rehybridization of the carbon from sp^3 to sp^2 and the inferred multiple bond character between the phosphorus and carbon atoms. As both phosphorus atoms are quarternized, $^1J(P-C)$ is likely to be positive such that Fermi contact arguments may be used. The increase in $^1J(P-C)$ upon deprotonation could be a consequence of the increase in s -character about the carbon nucleus. Again, the changes in $^2J(P-P)$ maybe due to several factors: i) increased s -character in the hybrid orbitals between the nuclei, ii) contraction of the distance between the nuclei due to the increase in the P-C bond order, iii) different conformational populations (i.e. the anion will probably prefer a planar configuration of the S-P-C-P-S atoms, Scheme 2.15).

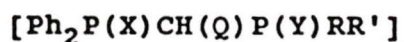
Scheme 2.15



A similar but smaller increase in ${}^2J(\text{P-P})$ is seen with $[(\text{EtO})_2\text{P}(\text{O})\text{CH}_2\text{P}(\text{O})(\text{OEt})_2]$. Deprotonation of the central methylene carbon raises ${}^2J(\text{P-P})$ from being very small to >25 Hz.⁴⁶ The possibility of electron delocalization seems important in both cases.

In summary, the ligands represented by $[\text{Ph}_2\text{P}(\text{X})\text{CH}(\text{Q})\text{P}(\text{Y})\text{RR}']$ were readily synthesized by the coupling of two phosphines, followed by reaction with the appropriate chalcogenide. Successive oxidation of the phosphorus atoms leads to a decrease in the value of ${}^2J(\text{P-P})$. This was rationalized in terms of changes in the relative populations of the possible conformers with respect to electron-pair/electron-pair, electron-pair/P=S and P=S/P=S steric interactions. The increase in ${}^1J(\text{P-C})$ upon oxidation of the phosphorus atoms could not be rationalized as it was necessary to know the sign of the coupling constant, which for these compounds was not determined. The observed trends, however, could be very useful synthetic structural probes. Within the range of compounds reported here and elsewhere, there appears to be no exception to the observed trends.

TABLE 2.1. ^{31}P NMR Data for Phosphine compounds used in
Chemical Shift Assignments of the Ligands



Compound	$\delta(\text{P})^{\text{a}}$
Ph_2PMe	-169
$\text{Ph}_2\text{PCH}_2\text{PPh}_2$	-164
$\text{MeP}(\text{NEt}_2)_2$	-61
$\text{MeP}(\text{NMe}_2)_2$	-55
$\text{MeP}(\text{S})\text{Ph}_2$	-106
$\text{MeP}(\text{O})(\text{NMe}_2)_2$	-103
$\text{PhP}(\text{O})(\text{NMe}_2)_2$	-113
$\text{PhP}(\text{O})(\text{NEt}_2)_2$	-103

Notes: ^a chemical shift in ppm relative to TMP

Reference: Crutchfield, M. M.; Dungan, J. H.; Letcher, J.

H.; Mark, V. Van Wazer, J. R. *Topics in Phosphorus Chemistry*

Vol. 5 (1965).

TABLE 2.2 ^{31}P NMR Data for $[\text{Ph}_2\text{P}(\text{X})\text{CH}(\text{Q})\text{P}(\text{Y})\text{RR}']$ Ligands

Compound	$\delta\text{P}_a^{\text{a,b}}$	$\delta\text{P}_b^{\text{a,c}}$	$J(\text{P}_a-\text{P}_b)^{\text{d}}$
$\text{Ph}_2\text{PCH}_2\text{P}(\text{NEt}_2)_2^{\text{f}}$	-59.96	-163.36	146
$\text{Ph}_2\text{PCH}_2\text{P}(\text{N}(\text{CH}_2\text{CH}_2)_2\text{CH})_2^{\text{f}}$	-78.41	-163.33	140
$\text{Ph}_2\text{PCH}_2\text{P}(\text{NMe}_2)_2^{\text{e}}$	-52.82	-163.54	142
$\text{Ph}_2\text{PCH}_2\text{P}(\text{NEt}_2)\text{Ph}^{\text{f}}$	-89.39	-163.17	132
$\text{Ph}_2\text{P}(\text{S})\text{CH}_2\text{P}(\text{NEt}_2)_2^{\text{f}}$	-67.46	-101.18	102
$\text{Ph}_2\text{PCH}_2\text{P}(\text{O})(\text{NEt}_2)_2^{\text{e}}$	-111.55	-167.78	65
$\text{Ph}_2\text{P}(\text{S})\text{CH}_2\text{P}(\text{S})(\text{NEt}_2)_2^{\text{f}}$	-71.15	-106.00	3
$\text{Ph}_2\text{P}(\text{S})\text{CH}(\text{Li})\text{P}(\text{S})(\text{NEt}_2)_2^{\text{g}}$	-62.70	-101.57	44

Notes: **a** chemical shift in ppm relative to TMP
b aminophosphine
c diphenylphosphine
d in Hz
e TT14 with external C_6D_6 reference
f CDCl_3
g d^8THF .

TABLE 2.3. ^{13}C NMR^a Data for $[\text{Ph}_2\text{P}(\text{X})\text{CH}(\text{Q})\text{P}(\text{Y})\text{RR}']$ Ligands

Compound	$\delta\text{-CH}_2$ ^{b,c}	$\delta\text{PNCH}_2\text{CH}_3$ ^b	$\delta\text{PNCH}_2\text{CH}_3$ ^c	δPh ^d
$\text{Ph}_2\text{PCH}_2\text{P}(\text{NEt}_2)_2$ ^e	29.19(t) (20) [20]	15.04(s)	42.39(d) [17]	128.6-133.5
$\text{Ph}_2\text{PCH}_2\text{P}(\text{NEt}_2)\text{Ph}$ ^f	29.15(dd) (23) [29]	15.03(s)	44.20(d) [15]	127.5-133.7
$\text{Ph}_2\text{P}(\text{S})\text{CH}_2\text{P}(\text{NEt}_2)_2$ ^f	34.71(dd) (53) [27]	14.58(d) [3]	42.82(d) [18]	128.0-134.6
$\text{Ph}_2\text{P}(\text{S})\text{CH}_2\text{P}(\text{S})(\text{NEt}_2)_2$ ^f	36.63(dd) (51) [82]	14.16(s)	39.96(s)	128.0-134.2
$\text{Ph}_2\text{P}(\text{S})\text{CH}(\text{Li})\text{P}(\text{S})(\text{NEt}_2)_2$ ^g	23.56(dd) (117) [152]	15.34(d) [5]	41.08(d) [4]	127.6-142.9

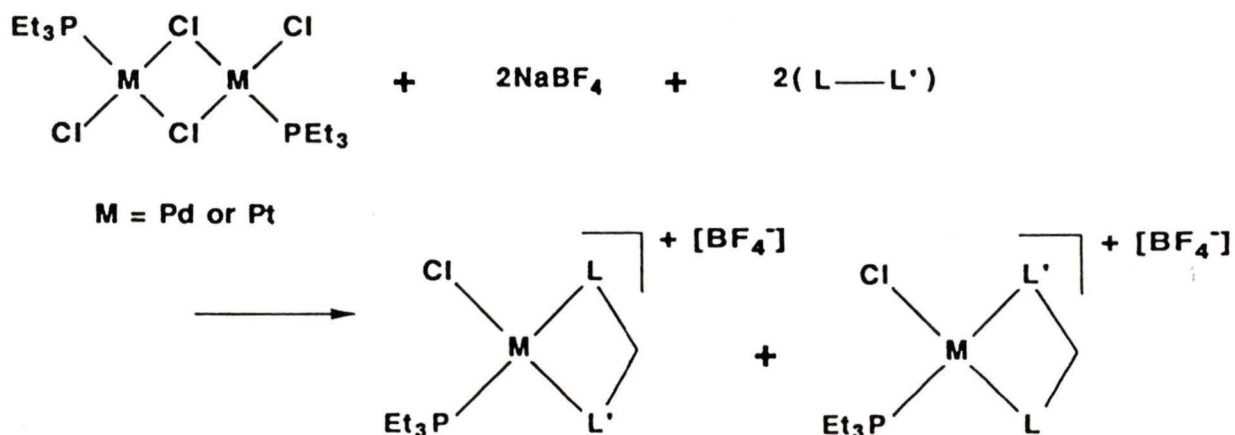
- Notes: ^a chemical shift in ppm relative to TMS
^b () coupling to phenylphosphine in Hz
^c [] coupling to aminophosphine in Hz
^d multiplets
^e C_6D_6
^f CDCl_3
^g d^8THF .

**CHAPTER 3: Coordination Chemistry and Reactivity of the
Ligands $[\text{Ph}_2\text{PCH}_2\text{P}(\text{NEt}_2)_2]$ and $[\text{Ph}_2\text{PCH}_2\text{P}(\text{NEt}_2)\text{Ph}]$**

3.1. Introduction

A convenient route to the formation of transition-metal complexes of monodentate or bidentate ligands, involves the cleavage of neutral chloro-bridged dimers of the type $[M_2Cl_2(\mu-Cl)_2(PEt_3)_2]$; where $M = Pd$ or Pt ⁴⁷ and $[M_2(\mu-Cl)_2(\eta^4-cod)_2]$; where $M = Rh$ ⁴⁸ or Ir .⁴⁹ Cleavage of the platinum and palladium dimers with asymmetric bidentate chelating ligands (L-L') can generate *cis* and/or *trans* isomers, Scheme 3.1. Cleavage of the rhodium and iridium dimers, however, only generates one product owing to the symmetry of the 1,5-cyclooctadiene ligand, Scheme 3.2.

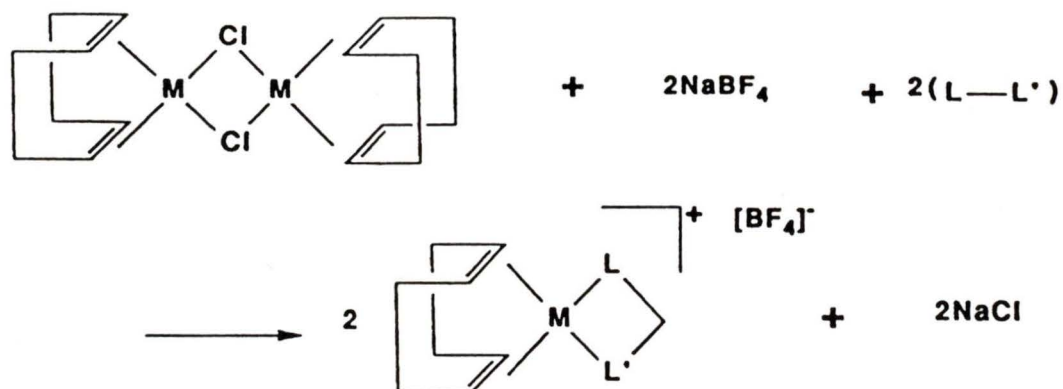
Scheme 3.1



Cleavage of $[Pt_2Cl_2(\mu-Cl)_2(PEt_3)_2]$ and $[Pd_2Cl_2(\mu-Cl)_2(PEt_3)_2]$ requires the addition of NaBF_4 in order to provide the $[\text{BF}_4]^-$ counter-ion. In the absence of an alternative counter-ion⁵⁰ the metal counter-ion $[\text{Cl}_3\text{M}(\text{PEt}_3)]^-$ ($\delta^{31}\text{P} =$

-138 ppm; $^1J(\text{Pt-P}) = 3710 \text{ Hz}$) is generated, which constitutes a waste of metal and causes unnecessary confusion during NMR analysis.

Scheme 3.2



The following Chapter contains the results and discussion of reactions to generate transition metal complexes of the ligands $[\text{Ph}_2\text{PCH}_2\text{P}(\text{NEt}_2)\text{Ph}]$, $[\text{Ph}_2\text{PCH}_2\text{P}(\text{NEt}_2)_2]$ and $[\text{Ph}_2\text{PCH}_2\text{P}\{\text{N}(\text{CH}_2\text{CH}_2)_2\text{CH}\}_2]$. The latter half of the Chapter covers the results on phosphorus-nitrogen reactivity of the complexed ligands $[\text{Ph}_2\text{PCH}_2\text{P}(\text{NEt}_2)_2]$ and $[\text{Ph}_2\text{PCH}_2\text{P}(\text{NEt}_2)\text{Ph}]$.

3.2.1. Reaction of $[\text{Pt}_2\text{Cl}_2(\mu\text{-Cl})_2(\text{PEt}_3)_2]$ with $[\text{Ph}_2\text{PCH}_2\text{P}(\text{NEt}_2)_2]$

The reaction of $[\text{Ph}_2\text{PCH}_2\text{P}(\text{NEt}_2)_2]$ with $[\text{Pt}_2\text{Cl}_2(\mu\text{-Cl})_2(\text{PEt}_3)_2]$ was the first of a series of reactions designed to promote nitrogen-metal coordination through ring strain of

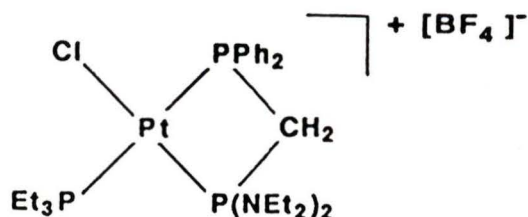
the chelate, as mentioned in Chapter 2: generation of the more stable five-membered ring complex over the four-membered ring complex,¹ Figure 2.1. Bisphosphines of type $[R_2PCH_2PR_2]$ normally form four-membered metal chelates.

The following section, apart from discussing the chemistry involved, will briefly outline the power of phosphorus NMR in conjunction with a spin active metal such as platinum-195, for complex structure elucidation. Throughout this thesis, *cis* and *trans* will refer to the position of the aminophosphine relative to the triethylphosphine. A summary of the NMR data for this Chapter is given in Tables 3.1 to 3.6.

Reaction of $[Pt_2Cl_2(\mu-Cl)_2(PEt_3)_2]$ with two equivalents of $[Ph_2PCH_2P(NEt_2)_2]$ and sodium tetrafluoroborate, initially generated a product having the $^{31}P\{^1H\}$ NMR spectrum shown in Figure 3.1. Recrystallization of this initial product from dichloromethane/hexane afforded colourless crystals. The $^{31}P\{^1H\}$ NMR of the crystals (Figure 3.2a) was significantly different from that of the original product and is considered to be that of the *cis*-isomer; discussion to follow.

The major resonances in Figure 3.2 (doublet, doublet and doublet of doublets; at -119.27, -130.91 and -182.04 ppm respectively) are characteristic of an AMX spin-system with slight second order distortion (i.e. intensity tenting in

the group of resonances at -119.27 and -182.04 ppm, caused by a strong coupling constant and relatively close chemical shifts). The $^{31}\text{P}\{^1\text{H}\}$ NMR shown in Figure 3.2 was assigned to the complex:



The $^{31}\text{P}\{^1\text{H}\}$ NMR of $\text{cis-}[\text{PtCl}(\text{PEt}_3)\{\text{Ph}_2\text{PCH}_2\text{P}(\text{NEt}_2)_2\}\text{-P,P'}]\text{BF}_4$ (Figure 3.2a), shows a resonance to low frequency (assigned to Ph_2P by comparison with analogous compounds) with a low $J(\text{Pt-P})$ value of 2150 Hz. This is indicative of a platinum-phosphorus single bond, with the phosphorus in question *trans* to a ligand with a strong *trans*-influence; presumably another phosphine. The two remaining phosphorus resonances (doublets) at -119.27 and -130.91 ppm are the triethylphosphine and bis(diethylamino)phosphino group respectively (the triethylphosphine resonance was assigned by comparison with other results from this research group). The aminophosphine-platinum coupling of 3806 Hz is indicative of a phosphorus-platinum single bond, with the phosphorus *trans* to a ligand of weaker *trans*-influence, such as a halide; in this case chloride.

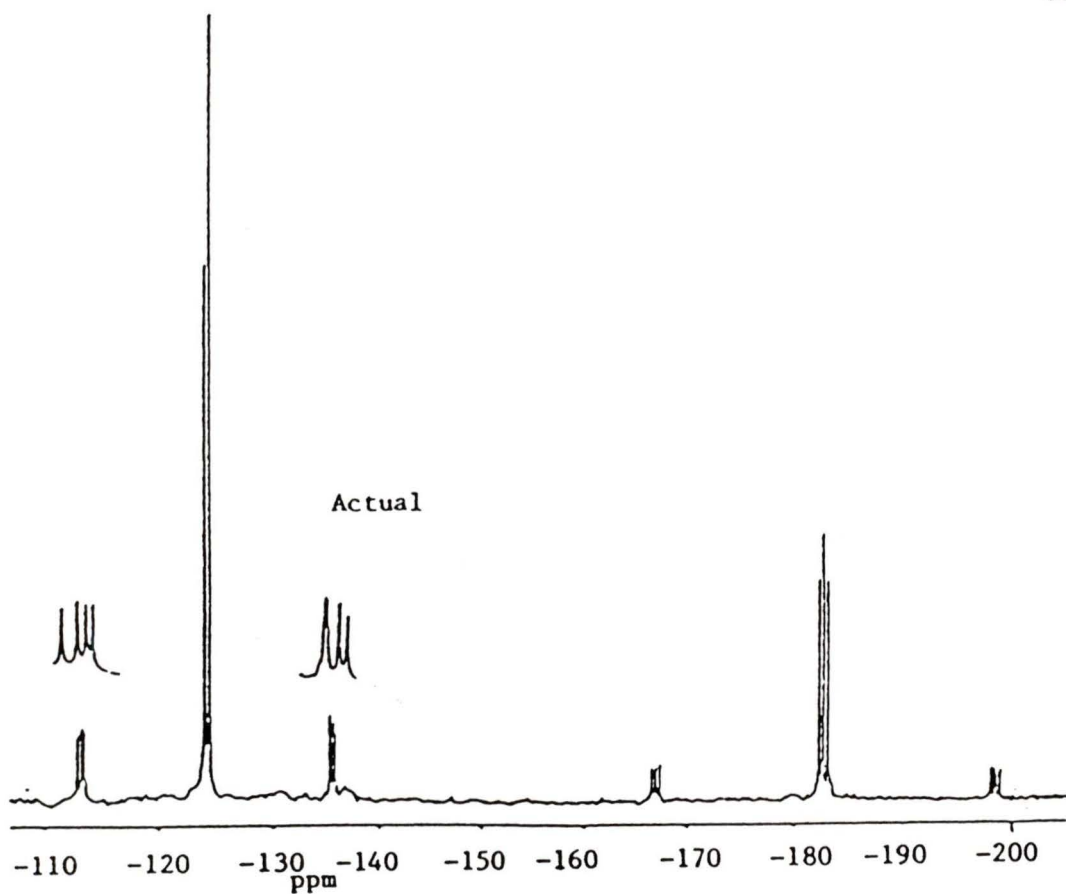
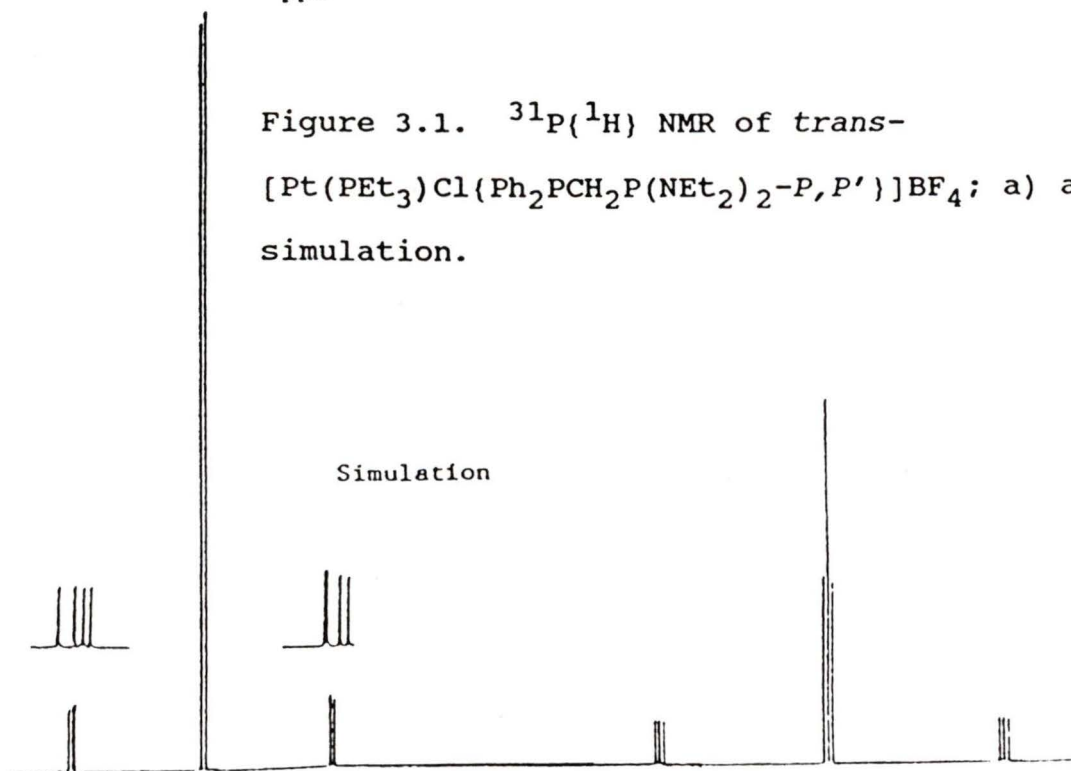


Figure 3.1. ^{31}P (^1H) NMR of *trans*-
[Pt(PEt₃)Cl(Ph₂PCH₂P(NEt₂)₂-*P,P'*)]BF₄; a) actual, b)
simulation.



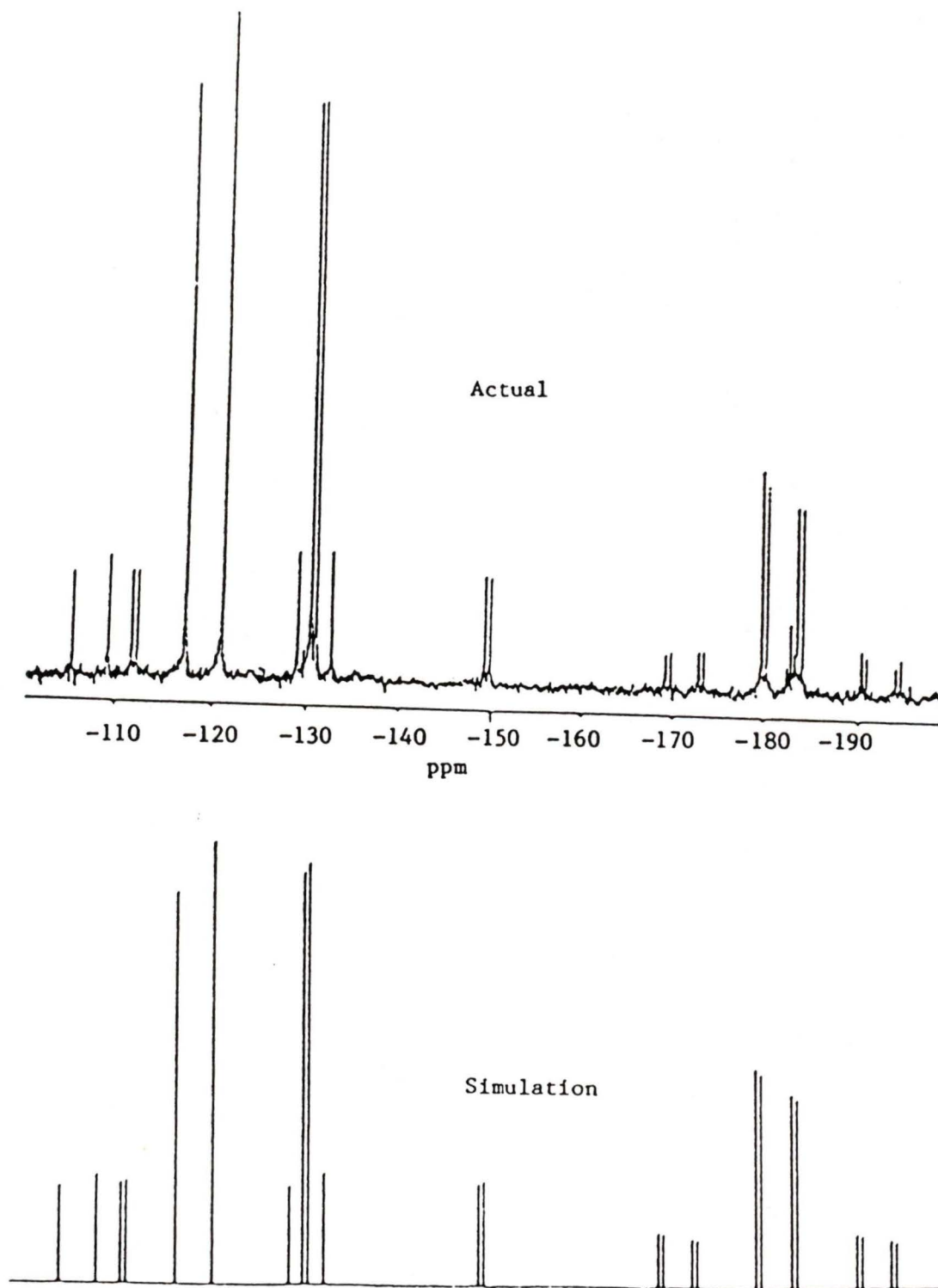


Figure 3.2. $^{31}\text{P}\{^1\text{H}\}$ NMR of $\text{cis-}[\text{Pt}(\text{PEt}_3)\text{Cl}(\text{Ph}_2\text{PCH}_2\text{P}(\text{NEt}_2)_2\text{-}P,P')]\text{BF}_4$; a) actual, b) simulation

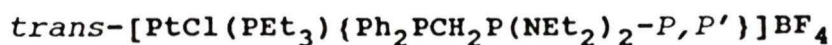
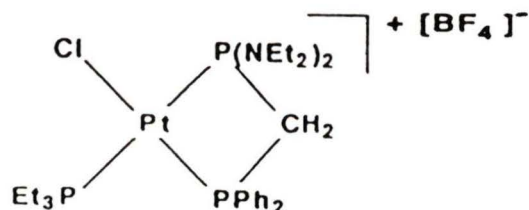
The above information alone indicates a *cis*-P,P' metal chelate. The expected nitrogen coordination was not observed. Further evidence for the formation of the four-membered ring complex in preference to five-membered ring complex comes from the chemical shift changes upon coordination with respect to uncoordinated bisphosphine. When dppm or any other similar P-X-P phosphine, coordinates with a metal to form a four-membered chelate ring the phosphorus chemical shifts move to lower frequency. Conversely, when dppe (bis(diphenylphosphino)ethane) and similar P-X-X-P phosphines coordinate with a metal to form a five-membered chelate ring, the phosphorus chemical shifts move to higher frequency.^{52,1} In the present example the chemical shifts of both bis(diethylamino)phosphino group and diphenylphosphino group move to lower frequency upon coordination ($\Delta\delta = -70.95$ and -18.67 ppm respectively), implying a four-membered chelate.

The second order distortion seen in Figure 3.2 is due to the strong, *trans* two bond phosphorus-phosphorus coupling constant between the diphenylphosphino group and the triethylphosphine of 381 Hz. $^2J(\text{P-P})_{\text{trans}}$ couplings are typically found to be greater than 350 Hz. Consequently, the coupling constants and chemical shifts obtained from a first order analysis are not their true values. Their true values can be obtained by calculations on the spectral resonance positions either by hand for simple spectra, or by computer for more complicated spectra. The computer simulated spectrum

for the *cis*-isomer is shown in Figure 3.2.

The unresolved coupling between the bis(diethylamino)phosphino group and the triethylphosphine is typical for a *cis* phosphorus-phosphorus couplings, which are usually small and negative.²⁹ The intra-chelate coupling was reduced from 146 Hz in $[\text{Ph}_2\text{PCH}_2\text{P}(\text{NEt}_2)_2]$ to 59 Hz upon coordination. This is thought to be a consequence of having a negative coupling path through the metal (*cis* arrangement) cancelling some of the positive coupling, through the chelate backbone.⁵³ It could also be due to the restricted conformation of the bisphosphine and rehybridization upon coordination. That is, following the discussion in chapter 2 the conformation adopted may be that of a low J(P-P) pathway.

The initial product formed by the reaction of $[\text{Pt}_2\text{Cl}_2(\mu\text{-Cl})_2(\text{PEt}_3)_2]$ with $[\text{Ph}_2\text{PCH}_2\text{P}(\text{NEt}_2)_2]$ is then probably the *trans*-isomer:



Trans- $[\text{PtCl}(\text{PEt}_3)\{\text{Ph}_2\text{PCH}_2\text{P}(\text{NEt}_2)_2\text{-P,P'}\}]\text{BF}_4$ is expected to have a strongly coupled ABX spin pattern for its $^{31}\text{P}\{^1\text{H}\}$

have a strongly coupled ABX spin pattern for its $^{31}\text{P}(^1\text{H})$ NMR: triethylphosphine and bis(diethylamino)phosphino group having a large coupling constant ($^2J(\text{P-P})_{\text{trans}} > 350 \text{ Hz}$) and close chemical shifts. The $^{31}\text{P}(^1\text{H})$ NMR (Figure 3.1), however, appears as a simple triplet and doublet (main resonances); typical of an A_2X spin system. The probability of obtaining an A_2X , or even an $\text{AA}'\text{X}$ spin system, is extremely low since triethylphosphine and bis(diethylamino)phosphino groups are unlikely to have coincidental chemical shifts. In short, the central resonances may be described as that of a "deceptively simple spectrum";⁵⁴ that is, the spectral pattern portrays a simpler situation than actually exists. The ABX appears as an A_2X , with the directly measured coupling being the average of J_{AX} and J_{BX} . The deceptively simple ABX pattern for *trans*- $[\text{PtCl}(\text{PET}_3)(\text{Ph}_2\text{PCH}_2\text{P}(\text{NET}_2)_2\text{-P,P}')]\text{BF}_4$ is probably due to the large *trans* phosphorus-phosphorus coupling between the triethylphosphine and bis(diethylamino)phosphino group.

The gradual distortion from an ABX to an apparent A_2X spin pattern is shown diagrammatically in Figure 3.3. The ratio $J/\Delta\delta$ is gradually increased from 0.6 to 60.0, where the spectrum finally collapses to a doublet and a triplet.

Deceptively simple spectra are notoriously difficult to solve because of the lack of information available (few spectral lines) and their many possible solutions. The

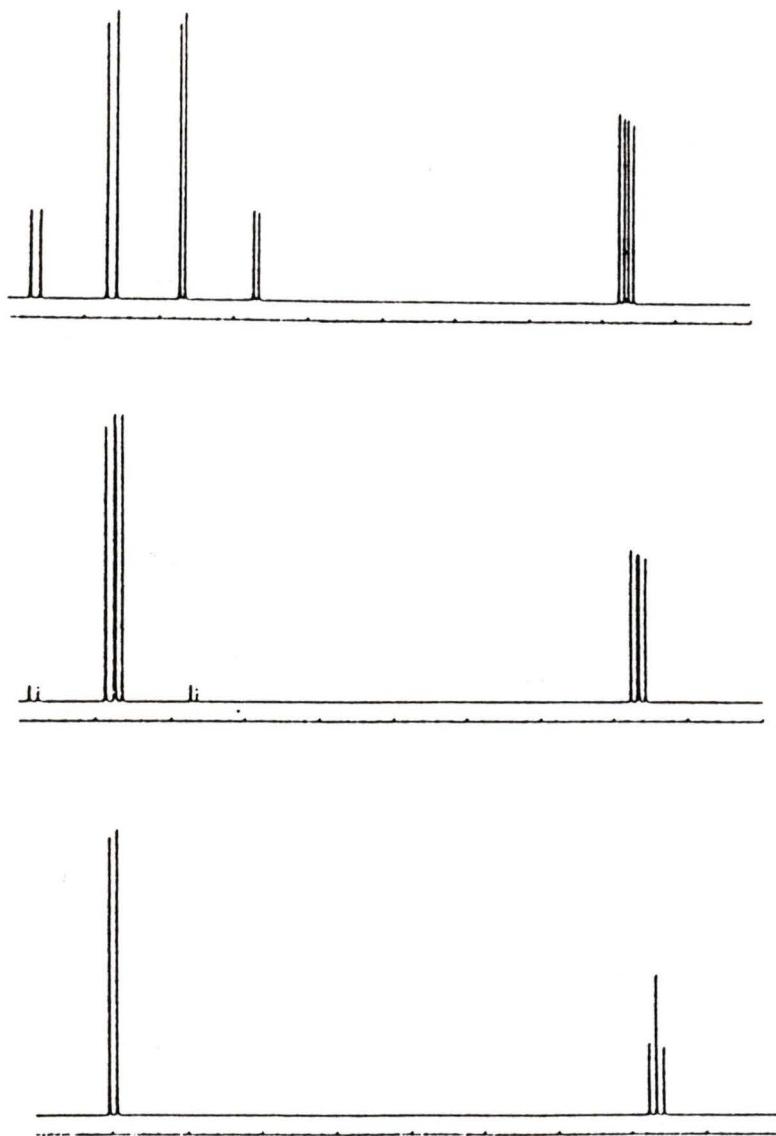
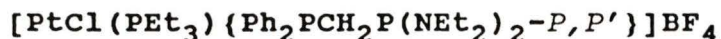


Figure 3.3 A series of simulated spectra showing the gradual transformation of an ABX spin-system to a deceptively simple A_2X spin-system by increasing the ratio of $J/\Delta\delta$. a) $J/\Delta\delta = 0.6$; b) $J/\Delta\delta = 5.0$; c) $J/\Delta\delta = 60.0$

example in Figure 3.3 shows just one particular way of obtaining a deceptively simple spectrum. Extra information, however, can normally be obtained from the platinum satellites. The large platinum couplings can spread out the contents of the centre spectrum by a process called "effective chemical shift" (which derives from the mathematics involved in the solution of an ABMX spin-system). Asymmetry in the satellites is due to the different combinations of chemical shifts and coupling constants, therefore giving different effective chemical shifts. However, due to the low intensity of the satellites only the strong centre resonances of the AB quartets were observed, which only convey the value of $[J_{AX} + J_{BX}]$, see Figure 3.3b for example. The smaller outer resonances of the AB quartets were lost in the base-line noise, therefore the value of J_{AB} cannot be determined.

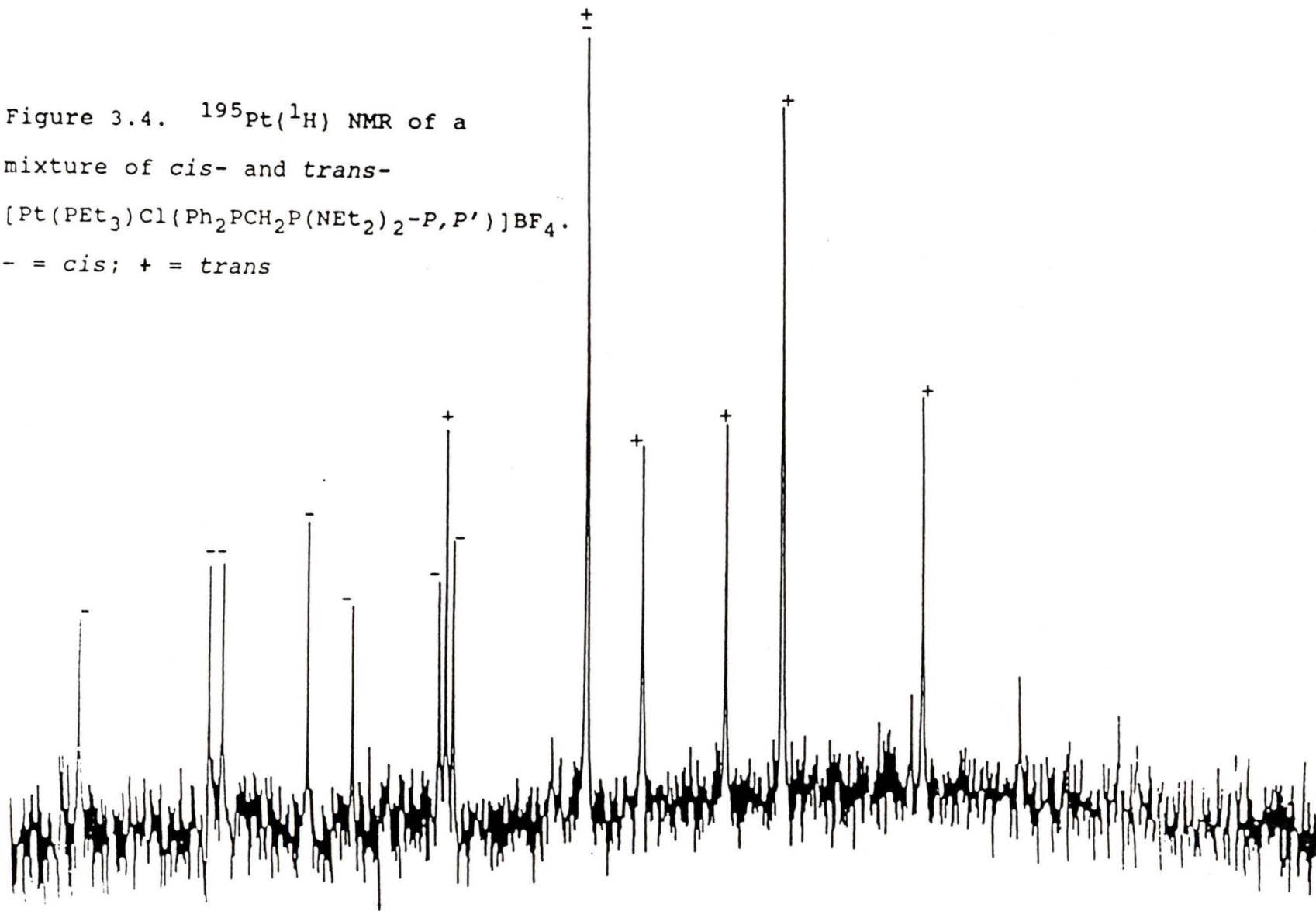
Solving the spin-system employing intuitive guesses and a computer simulation program was attempted. The results are shown graphically in Figure 3.1 and Table 3.1. The solution, however, is not unique owing to the lack of spectral information.

3.2.2. Discussion on the Platinum-195 NMR of



The $^{195}\text{Pt}\{^1\text{H}\}$ NMR of *cis* and *trans*- $[\text{PtCl}(\text{PEt}_3)(\text{Ph}_2\text{PCH}_2\text{-P}(\text{NEt}_2)_2\text{-}P,P')]\text{BF}_4$ is shown in Figure 3.4. The $^{195}\text{Pt}\{^1\text{H}\}$

Figure 3.4. $^{195}\text{Pt}(^1\text{H})$ NMR of a mixture of *cis*- and *trans*-
 $[\text{Pt}(\text{PEt}_3)\text{Cl}(\text{Ph}_2\text{PCH}_2\text{P}(\text{NEt}_2)_2\text{-}P,P')]\text{BF}_4$.
- = *cis*; + = *trans*



NMR spectrum of the *cis*-isomer was also obtained separately. The *cis*-isomer pattern is as expected; eight lines representing a doublet of doublet of doublets from coupling to the three different phosphines.

The *trans*-isomer, however, is an overlapping doublet of triplets ($^1J(\text{Pt-P}) = 3188$ and 2266 Hz), caused by second order distortion. The triplet coupling constant is an average of the two phosphorus-platinum couplings corresponding to the triethylphosphine and bis(diethylamino)phosphino group ($^1J(\text{Pt-P}_{\text{amine}}) = 2414$ Hz, $^1J(\text{Pt-P}_{\text{phenyl}}) = 2119$ Hz; $(2414 + 2119)/2 = 2266$ Hz). It was hoped that the $^{195}\text{Pt}\{^1\text{H}\}$ NMR of the *trans*-isomer would allow the values of each $^1J(\text{Pt-P})$ to be measured directly. However, the strong *trans* coupling between the aminophosphino group and triethylphosphine makes them "appear" the same to the platinum centre. This process can be explained if one simplifies the spin-system from an ABMX to an ABX, i.e. treating the triplets separately by considering only the bis(diethylamino)phosphino group (A), the triethylphosphine (B) and the platinum (X).

The line positions of the X region of an ABX have been shown to be:⁵⁴

$\nu_X - 1/2(J_{AX} + J_{BX})$	line 1
$\nu_X + D_+ - D_-$	line 2
$\nu_X - D_+ + D_-$	line 3
$\nu_X + 1/2(J_{AX} + J_{BX})$	line 4

where

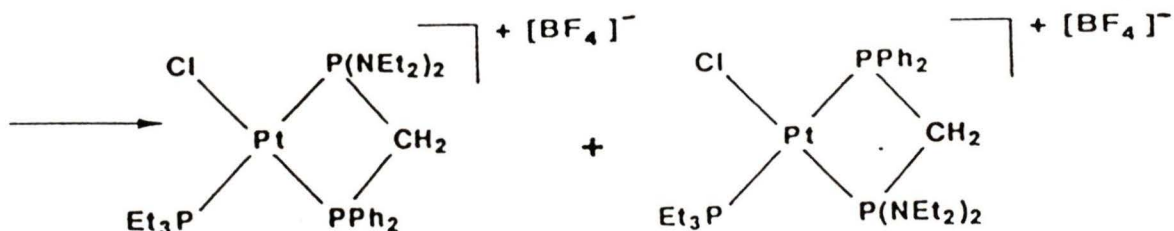
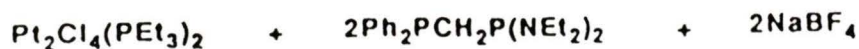
$$2D_+ = \{[(\nu_A - \nu_B) + 1/2(J_{AX} - J_{BX})]^2 + J_{AB}^2\}^{1/2}$$

$$2D_- = \{[(\nu_A - \nu_B) - 1/2(J_{AX} - J_{BX})]^2 + J_{AB}^2\}^{1/2}$$

Using the values derived from the simulation of the $^{31}\text{P}\{^1\text{H}\}$ NMR of $t\text{-}[\text{PtCl}(\text{PEt}_3)\{\text{Ph}_2\text{PCH}_2\text{P}(\text{NEt}_2)_2\text{-}P,P'\}]\text{BF}_4$; $D_- \approx D_+$. This makes line 2 and line 3 equal to ν_X , thus the two central resonances become one under the resolution of the NMR machine (≈ 10 Hz). Also the distance between the centre and outer resonances is shown to be $1/2(J_{AX} + J_{BX})$.

In summary: $[\text{Ph}_2\text{PCH}_2\text{P}(\text{NEt}_2)_2]$ cleaves $[\text{Pt}_2\text{Cl}_2(\mu\text{-Cl})_2(\text{PEt}_3)_2]$ to yield *cis* and *trans* P-P' coordinated chelate complexes, Scheme 3.3, in preference to five-membered P,N coordinated chelate complexes.

Scheme 3.3

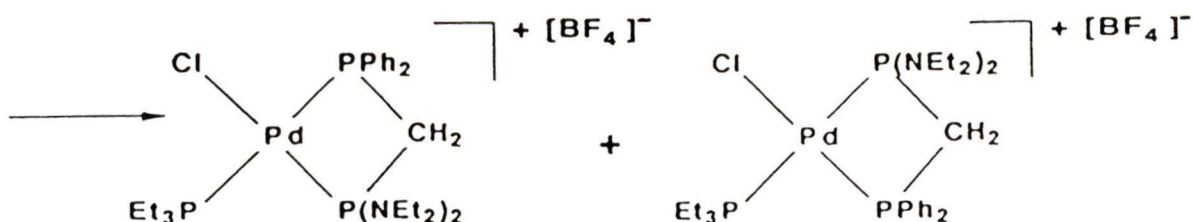


3.3. Reaction of $[\text{Ph}_2\text{PCH}_2\text{P}(\text{NEt}_2)_2]$ and

$[\text{Ph}_2\text{PCH}_2\text{P}(\text{N}(\text{CH}_2\text{CH}_2)\text{CH})_2]$ with $[\text{Pd}_2\text{Cl}_2(\mu\text{-Cl})_2(\text{PEt}_3)_2]$.

Reaction of two equivalents of $[\text{Ph}_2\text{PCH}_2\text{P}(\text{NEt}_2)_2]$ and NaBF_4 with $[\text{Pd}_2\text{Cl}_2(\mu\text{-Cl})_2(\text{PEt}_3)_2]$ generated the *trans*-isomer of $[\text{PdCl}(\text{PEt}_3)(\text{Ph}_2\text{PCH}_2\text{P}(\text{NEt}_2)_2\text{-}P,P')]\text{BF}_4$, which over time, converted to the the *cis*-isomer, Scheme 3.4.

Scheme 3.4



There was initial confusion over this assignment as the $^{31}\text{P}(^1\text{H})$ NMR chemical shifts differed significantly between

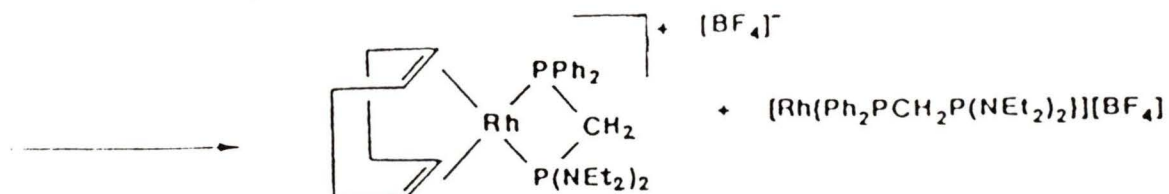
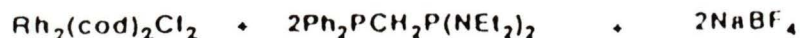
isomers, which was thought to be due to nitrogen-metal interaction. Therefore, the piperidine analogue of $[\text{Ph}_2\text{PCH}_2\text{P}(\text{NEt}_2)_2]$ was synthesized and reacted with $[\text{Pd}_2\text{Cl}(\mu\text{-Cl})_2(\text{PEt}_3)_2]$. It was thought that the bulk of the piperidine groups would reduce the possibility of nitrogen coordination and generate the P,P' coordinated complex for comparison. However, a similar spectrum was obtained, consequently $[\text{PdCl}(\text{PEt}_3)(\text{Ph}_2\text{PCH}_2\text{P}(\text{NEt}_2)_2)]\text{BF}_4$ complex must also be P,P' coordinated.

Again, nitrogen coordination was not observed. Review of the literature shows that the large chemical shift change (17 ppm) between the *cis*- and *trans*-isomers is not unusual for palladium-phosphine complexes.⁵⁵

3.4. Rhodium-Bisphosphine Complexes of $[\text{Ph}_2\text{PCH}_2\text{P}(\text{NEt}_2)_2]$
 Attempts at synthesizing $[\text{Rh}(\text{L-L})(\text{Ph}_2\text{PCH}_2\text{P}(\text{NEt}_2)_2)]\text{BF}_4$ where L-L is a bidentate ligand other than $[\text{Ph}_2\text{PCH}_2\text{P}(\text{NEt}_2)_2]$, in order to probe a different transition-metal triad for nitrogen coordination, were unsuccessful.

Reaction of $[\text{Rh}_2(\mu\text{-Cl})_2(\eta^4\text{-cod})_2]$ with $[\text{Ph}_2\text{PCH}_2\text{P}(\text{NEt}_2)_2]$ generated a mixture of compounds, Scheme 3.5.

Scheme 3.5



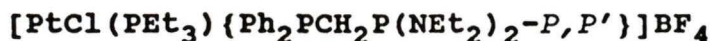
$[\text{Rh}(\text{cod})(\text{Ph}_2\text{PCH}_2\text{P}(\text{NEt}_2)_2\text{-}P,P')]\text{BF}_4$, the desired complex, was formed along with the bisphosphine substituted product $[\text{Rh}(\text{Ph}_2\text{PCH}_2\text{P}(\text{NEt}_2)_2\text{-}P,P')_2]\text{BF}_4$. Separation through crystallization were not successful. $[\text{Rh}(\text{Ph}_2\text{PCH}_2\text{P}(\text{NEt}_2)_2\text{-}P,P')_2]\text{BF}_4$ was not a desired product because of its complex $^{31}\text{P}\{^1\text{H}\}$ NMR pattern (AA'MM'X), and the isomeric forms possible (head-to-head and head-to-tail) making absolute identification difficult.

Attempts at synthesizing an analogous complex to that described above using $[\text{Rh}(\text{cod})(\text{bipyridyl})]\text{BF}_4$ (displacement of the cod and retention of the bipyridyl) were also unsuccessful. $[\text{Rh}(\text{Ph}_2\text{PCH}_2\text{P}(\text{NEt}_2)_2\text{-}P,P')_2]\text{BF}_4$ was again generated, together with the desired product, $[\text{Rh}(\text{bipy})(\text{Ph}_2\text{PCH}_2\text{-}P(\text{NEt}_2)_2\text{-}P,P')]\text{BF}_4$.

However, sufficient information was available from the $^{31}\text{P}\{^1\text{H}\}$ NMR of the mixtures to discount the possibility of rhodium-nitrogen coordination, as the rhodium-phosphorus

coupling constants ($J(\text{Rh-P}[\text{NEt}_2]_2) = 173$ and 162 Hz) are typical for single bond rhodium-phosphorus complexes (80 to 151 Hz).⁵⁵ Also the move to lower frequency of the phosphorus chemical shifts is indicative of the formation of a four-membered P,P' coordinated ring complex.

3.5. Discussion on the Crystal Structure of *cis*-



Reaction of $[\text{Ph}_2\text{PCH}_2\text{P}(\text{NEt}_2)_2]$ with $[\text{Pt}_2(\mu\text{-Cl})_2\text{Cl}_2(\text{PET}_3)_2]$, $[\text{Rh}_2(\mu\text{-Cl})_2(\eta^4\text{-cod})_2]$ and $[\text{Pd}_2(\mu\text{-Cl})_2\text{Cl}_2(\text{PET}_3)_2]$ to form platinum, rhodium and palladium complexes respectively, only generated P,P' coordinated complexes, which poses the question as to a reason for the lack of nucleophilicity of the nitrogen lone pair.

It is proposed that the lone pair is involved in an "extra bond" with the phosphorus atom, that is, a $p_\pi\text{-}d_\pi$ bonding interaction between the low lying d -orbitals on the phosphorus and the p -orbital containing the nitrogen lone-pair, Figure 3.5.

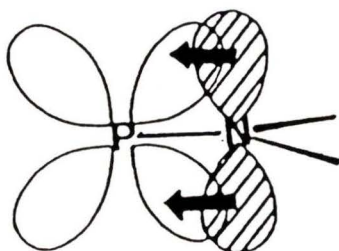


Figure 3.5. A diagrammatical representation of a $p_\pi\text{-}d_\pi$ bonding interaction between phosphorus and nitrogen atoms.

$p_{\pi}-d_{\pi}$ bonding interactions have been proposed many times, and they are the generally accepted explanations for abnormally short P-N, P=O and P=S bonds, and the restricted rotation often found about the P-N bond in aminophosphines. However there has been some doubt raised as to the validity of a $p_{\pi}-d_{\pi}$ interaction between phosphorus and nitrogen atoms. Most of the contentious arguments concern the energy difference between the nitrogen-2p and phosphorus-3d orbitals, and the expected diffuse character of the phosphorus-3d orbital in comparison to the nitrogen-2p orbital.¹⁷ That is, the orbitals may not be similar enough in energy and size to allow for significant overlap.

Evidence for $p_{\pi}-d_{\pi}$ interaction in the present work was found in the x-ray crystal structure of *cis*-[PtCl(PEt₃)(Ph₂PCH₂-P(NEt₂)₂-P,P')]BF₄, Figure 3.6. Pertinent data concerning the structure is given in Tables 3.7 - 3.12. The expected length of a phosphorus-nitrogen single bond is 1.80 Å, as calculated from the sum of the covalent radii.⁵⁶ Also the phosphoramidate ion, [H₃N-PO₃Na], is reported to have a phosphorus-nitrogen bond length of 1.77 - 1.79 Å.^{57,58} The phosphorus-nitrogen bond lengths in *cis*-[PtCl(PEt₃)(Ph₂PCH₂-P(NEt₂)₂-P,P')]BF₄ are 1.580 and 1.584 Å; significantly shorter than expected for phosphorus-nitrogen single bonds. If the length of a typical phosphorus-nitrogen double bond is taken to be 1.57 Å (as found in [Ph₃P=N-C₆H₄Br])⁵⁹ a

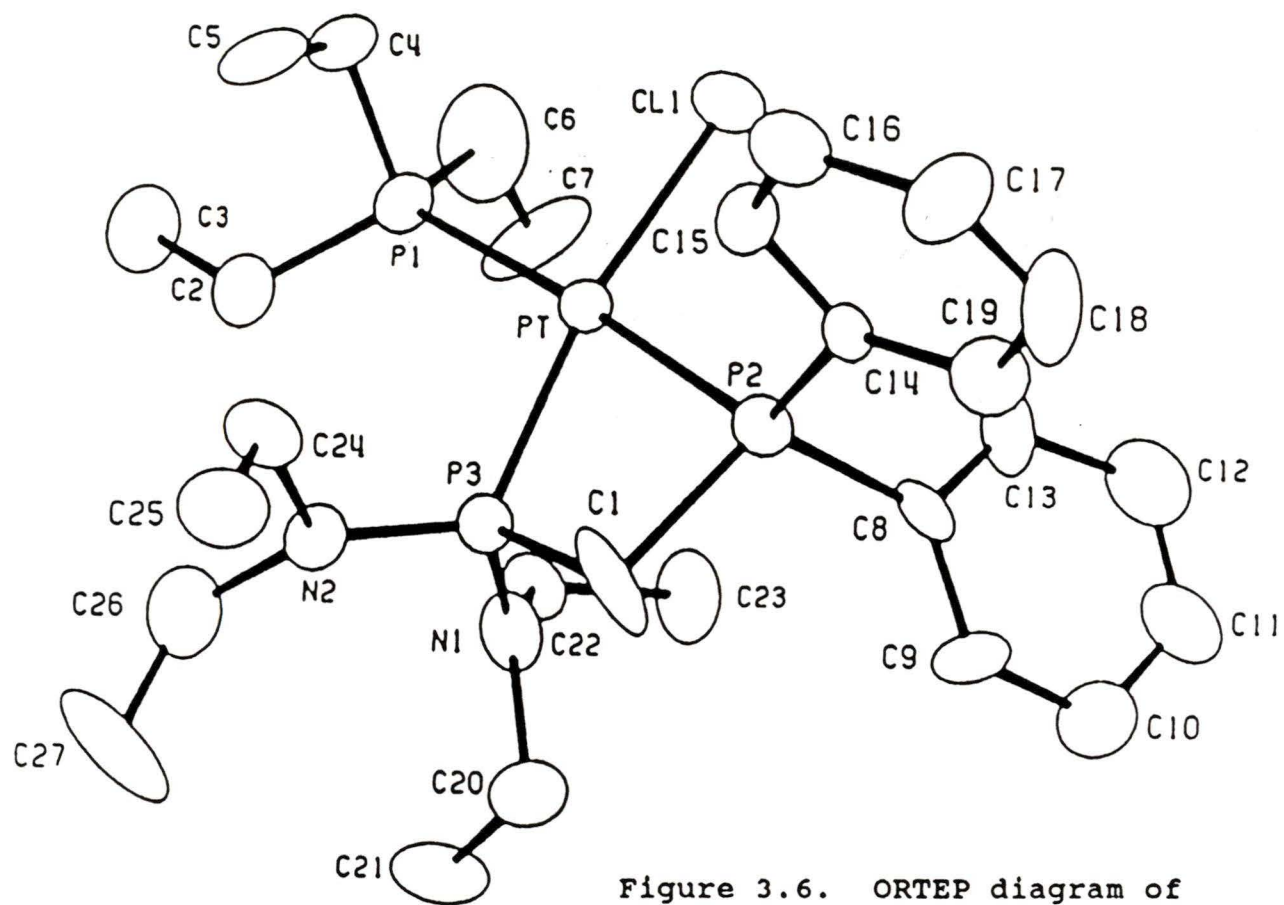


Figure 3.6. ORTEP diagram of
 $[\text{Pt}(\text{PEt}_3)\text{Cl}(\text{Ph}_2\text{PCH}_2\text{P}(\text{NEt}_2)_2\text{-P,P}')]\text{BF}_4$

significant amount of double bond character in the P-N bonds of *cis*-[PtCl(PEt₃)(Ph₂PCH₂P(NEt₂)₂-*P,P'*)]BF₄ can be implied.

The geometry about each nitrogen is expected to deviate from tetrahedral towards trigonal planar, depending on the extent of $p_{\pi}-d_{\pi}$ interaction. The tendency towards a trigonal planar configuration is shown in Figure 3.7. Nitrogens N1 and N2 of the amines are 0.052 and 0.128 Å above their respective planes, C20-C22-P3 and C24-C26-P3: a definite tendency towards trigonal planarity. Also, the sums of the angles around each nitrogen (N1 and N2) are 359.6 and 358 degrees respectively compared with the expected 360 degrees for a perfectly planar arrangement.

Cruickshank⁶⁰ assumed that because of the approximately tetrahedral environment of phosphorus(III), the two equi-energetic *d*-orbitals, $d_{x^2-y^2}$ and d_{z^2} , are of much more importance than the remaining three. He stated that for non-planar rings ($N_nP_n(NMe_2)_{2n}$) linear combinations of these two orbitals may give two hybrids at phosphorus, which are strongly bonding and which overlap equally well with orbitals of the neighbouring nitrogens. In the present case, however, the planes C20-C22-P3 and C24-C26-P3, shown in Figure 3.8, are nearly at right angles to one another (i.e. the two nitrogen lone-pairs are orthogonal to one another). This implies that the two hybrids at phosphorus are essen-

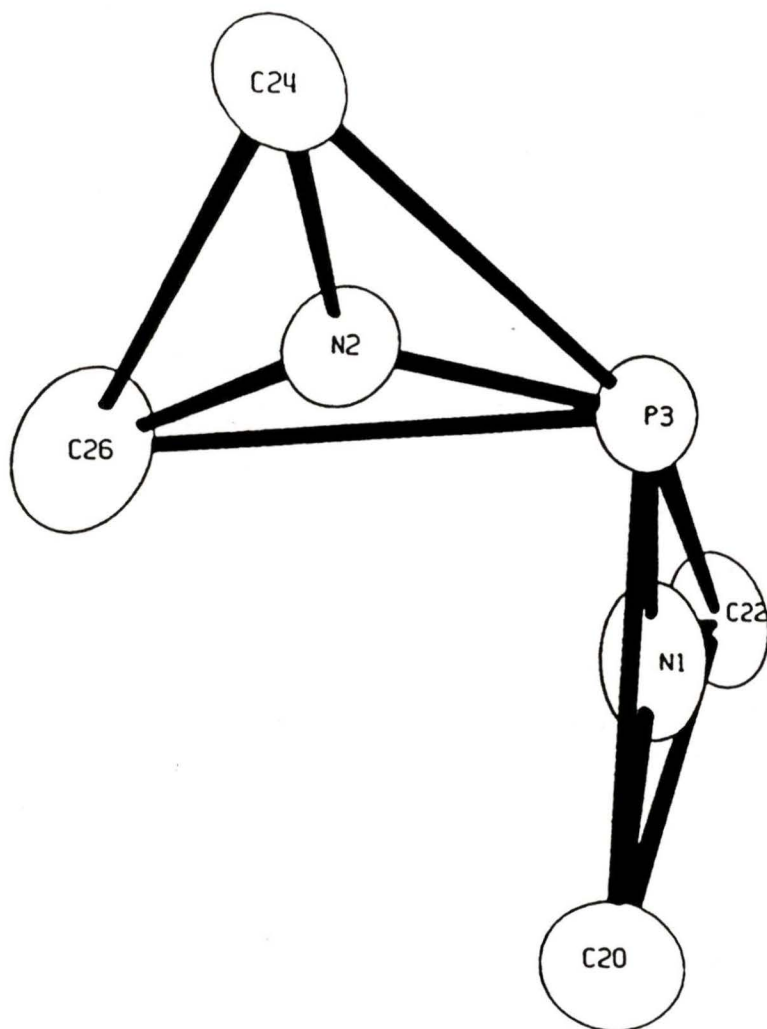


Figure 3.7. A selected ORTEP view of the bis(diethylamino)phosphino group in $[\text{Pt}(\text{PEt}_3)\text{Cl}(\text{Ph}_2\text{PCH}_2\text{P}(\text{NEt}_2)_2\text{-}P,P')]\text{BF}_4$ showing the planar arrangement of substituents around the nitrogen atoms

tially pure d_{z^2} and $d_{x^2-y^2}$, as in the phosphoryl linkage of $[\text{PO}_4]^-$ for example, Figure 3.8.

It is not expected that coordination to the platinum centre would weaken the $d_{\pi}-p_{\pi}$ interaction, but rather strengthen it. The phosphine will form a dative covalent bond with platinum through its lone-pair of electrons. However, π back donation from the platinum to the phosphorus atom will be into the d_{xz} orbital, and not into the d_{z^2} , $d_{x^2-y^2}$ mutually perpendicular ($d_{\pi}-p_{\pi}$) orbitals. So the increase in effective positive charge on the phosphorus from σ donation of its lone-pair will lower the d_{z^2} and $d_{x^2-y^2}$ orbital energies and improve the $d_{\pi}-p_{\pi}$ interactions.

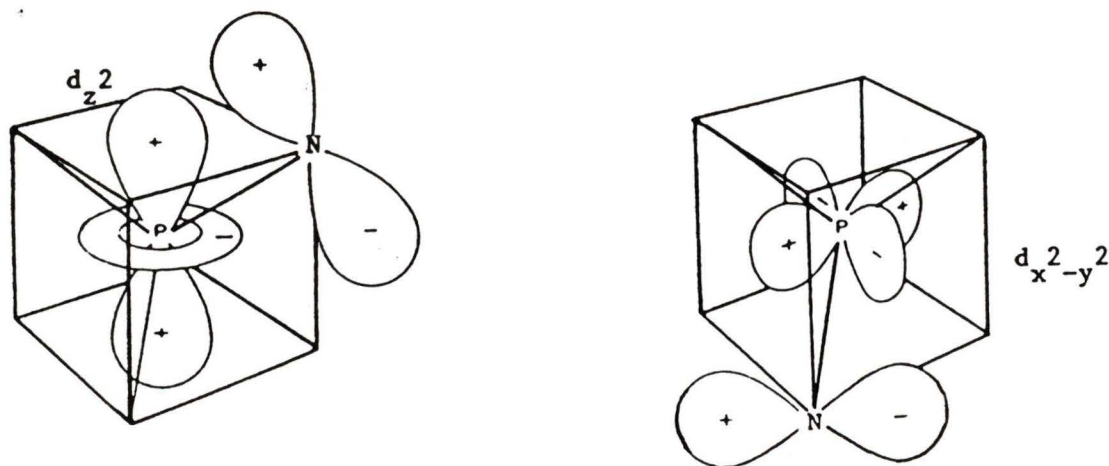


Figure 3.8. The orbitals used in the $p_{\pi}-d_{\pi}$ interaction present in the $\text{P}(\text{NEt}_2)_2$ group.

Therefore when the above discussion is taken into account, it is not surprising that the nitrogen atoms do not coor-

dinate. These results imply that the stabilization gained by forming a five-membered metal chelate complex compared to a four-membered is not enough to off-set the breaking of one partial ($p_{\pi}-d_{\pi}$) phosphorus-nitrogen bond.

3.6. Phosphorus-Nitrogen Bond Cleavage in Coordinated

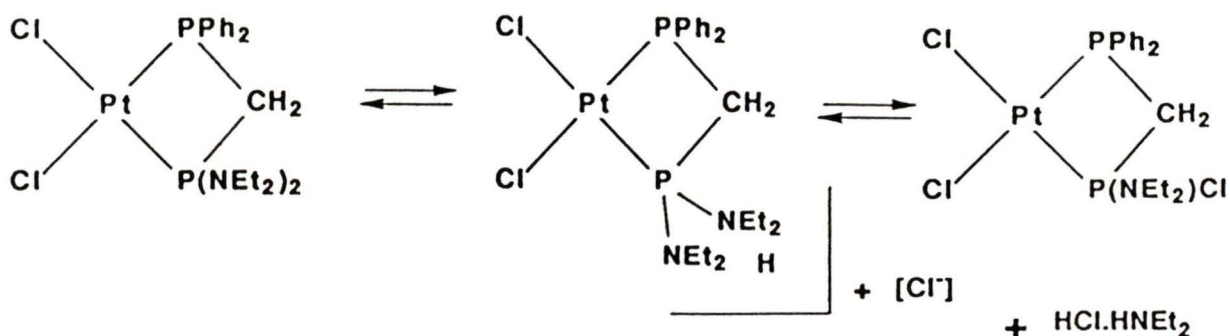
$[\text{Ph}_2\text{PCH}_2\text{P}(\text{NEt}_2)_2]$ and $[\text{Ph}_2\text{PCH}_2\text{P}(\text{NEt}_2)\text{Ph}]$

A second aim of the aminophosphine chemistry was to study phosphorus-nitrogen bond cleavage of the coordinated ligand. The complexes $[\text{PtCl}(\text{PEt}_3)\{\text{Ph}_2\text{PCH}_2\text{P}(\text{NEt}_2)_2\text{-P,P'}\}]\text{BF}_4$ and $[\text{PdCl}(\text{PEt}_3)\{\text{Ph}_2\text{PCH}_2\text{P}(\text{NEt}_2)_2\text{-P,P'}\}]\text{BF}_4$ were not suitable for such a study because of their complex NMR (second order), possibility of isomers, and the difficulty in obtaining them as pure solids. $[\text{PtCl}_2\{\text{Ph}_2\text{PCH}_2\text{P}(\text{NEt}_2)_2\text{-P,P'}\}]$ and $[\text{PdCl}_2\{\text{Ph}_2\text{PCH}_2\text{P}(\text{NEt}_2)_2\text{-P,P'}\}]$ were therefore synthesized by reaction of one equivalent of $[\text{Ph}_2\text{PCH}_2\text{P}(\text{NEt}_2)_2]$ with $[\text{PtCl}_2(\text{cod})]$ and PdCl_2 respectively. $^{31}\text{P}\{^1\text{H}\}$ NMR spectra of both products were simple doublets with no evidence for nitrogen-metal coordination.

3.6.1. Reaction of $[\text{PtCl}_2\{\text{Ph}_2\text{PCH}_2\text{P}(\text{NEt}_2)_2\text{-P,P'}\}]$ with Hydrogen Chloride

The result of reacting a solution of $[\text{PtCl}_2\{\text{Ph}_2\text{PCH}_2\text{P}(\text{NEt}_2)_2\text{-P,P'}\}]$ with hydrogen chloride gas are shown in Table 3.2 and Scheme 3.6.

Scheme 3.6



Arguments in favour of the proposed reaction Scheme are as follows:

1) All reactivity involves the bis(diethylamino)-phosphino group, as this is the only resonance to undergo an appreciable chemical shift change: $\Delta\delta P_{\text{amine}} = +18.6$ ppm; $\Delta\delta P_{\text{phenyl}} = -1.4$ ppm.

2) Comparing the final product with the precursor, $J(\text{Pt}-P_{\text{amine}})$ increases from 3656 Hz to 4056 Hz. This is as expected. When the electron-donating amino group is replaced by the electron-withdrawing chlorine the effective positive charge on the phosphorus will increase. The 3s orbital will then drop to lower energy and contract around the phosphorus nucleus. Increased s-orbital character around the phosphorus will increase $^1J(\text{Pt}-\text{P})$ (as for a Fermi contact argument).

Further evidence to this effect is seen with earlier work carried out in this group with $[\text{PtCl}_2\text{P}(\text{NR}_2)_{3-n}\text{Cl}_n]$ where n

= 0 or 1 and R = ethyl or methyl; Table 3.5.⁶¹ Comparing the three pairs as for the present discussion (i.e. Pt-P(NEt₂)₃ and Pt-P(NEt₂)₂Cl) there is always an increase in ¹J(Pt-P_{amine}) on replacing an amine with a chlorine.

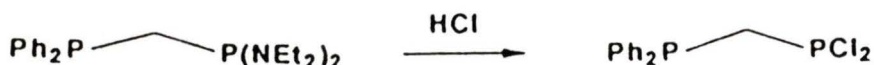
3) Only one phosphorus-nitrogen bond is cleaved in the reaction. It is expected that the increase in effective positive charge on the phosphorus associated with replacement of the amino group with chlorine not only lowers the 3s-orbital energy, but also the d_{x²-y²} and d_{z²} orbitals. This will lead to a better overlap with the nitrogen p-orbitals, so strengthening the remaining phosphorus-nitrogen bond and reducing its reactivity. Also the ³¹P{¹H} chemical shift of the aminophosphine, after reaction, is not deshielded enough for it to be a dichlorophosphine.

3.6.2. Reaction of [PtCl₂{Ph₂PCH₂P(NEt₂)Ph-P,P'}] with Hydrogen Chloride

Rather than reacting [PtCl₂{Ph₂PCH₂P(NEt₂)Cl-P,P'}] with an alkyllithium reagent to form [PtCl₂{Ph₂PCH₂P(NEt₂)R-P,P'}] followed by further reaction with hydrogen chloride in an attempt to cleave off the second amino group, the complex [PtCl₂{Ph₂PCH₂P(NEt₂)Ph-P,P'}] was synthesized and reacted with hydrogen chloride; and Scheme 3.7.

comparison purposes, $[\text{Ph}_2\text{PCH}_2\text{P}(\text{NEt}_2)_2]$ was reacted with hydrogen chloride; Scheme 3.8. Among other products, $[\text{Ph}_2\text{P-CH}_2\text{PCl}_2]$ was formed.

Scheme 3.8



Reaction of $[\text{Ph}_2\text{PCH}_2\text{PCl}_2]$ with $[\text{PtCl}_2(\text{cod})]$, however, did not generate the desired complex $[\text{PtCl}_2(\text{Ph}_2\text{PCH}_2\text{PCl}_2\text{-P,P'})]$ which should have had a simple $^{31}\text{P}\{^1\text{H}\}$ NMR pattern similar to that for $[\text{PtCl}_2(\text{Ph}_2\text{PCH}_2\text{P}(\text{NEt}_2)_2\text{-P,P'})]$, instead the $^{31}\text{P}\{^1\text{H}\}$ NMR was unidentifiable. Prolonged reaction of $[\text{PtCl}_2(\text{Ph}_2\text{PCH}_2\text{P}(\text{NEt}_2)_2\text{-P,P'})]$ with hydrogen chloride (one week) yielded an extremely viscous oil, the $^{31}\text{P}\{^1\text{H}\}$ NMR of which showed two broad resonances, each with broad platinum satellites ($\delta = -104.5$ ppm, $J(\text{Pt-P}) = 3946$ Hz; $\delta = 188.8$ ppm, $J(\text{Pt-P}) = 3237$ Hz). This may be $[\text{PtCl}_2(\text{Ph}_2\text{PCH}_2\text{PCl}_2\text{-P,P'})]$, although a hydrolysis product can not be discounted for such a long reaction.

In summary: It is possible to selectively cleave the amine groups off the ligand $[\text{Ph}_2\text{PCH}_2\text{P}(\text{NEt}_2)_2]$ by first coordinating to a metal. Corresponding reaction of the free ligand could not be controlled as well, such that the reaction of $[\text{Ph}_2\text{PCH}_2\text{P}(\text{NEt}_2)_2]$ with hydrogen chloride only formed $[\text{Ph}_2\text{P-CH}_2\text{PCl}_2]$; the mono-cleaved product was not observed. This

may indicate a possibility of observing nitrogen coordination as P-N cleavage by acids must go via a protonated-nitrogen intermediate else $[\text{PtCl}_2(\text{Ph}_2\text{PCH}_2\text{P}(\text{NEt}_2)_2\text{-P,P}')]]$ would not have acid cleaved.

An interesting observation in the ^1H NMR of $[\text{PtCl}_2(\text{Ph}_2\text{PCH}_2\text{-P}(\text{NEt}_2)\text{Ph-P,P}')]]$ (Figure 3.9) which will be useful in the next section, is the asymmetry seen in the methylene protons of the ligand (P- CH_2 -P). Making one of the phosphorus atoms chiral (in this case the aminophosphine) places the two protons in chemically different environments (Figure 3.10), creating an ABX₂ spectrum. The magnitude of the coupling between the two hydrogens of 16 Hz is reasonable for geminal hydrogens.

3.7. Attempts at Promoting Nitrogen Coordination on the complex $[\text{PtCl}_2(\text{Ph}_2\text{CH}_2\text{P}(\text{NEt}_2)_2\text{-P,P}')]]$

Reaction of $[\text{Pt}_2\text{Cl}_2(\mu\text{-Cl})_2(\text{PEt}_3)_2]$ with $[\text{PtCl}_2(\text{Ph}_2\text{PCH}_2\text{-P}(\text{NEt}_2)_2\text{-P,P}')]]$ in an effort to get the Et₂N-P-NEt₂ group to cleave open the dimer was unsuccessful. The nitrogen lone pairs appear unable to break open the dimer.

Reaction of $[\text{PtCl}_2(\text{Ph}_2\text{PCH}_2\text{P}(\text{NEt}_2)_2\text{-P,P}')]]$ with $[\text{Rh}(\text{cod})\text{-}(\text{MeCN})_2]\text{BF}_4$, however, was successful. It was hoped that the amines would displace the labile acetonitrile ligands with the driving force of reaction being the formation of a chelate. Although x-ray structural determination was not at

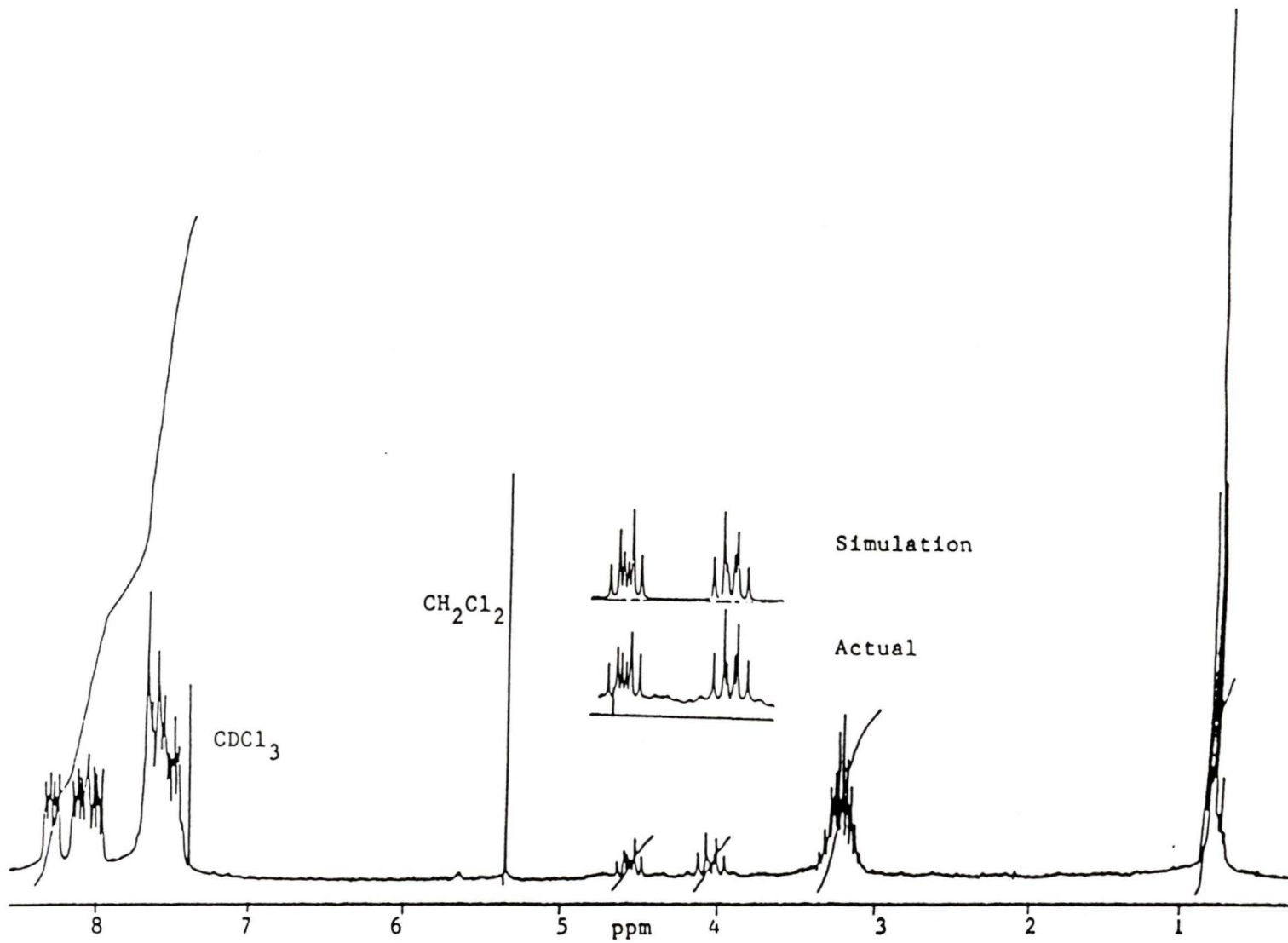


Figure 3.9. ^1H NMR of $[\text{PtCl}_2(\text{Ph}_2\text{PCH}_2\text{P}(\text{NEt}_2)\text{Ph-P,P}')]$

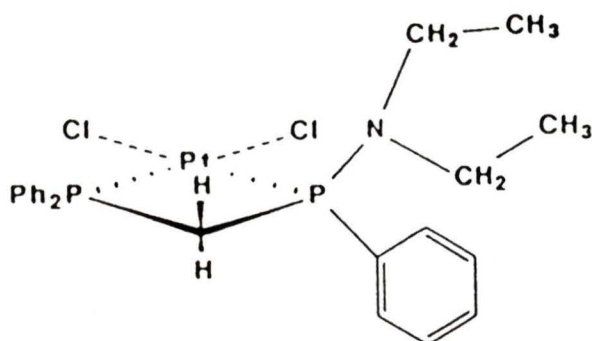


Figure 3.10. $[\text{PtCl}_2(\text{Ph}_2\text{PCH}_2\text{P}(\text{NEt}_2)\text{Ph-}P,P')]$ showing the two chemically different environments that the P-CH₂-P hydrogens reside.

tempted, the ^1H and $^{13}\text{C}\{^1\text{H}\}$ NMR indicated the formation of the metal dimer shown in Figure 3.11.

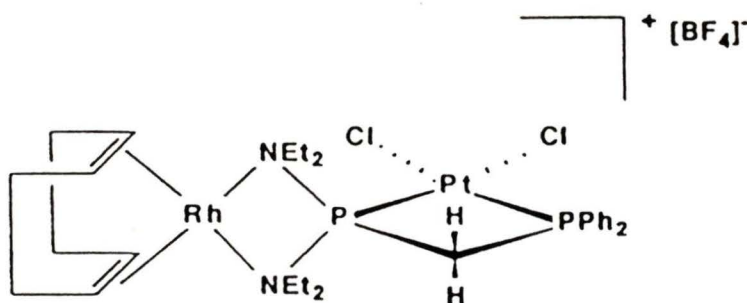
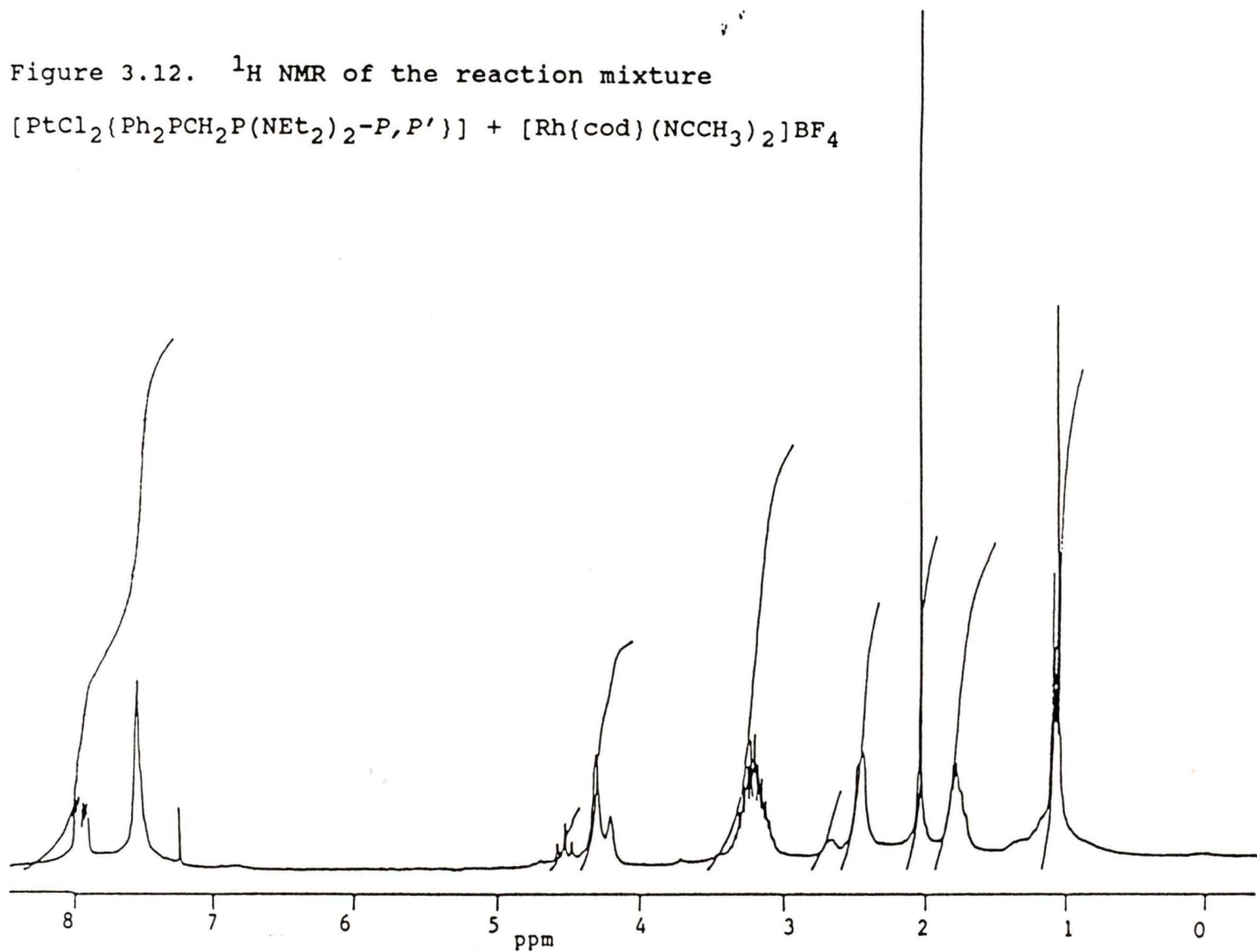
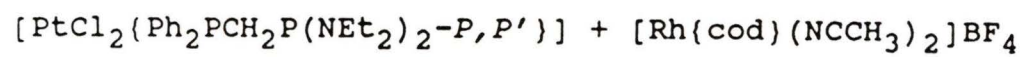


Figure 3.11. $[\text{PtCl}_2(\text{Ph}_2\text{PCH}_2\text{P}(\text{NEt}_2)_2\text{-}P,P')\{N,N\text{-Rh}(\text{cod})\}]\text{BF}_4$

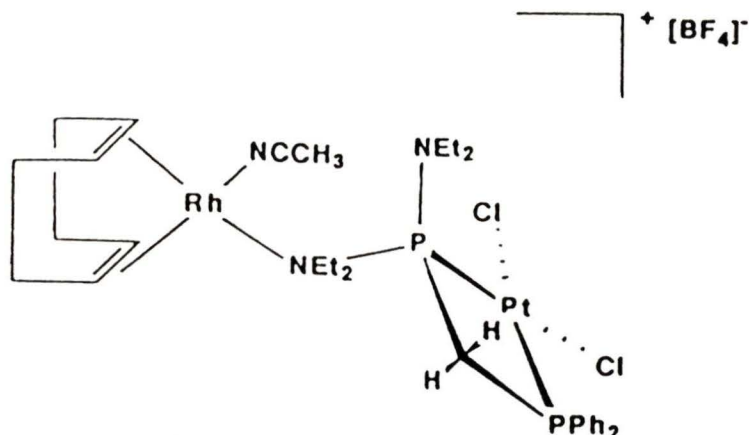
Firstly, the ^1H NMR of the reaction mixture, Figure 3.12, showed the liberation of acetonitrile, with a free acetonitrile resonance at 2.04 ppm. Coordinated acetonitrile was not observed. Upon work-up and leaving under reduced pressure for several hours the free acetonitrile resonance

Figure 3.12. ^1H NMR of the reaction mixture



disappeared.

If only one acetonitrile was displaced generating the complex



the aminophosphine phosphorus atom would be chiral, as in the complex $[\text{PtCl}_2(\text{Ph}_2\text{PCH}_2\text{P}(\text{NEt}_2)\text{Ph}-P,P')]$. The chirality of the aminophosphine phosphorus atom in $[\text{PtCl}_2(\text{Ph}_2\text{PCH}_2\text{-P}(\text{NEt}_2)\text{Ph}-P,P')]$ was reflected in the proton resonances of the P-CH₂-P group. The ¹H NMR of the present compound, however, showed only a triplet at 4.53 ppm signifying non-chirality at the phosphorus. Further evidence for the proposed structure is seen in the asymmetry of the cod resonances due to the lack of a plane of symmetry cutting the cod ligand (i.e. that plane containing the atoms; Rh-N-N-P), Figure 3.12.

An ideal NMR probe to verify the N,N bonded dimer would be nitrogen-15 NMR. One would expect the nitrogen nuclei to show coupling to the rhodium and both phosphorus nuclei generating a doublet of doublet of doublets. If only one of

the nitrogen atoms was coordinated, a similar set of resonances would be expected for the coordinated nitrogen and a doublet of doublets for the uncoordinated nitrogen. The coordinated acetonitrile would also be observed as a doublet. Nitrogen J couplings are also particularly valuable in structure determinations because of their sensitivity to the presence and orientation of the nitrogen lone-pair.

Because of the low natural abundance (0.37%), low sensitivity (0.101 relative to ^1H at constant field), relaxation problems and negative NOE (γ being small and negative at $-2.7 \times 10^7 \text{ rad s}^{-1} \text{ T}^{-1}$), working with natural abundance nitrogen-15 NMR presents various problems, especially with the signal to noise ratio. A nitrogen-15 labeled sample would have been extremely expensive to prepare owing to the many steps involved in the complex synthesis and the waste of amine during the chloroaminophosphine synthesis, Scheme 2.5.

The sensitivity of natural abundance nitrogen-15 NMR can, however, be improved by the use of higher magnetic fields, wider-bore spectrometers and proton decoupling. Pulse sequences, which transfer polarization (magnetization) from a more sensitive coupled nucleus, usually the proton, can also be used. Pulse sequence methods can produce some of the most dramatic enhancements.⁶⁵ The enhancement is a product of the ratio $(\gamma^{1\text{H}}/\gamma^{15\text{N}})$ and a factor owing to the ability

to pulse at a rate determined by the fast proton relaxation. For slowly relaxing nitrogens the enhancement can be a hundred-fold or more. The method used here was DEPT (Distortionless Enhancement by Polarization Transfer).

For comparison purposes the $^{15}\text{N}\{^1\text{H}\}$ NMR of the free ligand $[\text{Ph}_2\text{PCH}_2\text{P}(\text{NEt}_2)_2]$, the precursor complex $[\text{PtCl}_2\{\text{Ph}_2\text{PCH}_2\text{P}(\text{NEt}_2)_2\text{-P,P'}\}]$ then the bimetallic complex $[\text{PtCl}_2\{\text{Ph}_2\text{PCH}_2\text{P}(\text{NEt}_2)_2\text{-P,P'}\}\{N,N\text{-Rh(cod)}\}]\text{BF}_4$ were to be run.

The $^{15}\text{N}\{^1\text{H}\}$ NMR of the free ligand is shown in Figure 3.13. As expected the amino group appears as a doublet of doublets through coupling to both phosphorus nuclei. The magnitude of the single bond phosphorus-nitrogen coupling of 75 Hz is similar to that found for $\text{P}(\text{NMe}_2)_3$ at 59.1 Hz.⁴⁰ The phosphorus-nitrogen three bond coupling is then the 4 Hz splitting. The position of the amine resonance at 317.40 ppm relative to external $\text{CD}_3^{15}\text{NO}_2$ falls within the range normally expected for a phosphorus-bound nitrogen atom.⁶⁵

An interesting extension to this study would have been to observe the change in $J(\text{P-N})$ upon coordinating the bisphosphine to platinum as in $[\text{PtCl}_2\{\text{Ph}_2\text{PCH}_2\text{P}(\text{NEt}_2)_2\text{-P,P'}\}]$. However it was found impossible to generate an $^{15}\text{N}\{^1\text{H}\}$ NMR of $[\text{PtCl}_2\{\text{Ph}_2\text{PCH}_2\text{P}(\text{NEt}_2)_2\text{-P,P'}\}]$. The problem was not the quantity of complex that could be generated but in obtaining a concentrated sample. Continuation to the bimetallic che-

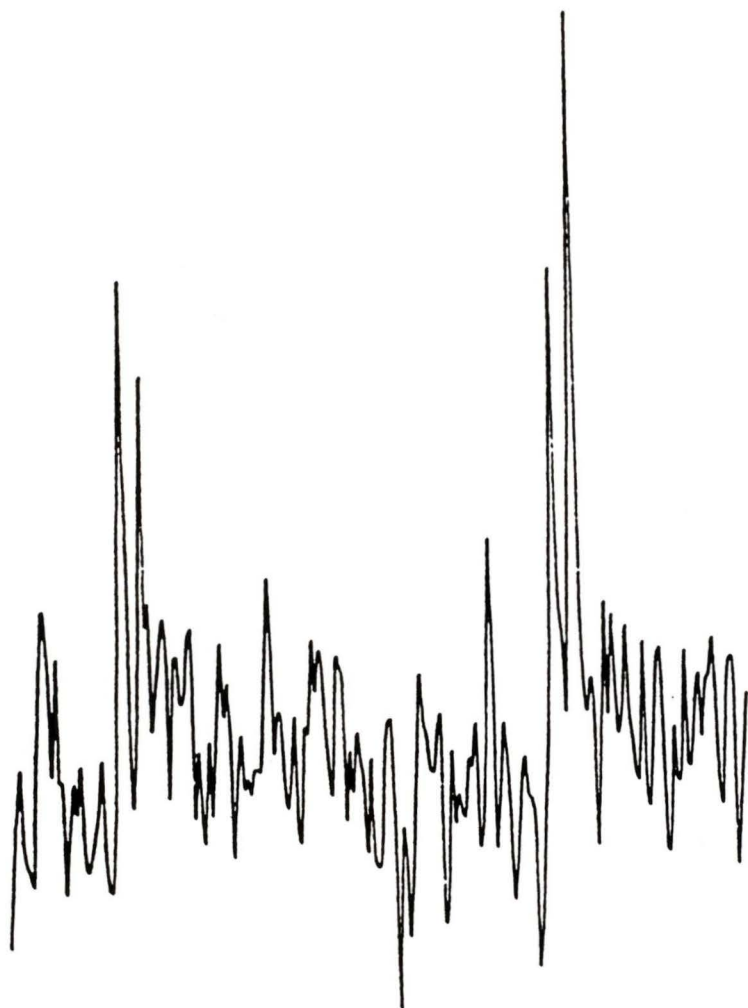


Figure 3.13. Natural abundance $^{15}\text{N}(^1\text{H})$ NMR of
[Ph₂PCH₂P(NEt₂)₂]

late was then deemed unnecessary as the complex would probably degrade in the time for a reasonable signal to noise ratio to be established. Thus the only options remaining in order to continue such a study would be to use ^{15}N enriched samples or maybe a higher field NMR spectrometer. The sensitivity and solubility problems discussed above probably account for the lack of natural abundance nitrogen-15 NMR studies of nitrogen containing complexes in the literature.

The complex $[\text{PtCl}_2\{\text{Ph}_2\text{PCH}_2\text{P}(\text{NEt}_2)_2\text{-P,P'}\}\{\text{N,N-Rh}(\text{cod})\}]\text{BF}_4$ is interesting in view of earlier results where the nitrogen atoms could not be forced to coordinate. As was mentioned, compounds containing quarternary phosphorus-bound nitrogen atoms are scarce. The few examples are usually BH_3 adducts of the rigid cyclic tris(dialkylamino)phosphines,^{66,64} molybdenum complexes of the cyclamphosporanide ligand (which is not strictly of the type discussed)⁶⁸ and the protonated cyclamphosphoranide.^{63,64}

In summary the bisphosphine $[\text{Ph}_2\text{PCH}_2\text{P}(\text{NEt}_2)_2]$ prefers to coordinate to platinum group metals (Pt, Rh, Pd) so as to form four-membered P,P' coordinated ring complexes instead of the expected more stable five-membered P,N bonded ring complexes. The absence of any nitrogen coordinated complexes was rationalized by extensive $p_\pi\text{-}d_\pi$ interaction between the nitrogen lone pair of electrons and low lying $3d$ orbitals on the phosphorus atom, as shown by the shorter

than expected phosphorus-nitrogen bond lengths in *cis*-
 $[\text{PtCl}(\text{PEt}_3)\{\text{Ph}_2\text{PCH}_2\text{P}(\text{NEt}_2)_2\text{-P,P}'\}]\text{BF}_4$ of 1.58 Å.

Nitrogen coordination was, however, promoted by first coordinating the phosphorus atoms to a metal as in $[\text{PtCl}_2\{\text{Ph}_2\text{PCH}_2\text{P}(\text{NEt}_2)_2\text{-P,P}'\}]$ then reacting the complex with the labile metal complex $[\text{Rh}(\text{cod})(\text{NCMe})_2]\text{BF}_4$ to form $[\text{PtCl}_2\{\text{Ph}_2\text{PCH}_2\text{P}(\text{NEt}_2)_2\text{-P,P}'\}(\text{N,N-Rh}(\text{cod}))]\text{BF}_4$. The driving force of reaction being the formation of another chelate complex. The energy liberated in forming the N,N chelate ring must be enough to offset the destruction of the $p_\pi\text{-}d_\pi$ interaction. Whereas the energy difference between a four-membered P,P' coordinated complex compared to a five-membered P,N coordinated complex is not enough to break the $p_\pi\text{-}d_\pi$ interaction. If the energy of the $p_\pi\text{-}d_\pi$ interaction is about 10 - 15 kJ/mol as determined from dynamic ^1H NMR experiments,⁶⁹ the difference in energy between the P,P' and P,N bonded forms is less than 10 kJ/mol and the energy of N,N chelate formation is greater than 15 kJ/mol.

TABLE 3.1. ^{31}P NMR Data for Cationic Complexes of the Bisphosphine $[\text{Ph}_2\text{PCH}_2\text{P}(\text{NR}_2)_2]$

Compound ^a	$\delta\text{P}_A^{\text{b,c,d}}$	$\delta\text{P}_B^{\text{b,e,d}}$	$\delta\text{P}_C^{\text{b,f,d}}$	$^2J_{(\text{P}_A\text{P}_B)}^{\text{g}}$	$^2J_{(\text{P}_A\text{P}_C)}^{\text{g}}$	$^2J_{(\text{P}_B\text{P}_C)}^{\text{g}}$
c- $[\text{Pt}(\text{PET}_3)\text{Cl}(\text{PPN}_2)]^{+\text{h}}$	-130.91 (3806)	-182.04 (2150)	-119.27 (2385)	59	0	381
t- $[\text{Pt}(\text{PET}_3)\text{Cl}(\text{PPN}_2)]^{+\text{h}}$	-124.34 (2414)	-183.01 (3188)	-124.57 (2119)	78	600	10
c- $[\text{Pd}(\text{PET}_3)\text{Cl}(\text{PPN}_2)]^{+\text{i}}$	-128.68	-183.56	-120.31	73	-31	387
t- $[\text{Pd}(\text{PET}_3)\text{Cl}(\text{PPN}_2)]^{+\text{i}}$	-128.04	-166.13	-121.74	107	572	-38
c- $[\text{Pd}(\text{PET}_3)\text{Cl}(\text{PPN}'_2)]^{+\text{i}}$	-107.57	-182.11	-114.67	80	-26	422
t- $[\text{Pd}(\text{PET}_3)\text{Cl}(\text{PPN}'_2)]^{+\text{i}}$	-128.79	-164.68	-120.95	104	571	-28
$[\text{Rh}(\text{cod})\text{PPN}_2]^{+\text{i}}$	-68.34 (185)	-144.44 (173)	-----	115	---	---
$[\text{Rh}(\text{bipy})\text{PPN}_2]^{+\text{i}}$	-79.81 (178)	-146.39 (162)	-----	122	---	---
$[\text{PtCl}_2\text{PPN}_2(\text{Rh}(\text{cod}))]^{+\text{i}}$	-158.09 (3732)	-192.80 (3443)	-----	78	---	---

Notes:

^a $\text{PPN}_2 = \text{Ph}_2\text{PCH}_2\text{P}(\text{NET}_2)_2$; $\text{PPN}'_2 = \text{Ph}_2\text{PCH}_2\text{P}(\text{N}(\text{CH}_2\text{CH}_2)_2\text{CH})_2$;
 cod = 1,5 - cyclooctadiene; bipy = bipyridyl;

tetrafluoroborate counter ion.

^b chemical shift in ppm relative to TMP

^c aminophosphino

^d {} coupling to metal in Hz

^e diphenylphosphino

^f triethylphosphine

^g coupling between phosphines in Hz

^h CD_2Cl_2

ⁱ CDCl_3

TABLE 3.2. ^{31}P NMR Data for Neutral Complexes of the Bisphosphine $[\text{Ph}_2\text{PCH}_2\text{PRR}']$ and the HCl Reaction Products.

Compound ^a	$\delta\text{P}_A^{\text{b,c,d}}$	$\delta\text{P}_B^{\text{b,e,d}}$	$^2J_{(\text{P}_A\text{P}_B)}^{\text{f}}$
$[\text{PdCl}_2(\text{PPN}_2)]^{\text{g}}$	-128.69	-180.86	71
$[\text{PtCl}_2(\text{PPN}_2)]^{\text{h}}$	-147.62 (3656)	-195.79 (3393)	72
$[\text{PtCl}_2(\text{PPNPh})]^{\text{i}}$	-164.47 (3343)	-201.91 (3198)	67
$[\text{PtCl}_2(\text{PPN}_2)] [\text{HCl}]^{\text{i}}$	-129.00 (3839)	-198.52 (3093)	69
$[\text{PtCl}_2(\text{PPNCl})]^{\text{i}}$	-135.32 (4056)	-197.22 (3062)	71
$[\text{PtCl}_2(\text{PPNPh})] [\text{HCl}]^{\text{j}}$	-151.95 (3566)	-201.48 (3016)	63
$[\text{PtCl}_2(\text{PPClPh})]^{\text{j}}$	-144.20 (3394)	-199.00 (3345)	68
$[\text{Ph}_2\text{PCH}_2\text{PCL}_2]^{\text{j}}$	+46.09	-167.10	142

Notes:

^a $\text{PPN}_2 = \text{Ph}_2\text{PCH}_2\text{P}(\text{NEt}_2)_2$; $\text{PPNPh} = \text{Ph}_2\text{PCH}_2\text{P}(\text{NEt}_2)\text{Ph}$;

$\text{PPNCl} = \text{Ph}_2\text{PCH}_2\text{P}(\text{NEt}_2)\text{Cl}$; $\text{PPClPh} = \text{Ph}_2\text{PCH}_2\text{P}(\text{Cl})\text{Ph}$

^b chemical shift in ppm relative to TMP

^c aminophosphino

^d {} coupling to metal in Hz

^e diphenylphosphino

^f coupling between phosphines in Hz

^g C_6D_6 external reference on TT14

^h CD_2Cl_2

ⁱ CDCl_3

^j C_6D_6 external reference on wm250

TABLE 3.3. Platinum-195 NMR Data For $[\text{Ph}_2\text{PCH}_2\text{P}(\text{NET}_2)_2]$, $[\text{Ph}_2\text{PCH}_2\text{P}(\text{NET}_2)\text{Ph}]$ and $[\text{Ph}_2(\text{S})\text{PCH}_2\text{P}(\text{S})(\text{NET}_2)_2]$ Complexes

Compound	$\delta_{\text{Pt}}^{\text{a,b}}$	Pt^{c}	$^1J_{(\text{Pt}-\text{P})}^{\text{d,e}}$	$^1J_{(\text{PtP})}^{\text{f,e}}$	$^1J_{(\text{PtP})}^{\text{g,e}}$
$\text{c}[\text{Pt}(\text{PET}_3)\text{Cl}(\text{Ph}_2\text{PCH}_2\text{P}(\text{NET}_2)_2)] [\text{BF}_4]^{\text{i}}$	341.7(ddd)	21.407311	3800	2154	2380
$\text{t}[\text{Pt}(\text{PET}_3)\text{Cl}(\text{Ph}_2\text{PCH}_2\text{P}(\text{NET}_2)_2)] [\text{BF}_4]^{\text{j}}$	207.6(dt)	21.404442	2266 ^h	3177	2266
$[\text{PtCl}_2(\text{Ph}_2\text{PCH}_2\text{P}(\text{NET}_2)_2)]^{\text{i}}$	651.1(dd)	21.413934	3664	3389	----
$[\text{PtCl}_2(\text{Ph}_2\text{PCH}_2\text{P}(\text{NET}_2)\text{Ph})]^{\text{j}}$	697.6(dd)	21.414929	3344	3198	----
$[\text{Pt}(\text{PET}_3)\text{Cl}(\text{Ph}_2(\text{S})\text{PCH}_2\text{P}(\text{S})(\text{NET}_2)_2)] [\text{BF}_4]^{\text{j}}$	391.1	21.408369	k	k	k

- Notes:
- a** chemical shift in ppm relative to 21.4 MHz
 - b** d, doublet; t, triplet
 - c** absolute frequency in MHz
 - d** aminophosphine
 - e** coupling in Hz
 - f** diphenylphosphine
 - g** triethylphosphine
 - h** simplified to a doublet of triplets by second order effects. Value is the average of the two couplings
 - i** in CD_2Cl_2
 - j** in CDCl_3
 - k** a mixture of *cis* and *trans* isomers made analysis difficult

TABLE 3.4. Some Phosphorus-Platinum Single-Bond Coupling Constants for $[P(NR_2)_3]$ and $[PCl(NR_2)_2]$ Phosphines.

Compound	$^1J(Pt-P)$ (Hz)	$^1J(Pt-P)$ (Hz)
$t-[PtCl_2(PEt_3)(P(NMe_2)_3)]$	3412	+125
$t-[PtCl_2(PEt_3)(PCl(NMe_2)_3)]$	3537	
$t-[PtCl_2(PEt_3)(P(NEt_2)_3)]$	3409	+97
$t-[PtCl_2(PEt_3)(PCl(NEt_2)_3)]$	3506	
$t-[PtCl_2(P(NEt_2)_3)_2]$	3226	+441
$t-[PtCl_2(PCl(NEt_2)_2)_2]$	3667	

Note: All complexes prepared by the reaction of the phosphine with a platinum precursor.

Reference: Hadj-Bagheri, N. *MSc. Thesis*, University of Victoria 1984.

TABLE 3.5. ^{13}C NMR^a data for Complexes Containing
 $[\text{Ph}_2\text{PCH}_2\text{P}(\text{NEt}_2)_2]$ and $[\text{Ph}_2\text{PCH}_2\text{P}(\text{NEt}_2)\text{Ph}]$

Compound ^{b,c}	$\delta(\text{CH}_2)$	$\delta(\text{PNCH}_2\text{CH}_3)$	$\delta(\text{PNCH}_2\text{CH}_3)$	$\delta(\text{PCH}_2\text{CH}_3)$	$\delta(\text{PCH}_2\text{CH}_3)$	$\delta(\text{Ph})^d$
c $[\text{PtCl}(\text{PEt}_3)(\text{PPN}_2)] [\text{BF}_4]$	-e	11.05(s)	41.04(d) (4)	5.00(s)	14.11(s)	124.9 - 135.1
$[\text{PdCl}(\text{PEt}_3)(\text{PPN}_2)] [\text{BF}_4]$	46.64 (29) (37) [8]	14.09(s)	41.16(s)	8.32(s)	11.69(s)	125.7 - 133.4
$[\text{PdCl}_2(\text{PPN}_2)]$	43.55(dd) (27) (36)	14.07(s)	41.36(d) (5)	-----	-----	129.3 - 133.6
$[\text{PtCl}_2(\text{PPN}_2)]$	47.99(dd) (33) (44) (150)	14.01(s)	40.90(d) (5)	-----	-----	127.2 - 133.2
$[\text{PtCl}_2(\text{PPNPh})]$	46.10(t) (32) (32)	13.90(d) (2)	42.49(d) (4) (22)	-----	-----	127.8 - 133.2

- Notes: ^a chemical shift in ppm relative to TMS.
 () = $^1\text{J}(\text{P}-\text{C})$ in Hz. [] = $^3\text{J}(\text{P}-\text{C})$ in Hz.
 { } = $\text{J}(\text{Pt}-\text{C})$ in Hz. d = doublet, t = triplet
 s = singlet.
- ^b $\text{PPN}_2 = [\text{Ph}_2\text{PCH}_2\text{P}(\text{NEt}_2)_2]$
 $\text{PPNPh} = [\text{Ph}_2\text{PCH}_2\text{P}(\text{NEt}_2)\text{Ph}]$
- ^c In CDCl_3
- ^d multiplet
- ^e not observed

TABLE 3.6. ^1H NMR^a data for Complexes Containing the Ligands $[\text{Ph}_2\text{PCH}_2\text{P}(\text{NEt}_2)_2]$ and $[\text{Ph}_2\text{PCH}_2\text{P}(\text{NEt}_2)\text{Ph}]$

Compound ^{b,c}	$\delta(\text{CH}_2)$	$\delta(\text{PNCH}_2\text{CH}_3)$	$\delta(\text{PNCH}_2\text{CH}_3)$	$\delta(\text{PCH}_2\text{CH}_3)$	$\delta(\text{PCH}_2\text{CH}_3)$	$\delta(\text{Ph})$
$c[\text{PtCl}(\text{PEt}_3)(\text{PPN}_2)] [\text{BF}_4]$	4.52 (t) (12) (12) (63)	1.02 (d) [7]	2.81 - 3.27 (m)	1.22 (dd) [8] (17)	2.05 ^d (m) [8] (ca. 8 - 9)	7.5 - 8.0 (m)
$[\text{PdCl}_2(\text{PPN}_2)]$	3.82 2H; (t) (11) (11)	1.04 12H; (t) [7]	3.25 8H; (dq) [7] [14]	-----	-----	7.5 - 8.1 10H; (m)
$[\text{PtCl}_2\text{PPN}_2]$	3.92 2H; (t) (12) (12) (72)	1.05 12H; (t) [7]	3.23 8H; (dq) [7] [15]	-----	-----	7.5 - 8.0 10H; (m)
$[\text{PtCl}_2\text{PPNPh}]$	4.52 1H; (dt) (10) (10) [16] 4.01 1H; (dt) (12) (12) [16]	0.93 6H; (t) [7]	3.11 - 3.35 4H; (m)	-----	-----	7.3 - 8.1 15H; (m)

- Notes: ^a chemical shift in ppm relative to TMS.
 () = J(P-H) in Hz. { } = J(Pt-H) in Hz.
 [] = J(H-H). d = doublet,
 t = triplet, m = multiplet, q = quartet.
- ^b $\text{PPN}_2 = [\text{Ph}_2\text{PCH}_2\text{P}(\text{NEt}_2)_2]$
 $\text{PPNPh} = [\text{Ph}_2\text{PCH}_2\text{P}(\text{NEt}_2)\text{Ph}]$
- ^c In CDCl_3
- ^d poorly resolved psuedo-quintet

TABLE 3.7. Crystallographic Parameters for
cis-[PtCl(PEt₃)(Ph₂PCH₂P(NEt₂)₂^{-P,P'})]BF₄

formula	PtClP ₃ F ₄ N ₂ C ₂₇ BH ₄₇
fw	809.9
space group	P2 ₁ 2 ₁ 2 ₁
a (Å)	15.285(4)
b (Å)	22.097(7)
c (Å)	10.270(4)
α (degrees)	90
β (degrees)	90
(degrees)	90
volume (Å ³)	3469
Z	4
calculated density (g cm ⁻³)	1.5509
crystal size (mm ³)	0.17 x 0.32 x 0.87
F(000) (e)	1616
μ (cm ⁻¹)	45.13
radiation (Å)	0.71069
temperature (K)	295
scan method	θ/2θ
data collected	0-50 in 2θ
total reflections collected	3455
unique data	2595
parameters refined	352
R	0.0734
R _w	0.0749
largest shift/esd	0.495 for BF ₄ , 0.04 for rest of molecule

TABLE 3.8 Fractional atomic coordinates and temperature parameters for $[\text{PtCl}(\text{PEt}_3)\{\text{Ph}_2\text{PCH}_2\text{P}(\text{NEt}_2)_2\text{-}P,P'\}]\text{BF}_4$

Atom	x/a	y/b	z/c	U_{eq}
Pt	38648(6)	41255(4)	-21572(10)	484(3)
Cl(1)	3315(6)	4666(4)	-346(8)	79(3)
P(1)	4942(5)	4863(3)	-2333(10)	70(3)
P(2)	2779(4)	3398(3)	-2162(9)	56(2)
P(3)	4170(4)	3488(3)	-3806(7)	54(2)
N(1)	488(2)	300(1)	-346(2)	8(1)
N(2)	433(1)	375(1)	-522(3)	6(1)
C(1)	309(2)	311(2)	-389(3)	9(2)
C(2)	567(3)	481(2)	-368(3)	10(2)
C(3)	631(3)	526(2)	-376(6)	16(3)
C(4)	449(2)	561(1)	-255(4)	8(1)
C(5)	394(3)	567(1)	-382(4)	11(2)
C(6)	558(4)	494(3)	-72(6)	18(3)
C(7)	596(4)	445(2)	-28(6)	17(3)
C(8)	281(2)	279(1)	-104(3)	6(1)
C(9)	269(2)	219(1)	-145(4)	7(1)
C(10)	273(2)	170(2)	-58(5)	10(2)
C(11)	281(2)	185(2)	83(5)	10(2)
C(12)	290(2)	243(2)	129(4)	11(2)
C(13)	296(2)	290(2)	28(4)	9(1)
C(14)	162(1)	364(1)	-214(3)	6(1)
C(15)	141(2)	423(1)	-270(3)	7(1)
C(16)	59(2)	442(1)	-288(3)	7(1)
C(17)	-8(2)	401(1)	-252(5)	10(2)
C(18)	9(2)	346(2)	-197(4)	11(2)
C(19)	99(2)	328(1)	-182(3)	8(1)
C(20)	484(2)	237(2)	-409(4)	9(1)
C(21)	576(3)	215(2)	-452(5)	12(2)
C(22)	555(2)	307(1)	-245(2)	6(1)
C(23)	540(3)	273(2)	-116(4)	10(2)
C(24)	371(2)	425(1)	-574(3)	8(1)
C(25)	315(3)	406(2)	-684(3)	11(2)
C(26)	518(3)	370(2)	-607(5)	11(2)
C(27)	509(4)	334(4)	-730(5)	20(3)
F(1)	657(3)	632(1)	-50(6)	28(3)
F(2)	703(7)	691(2)	71(8)	47(7)
F(3)	737(3)	603(2)	110(4)	23(2)
F(4)	783(3)	661(3)	-30(7)	27(3)
B(1)	729(5)	629(4)	0(12)	24(7)

Notes for Table 3.8.

Estimated standard deviations are given in parentheses.

Coordinates $\times 10^n$ where $n = 5$ for Pt; 4 for Cl,P; 3 otherwise

Temperature parameters $\times 10^n$ where $n = 4$ for Pt; 3 for Cl,P;
2 otherwise

U_{eq} = the equivalent isotropic temperature parameter.

$$U_{eq} = 1/3 \sum_i \sum_j U_{ij} a_i^* a_j^* (a_i \cdot a_j)$$

TABLE 3.9. Anisotropic temperature parameters (\AA^2) for
 $[\text{PtCl}(\text{PEt}_3)(\text{Ph}_2\text{PCH}_2\text{P}(\text{NEt}_2)_2\text{-}P,P')]\text{BF}_4$

Atom	U_{11}	U_{22}	U_{33}	U_{23}	U_{13}	U_{12}
Pt	433(4)	512(5)	507(5)	-15(5)	4(6)	-72(5)
Cl(1)	75(5)	87(5)	75(5)	-26(4)	4(5)	-8(4)
P(1)	56(4)	63(4)	91(6)	0(4)	9(5)	-20(3)
P(2)	44(4)	66(4)	58(4)	-11(4)	-2(5)	-14(3)
P(3)	45(4)	60(4)	56(4)	2(3)	3(3)	-3(3)
N(1)	7(2)	13(2)	4(1)	0(1)	-2(1)	-4(2)
N(2)	3(1)	7(1)	9(2)	1(1)	0(1)	0(1)
C(1)	3(1)	22(4)	2(1)	-1(2)	0(1)	0(2)
C(2)	13(3)	11(3)	6(2)	-1(2)	1(2)	-7(3)
C(3)	9(3)	17(4)	21(6)	1(4)	8(4)	-5(3)
C(4)	10(2)	5(1)	11(3)	0(2)	1(2)	0(2)
C(5)	17(4)	4(1)	12(3)	0(2)	-2(3)	2(2)
C(6)	15(5)	27(7)	12(4)	0(5)	-4(4)	-12(5)
C(7)	22(6)	7(2)	24(6)	6(3)	-15(5)	-1(3)
C(8)	6(2)	7(2)	4(1)	-1(1)	1(1)	3(1)
C(9)	6(2)	4(1)	12(3)	-1(2)	1(2)	1(1)
C(10)	5(2)	10(3)	15(4)	1(3)	0(2)	2(2)
C(11)	4(2)	15(4)	12(4)	-2(3)	1(2)	1(2)
C(12)	7(2)	15(4)	9(3)	1(3)	-2(2)	2(3)
C(13)	6(2)	13(3)	8(2)	1(2)	1(2)	-3(2)
C(14)	4(1)	6(1)	7(2)	-1(2)	3(2)	-1(1)
C(15)	8(2)	8(2)	6(2)	3(2)	0(2)	1(1)
C(16)	6(2)	11(2)	5(2)	0(2)	-2(2)	2(2)
C(17)	6(2)	7(2)	17(4)	4(3)	-1(2)	0(2)
C(18)	4(2)	15(3)	14(4)	6(3)	3(2)	-2(2)
C(19)	6(2)	9(2)	10(3)	0(2)	-1(2)	0(2)
C(20)	6(2)	8(2)	12(3)	-1(2)	-1(2)	-2(2)
C(21)	8(2)	11(3)	17(4)	-6(3)	4(3)	1(2)
C(22)	5(2)	11(2)	3(1)	-1(1)	-2(1)	0(2)
C(23)	9(3)	15(3)	7(2)	6(2)	-1(2)	1(2)
C(24)	7(2)	10(2)	6(2)	0(2)	-1(2)	3(2)
C(25)	16(4)	10(3)	7(2)	0(2)	-3(2)	4(3)
C(26)	9(3)	12(3)	11(3)	4(3)	0(3)	2(2)
C(27)	15(5)	34(8)	9(3)	-8(5)	5(3)	5(5)
F(1)	22(4)	15(3)	47(8)	4(4)	-20(5)	-5(3)
F(2)	92(20)	6(2)	42(9)	4(3)	-37(11)	-2(5)
F(3)	32(5)	17(3)	19(4)	-1(3)	6(4)	10(3)
F(4)	17(4)	24(5)	40(8)	8(5)	14(5)	-3(3)
B(1)	11(5)	25(11)	37(16)	25(12)	-13(8)	-15(7)

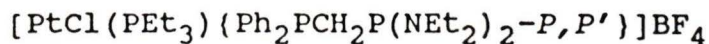
Notes for Table 3.9.

Estimated standard deviations are given in parentheses.

U values $\times 10^n$ where $n = 4$ for Pt; 3 for Cl,P; 2 otherwise

$$T = \exp -2\pi^2(U_{11}h^2a^{*2} + \dots + 2U_{23}klb^*c^* + \dots)$$

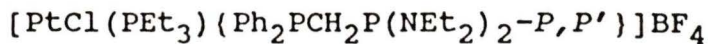
TABLE 3.10 Interatomic distances (Å) for



Atoms	Distance	Atoms	Distance
Cl(1) -Pt	2.365(8)	C(13) -C(8)	1.399(46)
P(1) -Pt	2.325(7)	C(10) -C(9)	1.391(48)
P(2) -Pt	2.310(6)	C(11) -C(10)	1.492(60)
P(3) -Pt	2.251(7)	C(12) -C(11)	1.354(58)
C(2) -P(1)	1.773(39)	C(13) -C(12)	1.477(53)
C(4) -P(1)	1.796(30)	C(15) -C(14)	1.462(36)
C(6) -P(1)	1.924(54)	C(19) -C(14)	1.296(36)
C(1) -P(2)	1.950(30)	C(16) -C(15)	1.348(37)
C(8) -P(2)	1.768(29)	C(17) -C(16)	1.405(44)
C(14) -P(2)	1.850(25)	C(18) -C(17)	1.364(45)
N(1) -P(3)	1.580(31)	C(19) -C(18)	1.444(41)
N(2) -P(3)	1.584(25)	C(21) -C(20)	1.563(48)
C(1) -P(3)	1.848(31)	C(23) -C(22)	1.530(40)
C(20) -N(1)	1.523(41)	C(25) -C(24)	1.476(46)
C(22) -N(1)	1.464(33)	C(27) -C(26)	1.499(72)
C(24) -N(2)	1.544(34)	B(1) -F(1)	1.214(63)
C(26) -N(2)	1.565(46)	F(4) -F(2)	1.736(5)
C(3) -C(2)	1.399(49)	B(1) -F(2)	1.600(58)
C(5) -C(4)	1.561(52)	B(1) -F(3)	1.277(84)
C(7) -C(6)	1.306(76)	B(1) -F(4)	1.120(55)
C(9) -C(8)	1.407(36)		

Estimated standard deviations are given in parentheses.

TABLE 3.11. Bond angles (°) for



Atoms	Angle	Atoms	Angle
P(1) -Pt -Cl(1)	87.6(3)	C(3) -C(2) -P(1)	116.5(31)
P(2) -Pt -Cl(1)	95.6(3)	C(5) -C(4) -P(1)	113.7(21)
P(2) -Pt -P(1)	175.4(4)	C(7) -C(6) -P(1)	116.8(50)
P(3) -Pt -Cl(1)	168.9(3)	C(9) -C(8) -P(2)	121.5(23)
P(3) -Pt -P(1)	103.5(3)	C(13)-C(8) -P(2)	120.3(25)
P(3) -Pt -P(2)	73.3(3)	C(13)-C(8) -C(9)	118.2(30)
C(2) -P(1)-Pt	117.4(11)	C(10)-C(9) -C(8)	122.4(35)
C(4) -P(1)-Pt	112.1(11)	C(11)-C(10)-C(9)	116.7(36)
C(4) -P(1)-C(2)	101.7(18)	C(12)-C(11)-C(10)	123.9(44)
C(6) -P(1)-Pt	110.7(18)	C(13)-C(12)-C(11)	114.9(41)
C(6) -P(1)-C(2)	111.0(21)	C(12)-C(13)-C(8)	123.2(35)
C(6) -P(1)-C(4)	102.8(27)	C(15)-C(14)-P(2)	117.0(18)
C(1) -P(2)-Pt	93.0(11)	C(19)-C(14)-P(2)	123.0(22)
C(8) -P(2)-Pt	120.4(10)	C(19)-C(14)-C(15)	119.4(26)
C(8) -P(2)-C(1)	109.7(15)	C(16)-C(15)-C(14)	122.3(26)
C(14)-P(2)-Pt	119.4(8)	C(17)-C(16)-C(15)	116.3(27)
C(14)-P(2)-C(1)	109.8(13)	C(18)-C(17)-C(16)	123.1(28)
C(14)-P(2)-C(8)	103.7(12)	C(19)-C(18)-C(17)	118.3(28)
N(1) -P(3)-Pt	113.8(10)	C(18)-C(19)-C(14)	120.5(29)
N(2) -P(3)-Pt	119.6(9)	C(21)-C(20)-N(1)	111.6(26)
N(2) -P(3)-N(1)	110.7(13)	C(23)-C(22)-N(1)	117.4(25)
C(1) -P(3)-Pt	97.8(11)	C(25)-C(24)-N(2)	115.0(28)
C(1) -P(3)-N(1)	108.3(16)	C(27)-C(26)-N(2)	115.8(39)
C(1) -P(3)-N(2)	104.8(12)	B(1) -F(2) -F(4)	39.0(30)
C(20)-N(1)-P(3)	119.6(20)	B(1) -F(4) -F(2)	63.9(78)
C(22)-N(1)-P(3)	124.6(23)	F(2) -B(1) -F(1)	85.7(83)
C(22)-N(1)-C(20)	115.4(27)	F(3) -B(1) -F(1)	118.8(69)
C(24)-N(2)-P(3)	118.7(18)	F(3) -B(1) -F(2)	90.8(95)
C(26)-N(2)-P(3)	127.6(20)	F(4) -B(1) -F(1)	121.0(67)
C(26)-N(2)-C(24)	111.7(23)	F(4) -B(1) -F(2)	77.1(67)
P(3) -C(1)-P(2)	91.5(15)	F(4) -B(1) -F(3)	117.5(69)

Estimated standard deviations are given in parentheses.

TABLE 3.12. Selected intermolecular distances (Å) for
 $[\text{PtCl}(\text{PEt}_3)(\text{Ph}_2\text{PCH}_2\text{P}(\text{NEt}_2)_2^{-P,P'})]\text{BF}_4$

Atoms	Distance	Sym	T _x	T _y	T _z
C(25) ...Cl(1)	3.848	1	0	0	-1
C(5) ...Cl(1)	3.856	2	0	1	-1
C(15) ...Cl(1)	3.680	2	0	1	-1
C(16) ...Cl(1)	3.649	2	0	1	-1
C(24) ...Cl(1)	3.935	2	0	1	-1
C(25) ...Cl(1)	3.907	2	0	1	-1
F(2) ...C(1)	3.245	3	1	0	-1
F(3) ...C(2)	3.533	2	1	1	0
F(3) ...C(3)	3.487	2	1	1	0
C(10) ...C(3)	3.573	3	1	-1	-1
F(2) ...C(11)	3.567	3	1	0	0
F(2) ...C(12)	3.285	3	1	0	0
F(1) ...C(20)	3.203	3	1	0	-1
F(2) ...C(20)	3.464	3	1	0	-1
F(4) ...C(21)	3.586	2	1	1	0
F(4) ...C(26)	3.221	2	1	1	0

Symmetry positions for the second atom are, 1: x, y, z
 2: $\frac{1}{2}-x, y, \frac{1}{2}+z$
 3: $-x, \frac{1}{2}+y, \frac{1}{2}-z$

Negative symmetry positions denote inversion and the translations are applied after the symmetry position has been defined.

Chapter 4: Coordination Chemistry of $[\text{Ph}_2\text{P}(\text{S})\text{CH}_2\text{P}(\text{NET}_2)_2]$,
 $[\text{Ph}_2\text{P}(\text{S})\text{CH}_2\text{P}(\text{S})(\text{NET}_2)_2]$ and $[\text{Ph}_2\text{P}(\text{S})\text{CHP}(\text{S})(\text{NET}_2)_2]\text{Li}$ with
Some of the Platinum Group Metals.

4.1. The Coordination Chemistry of $[\text{Ph}_2\text{P}(\text{S})\text{CH}_2\text{P}(\text{NEt}_2)_2]$ with Platinum, Palladium and Rhodium

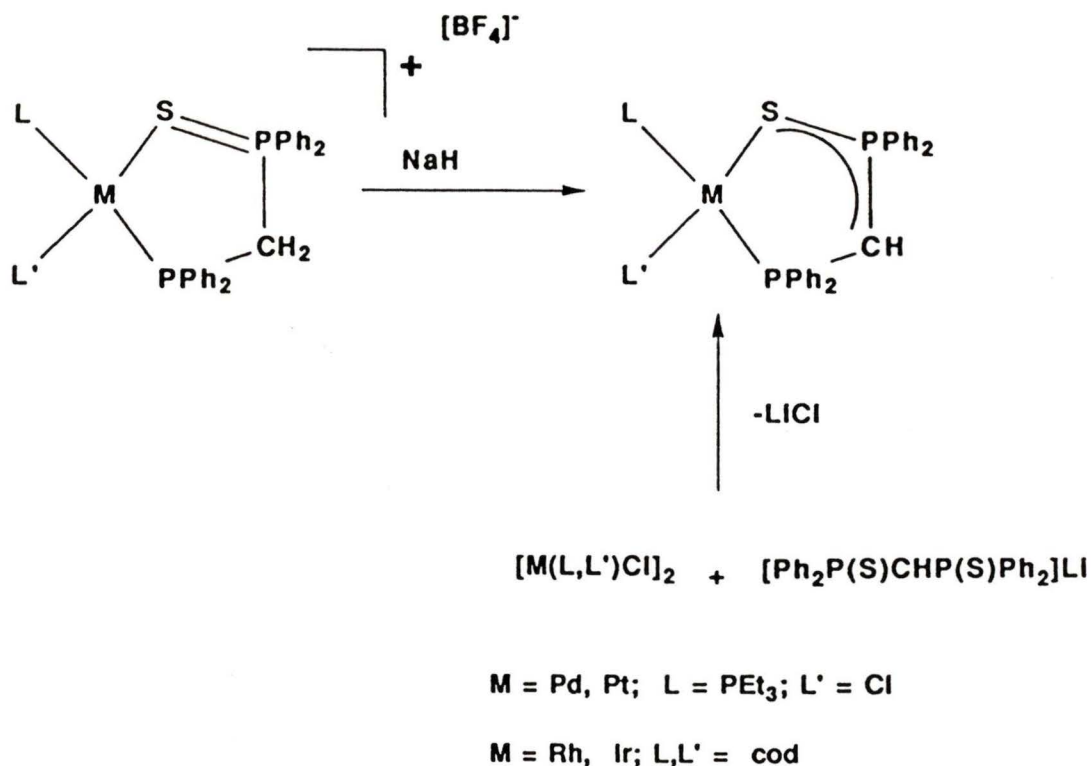
Over the past decade many papers have been published concerning the synthesis and coordination of the ligands $[\text{RR}'\text{P}(\text{X})\text{CH}_n\text{PR}''\text{R}''']^{(n-2)}$ (where $\text{X} = \text{O}, \text{S}$ or Se ; $n = 1$ or 2 and $\text{R}, \text{R}', \text{R}'', \text{R}''' =$ alkyl or aryl groups). The studies have generally focused on $^{31}\text{P}\{^1\text{H}\}$ NMR and in consequence the structural assignments derived in this section are based on a wealth of NMR data and several crystal structures.

The ligands, $[\text{R}_2\text{PCH}_2\text{P}(\text{X})\text{R}'_2]$, were initially synthesized by Grim and co-workers^{24,30,31,54,70} as part of an on-going interest in the $^{31}\text{P}\{^1\text{H}\}$ NMR of unsymmetrical, potentially bidentate, phosphorus ligands, where the phosphorus atoms are in chemically different environments. In addition to the $^{31}\text{P}\{^1\text{H}\}$ and $^{13}\text{C}\{^1\text{H}\}$ NMR parameters of the free ligand, they also reported the coordination chemistry of the ligands with chromium, molybdenum and tungsten carbonyls.

Dixon and co-workers⁷¹ have shown that cleavage of the chloro-bridged dimers $[\text{M}_2\text{Cl}_2(\mu\text{-Cl})_2(\text{PEt}_3)_2]$ (where $\text{M} = \text{Pt}$ or Pd) and $[\text{M}_2(\mu\text{-Cl})_2(\text{cod})_2]$ (where $\text{M} = \text{Rh}$ or Ir) with $[\text{Ph}_2\text{P}(\text{X})\text{CH}_2\text{PPh}_2]$ forms P,X coordinated five-membered ring complexes. Contrary to expectations, the anionic ligand $[\text{Ph}_2\text{P}(\text{X})\text{CHPPh}_2]^-$ also forms P,X coordinated five-membered ring complexes in preference to C,X coordinated four-membered ring complexes. The specific coordination mode of

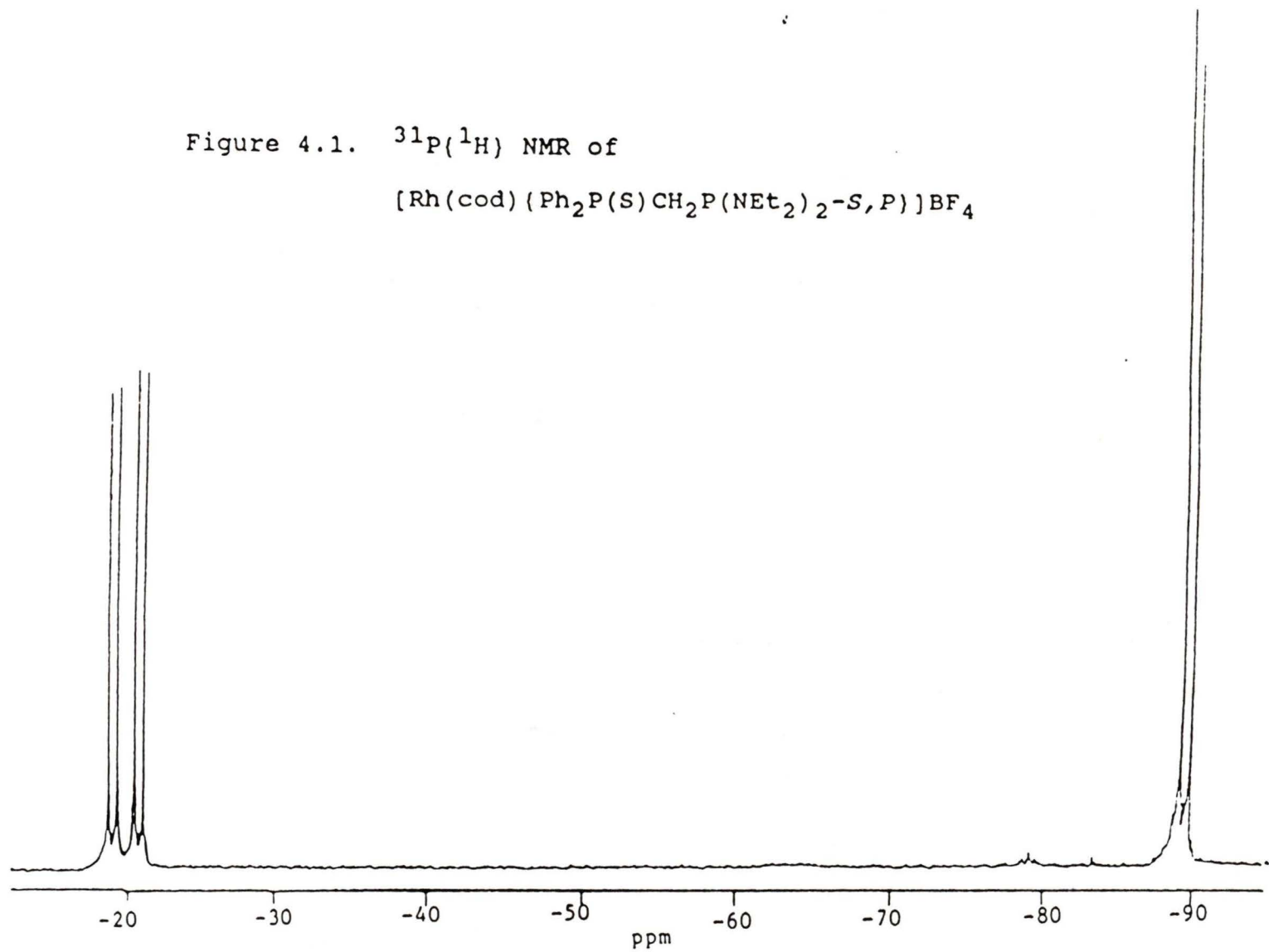
$[\text{Ph}_2\text{P}(\text{X})\text{CHPh}_2]\text{Li}$ was attributed to the stability of a five-membered ring complex, Scheme 4.1.

Scheme 4.1



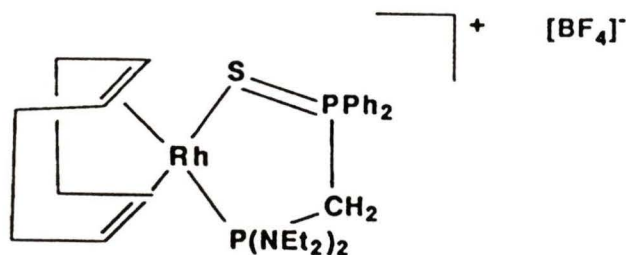
In the present research it was hoped that $[\text{Ph}_2\text{P}(\text{S})\text{CH}_2\text{-P}(\text{NET}_2)_2]$ would coordinate with transition-metals to form six-membered ring complexes, involving nitrogen coordination, in preference to P,S coordinated, five-membered ring complexes as generated in the chemistry discussed above. Again, $^{31}\text{P}\{^1\text{H}\}$ NMR was the important structural probe, primarily because of the amount of supportive data available and because reactivity was expected to be either at or near the

Figure 4.1. $^{31}\text{P}(^1\text{H})$ NMR of
 $[\text{Rh}(\text{cod})(\text{Ph}_2\text{P}(\text{S})\text{CH}_2\text{P}(\text{NEt}_2)_2\text{-S,P})]\text{BF}_4$



phosphorus atoms. The $^{31}\text{P}\{^1\text{H}\}$ NMR data for this section are summarized in Table 4.1.

Reaction of $[\text{Ph}_2\text{P}(\text{S})\text{CH}_2\text{P}(\text{NEt}_2)_2]$ with $[\text{Rh}_2(\mu\text{-Cl})_2(\text{cod})_2]$ generated the P,S coordinated complex;



as deduced from the magnitude of the rhodium-phosphorus couplings and $^{31}\text{P}\{^1\text{H}\}$ NMR chemical shifts; Figure 4.1. The very small rhodium-(diphenylphosphinosulphide) coupling of 2 Hz is typical of a two bond rhodium-phosphorus coupling. For example, $^2J(\text{Rh}-\text{O}=\text{P}) = 4.8$ Hz in *cis*- $[\text{RhCl}(\text{CO})\{\text{Ph}_2\text{PCH}_2\text{-P}(\text{O})\text{Ph}_2\text{-P},\text{O}\}]$.⁶ However, rhodium coupling to the bis(diethylamino)phosphino group at 178 Hz, is too large to be considered that through a coordinated nitrogen and is typical of a single bond rhodium-phosphorus coupling as seen with $[\text{Rh}(\text{cod})\{\text{Ph}_2\text{PCH}_2\text{P}(\text{NEt}_2)_2\text{-P},\text{P}'\}]\text{BF}_4$.

The $^{31}\text{P}\{^1\text{H}\}$ NMR chemical shift changes of the ligand upon coordination are also supportive of a five-membered ring complex. $\text{Ph}_2\text{P}(\text{S})$ and $(\text{NEt}_2)_2\text{P}$ both move to higher frequency upon coordination (+15.22 and +76.4 ppm respectively). A six-membered ring complex (if nitrogen coordinated) would have caused a relatively small shift, possibly to lower

frequency.^{1,52}

Formation of a five-membered ring complex was not surprising in view of the results obtained from the bisphosphine system (Chapter 3). That is, the difference in stability between four- and five-membered metal chelate complexes is far greater than that between five- and six-membered.^{1,7} This difference in the ring strain is observed in the coordination shift. A far greater change in chemical shift is usually encountered on going to a four- or five-membered ring complex compared to the relatively small change on going to a six-membered ring complex. A component of the chemical shift change is thought to be the rearrangement of the substituents around the phosphorus nucleus (i.e. the cone angle that the substituents fill). Chelate ring strain will alter the geometry about each phosphorus such that low ring strain will result in a small coordination shift.⁵²

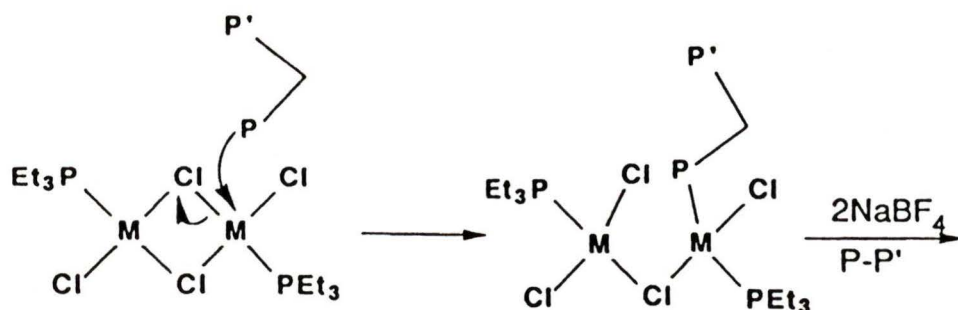
Cleavage of the dimers $[M_2Cl_2(\mu-Cl)_2(PEt_3)_2]$ (where M = Pt or Pd) with $[Ph_2P(S)CH_2P(NEt_2)_2]$ also forms P,S coordinated complexes as identified by their $^{31}P\{^1H\}$ NMR parameters. *Trans*- $[PtCl(PEt_3)\{Ph_2P(S)CH_2P(NEt_2)_2-S,P\}]BF_4$ shows high frequency shifts for the diphenylphosphinosulphide and bis-(diethylamino)phosphino groups of +13.36 and +21.64 ppm respectively relative to the uncoordinated ligand. The respective platinum-phosphorus coupling constants of 2849 and 127 Hz are indicative of one- and two-bond couplings.

The strong *trans* bis(diethylamino)phosphino-triethylphosphine coupling of 500 Hz (not available in the rhodium system) also implies the lack of nitrogen coordination.

The palladium system, although without the help of a spin-active metal, is assigned to the S,P coordinated complex with reference to the strong *trans* phosphorus-phosphorus coupling of 581 Hz in *trans*-[PdCl(PEt₃)(Ph₂P(S)CH₂-P(NEt₂)₂,S,P)]BF₄ and also by the coordination shift of the phosphorus resonances ($\Delta\delta\text{Ph}_2\text{P(S)} = +11.23$ ppm; $\Delta\delta\text{P(NEt}_2)_2$, +27.25 ppm).

An interesting point to note is that in cleavage reactions with [Ph₂PCH₂P(NEt₂)₂] and [Ph₂P(S)CH₂P(NEt₂)₂] the *trans*-isomer is always generated first (i.e. the kinetic product). This can be attributed to the *trans*-labilizing effect of the triethylphosphine relative to the bridging chloride. That is, the triethylphosphine weakens the chloride bond *trans* to itself such that the more basic end of the incoming bisphosphine is able to cleave the chloride bridge; Scheme 4.2.

Scheme 4.2



Reaction of a second molecule of the bisphosphine then probably cleaves the remaining chloride bridge. Extrusion of a chloride-ion through the formation of a chelate complex generates the final product. Such singly-bridged intermediates, as that in Scheme 4.2, have been proposed before for the cleavage of metal dimers with mono-phosphines⁵⁰, and other coordinating ligands.⁷²⁻⁷⁴

A problem was encountered when synthesizing platinum and palladium complexes of $[\text{Ph}_2\text{P}(\text{S})\text{CH}_2\text{P}(\text{NEt}_2)_2]$ if the ligand employed was generated using the lithium bromide complex of methyllithium (see Scheme 2.8). During ligand work-up, it was found impossible to remove all the lithium salts generated. The excess halide (Br^-) then exchanged with the coordinated halide (Cl^-) leading to the formation of both $[\text{PtBr}(\text{PET}_3)\{\text{Ph}_2\text{P}(\text{S})\text{CH}_2\text{P}(\text{NEt}_2)_2\text{-S,P}\}]\text{BF}_4$ and $[\text{PtCl}(\text{PET}_3)\{\text{Ph}_2\text{P}(\text{S})\text{CH}_2\text{P}(\text{NEt}_2)_2\text{-S,P}\}]\text{BF}_4$ *trans*-isomers (causing confusion in the $^{31}\text{P}\{^1\text{H}\}$ NMR). In order to push the exchange to completion, excess lithium bromide was added to the reaction

mixtures. This converted all the platinum complex to the monobromide analogue, plus some $[\text{PtBr}_2(\text{Ph}_2\text{P}(\text{S})\text{CH}_2\text{P}(\text{NET}_2)_2\text{-S,P})]$ (5%) through halide-phosphine exchange. The palladium analogue $[\text{PdCl}(\text{PEt}_3)(\text{Ph}_2\text{P}(\text{S})\text{CH}_2\text{P}(\text{NET}_2)_2\text{-S,P})]\text{BF}_4$ exchanged to completion, generating only $[\text{PdBr}_2(\text{Ph}_2\text{P}(\text{S})\text{CH}_2\text{P}(\text{NET}_2)_2\text{-S,P})]$. The difference in the product ratios reflects the difference in ligand lability between the two metals. As pointed out by Balch et al.,⁷⁵ such halide exchange (and halide scrambling) reactions have often led to confusion in palladium chemistry.

In summary, the reaction of $[\text{Ph}_2\text{P}(\text{S})\text{CH}_2\text{P}(\text{NET}_2)_2]$ with $[\text{M}_2\text{Cl}_2\text{-}(\mu\text{-Cl})_2(\text{PEt}_3)_2]$ ($\text{M} = \text{Pt}$ and Pd) and $[\text{Rh}_2(\mu\text{-Cl})_2(\text{cod})_2]$ generated S,P coordinated complexes. The hoped for nitrogen coordination was not observed and this was attributed to the particular stability of five-membered ring complexes.

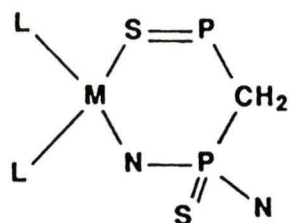
4.2.1. The Coordination Chemistry of

$[\text{Ph}_2\text{P}(\text{S})\text{CH}_2\text{P}(\text{S})(\text{NET}_2)_2]$ with Palladium, Platinum, Rhodium and Iridium.

There has been a wealth of chemistry generated both by our research group and others with regards to the coordination of neutral bischalcogenide-bisphosphine ligands having the general formula $[\text{RR}'\text{P}(\text{X})\text{YP}(\text{X})\text{R}''\text{R}''']$ where R, R', R'' and R''' are either alkyl or aryl substituents; X is oxygen, sulphur or selenium and combinations thereof and Y is S, NH, CH₂ or O.⁷⁶⁻⁸⁹ Of course all possible combinations have not

been studied but representative examples have been coordinated with the late transition-metals; Pd, Pt, Ni, Co, Rh, Ir and Fe. The complexes formed were generally found to be X,X coordinated complexes, with the geometry dependent on the metal used.

It was, therefore, of interest to see if oxidizing the bis-(diethylamino)phosphino group with sulphur to generate the disulphide $[\text{Ph}_2\text{P}(\text{S})\text{CH}_2\text{P}(\text{S})(\text{NEt}_2)_2]$, would make the amine nitrogens more competitive Lewis bases towards coordination. That is upon coordination to metals, the following metal-chelate complex might be formed.



In earlier work, nitrogen coordination was to be identified by the appearance of two-bond metal-phosphorus couplings. However, in the present example this nitrogen coordination probe is useless as in both possible cases (S,S and N,S coordinated complexes) the metal-phosphorus couplings will be over two bonds. ^1H NMR was therefore used as the structural probe. If nitrogen coordination occurred the ethyl resonances of the two amines would be different, that is, they would be in chemically different environments (one coordinated and one free).

The reactions of $[\text{Ph}_2(\text{S})\text{PCH}_2\text{P}(\text{S})(\text{NEt}_2)_2]$ with $[\text{M}_2\text{Cl}_2(\mu\text{-Cl})_2(\text{PEt}_3)_2]$ ($\text{M} = \text{Pt}$ and Pd) and $[\text{M}_2(\mu\text{-Cl})_2(\text{cod})_2]$ ($\text{M} = \text{Ir}$ and Rh) formed products whose $^{31}\text{P}\{^1\text{H}\}$ NMR spectra were as expected. Both *cis*- and *trans*-isomeric forms were observed for the platinum and palladium reactions; Table 4.2. For example, the $^{31}\text{P}\{^1\text{H}\}$ NMR of the platinum product is shown in Figure 4.2. The resonances around -130 ppm are associated with platinum satellites with the corresponding platinum-phosphorus coupling constants consistent with single bond platinum-phosphorus species ($^1\text{J}(\text{Pt-P}) = 3236$ and 3310 Hz). Therefore these resonances are assigned to the triethylphosphine ligands of the two isomers. *Cis* and *trans* geometries of the chelate ligand with respect to the triethylphosphine were assignable by reference to the magnitudes of the platinum couplings. Large platinum-phosphorus couplings will arise when the phosphorus atoms are *trans* to the weaker *trans*-influencing chloride, and small platinum-phosphorus couplings will arise when the phosphorus atoms are *trans* to the strongly *trans*-influencing triethylphosphine. Therefore, for example, the group of resonances at -106.77 ppm represents the diphenylphosphinosulphide group *trans* to the triethylphosphine ($^2\text{J}(\text{Pt-P}) = 48$ Hz). The respective bis-(diethylamino)phosphinosulphide at -84.47 ppm, having a larger platinum coupling of 143 Hz, is *trans* to the chloride ligand, thus the overall complex geometry is *cis* (as defined by the position of the bis(diethylamino)phosphinosulphide

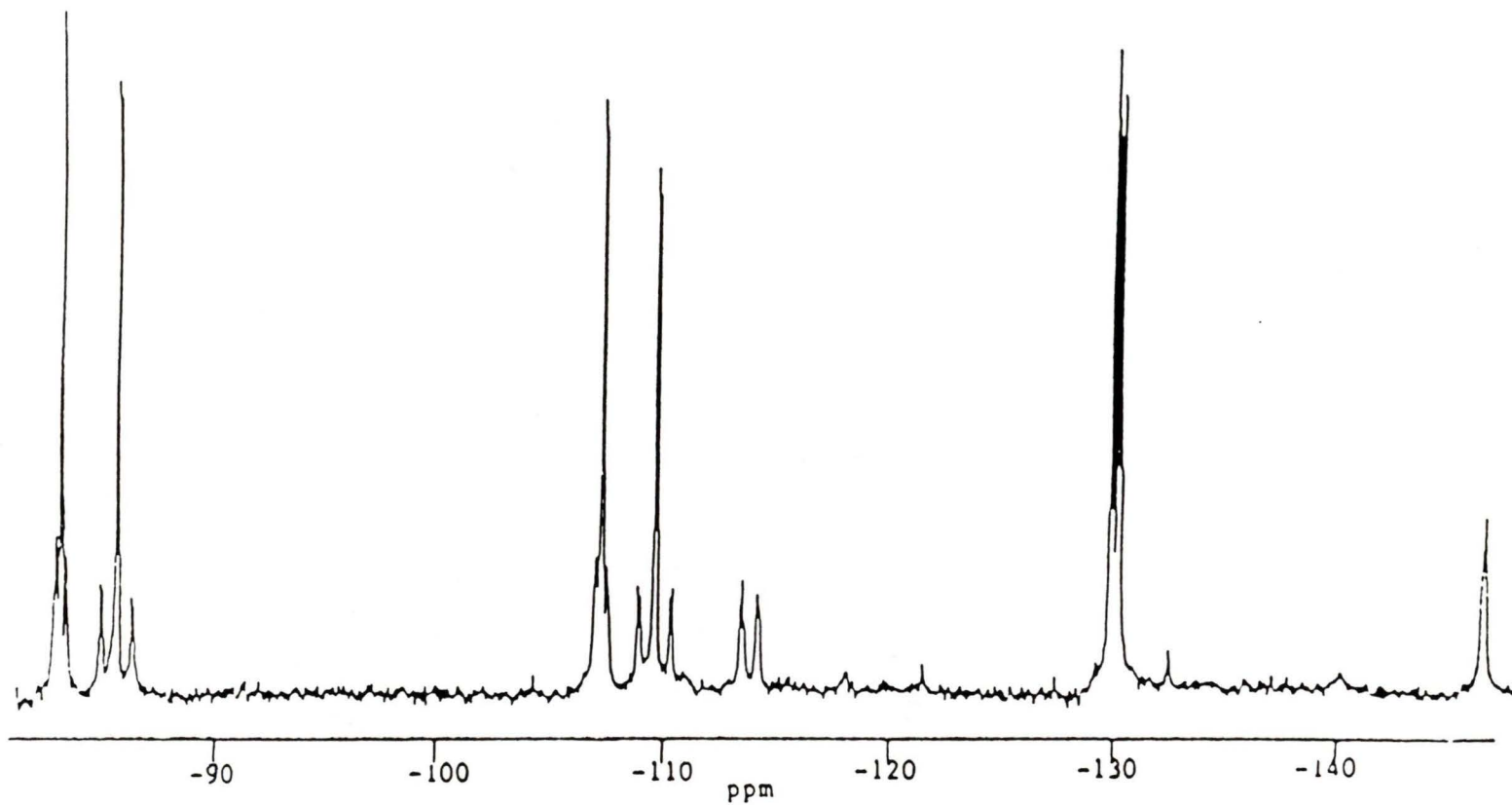
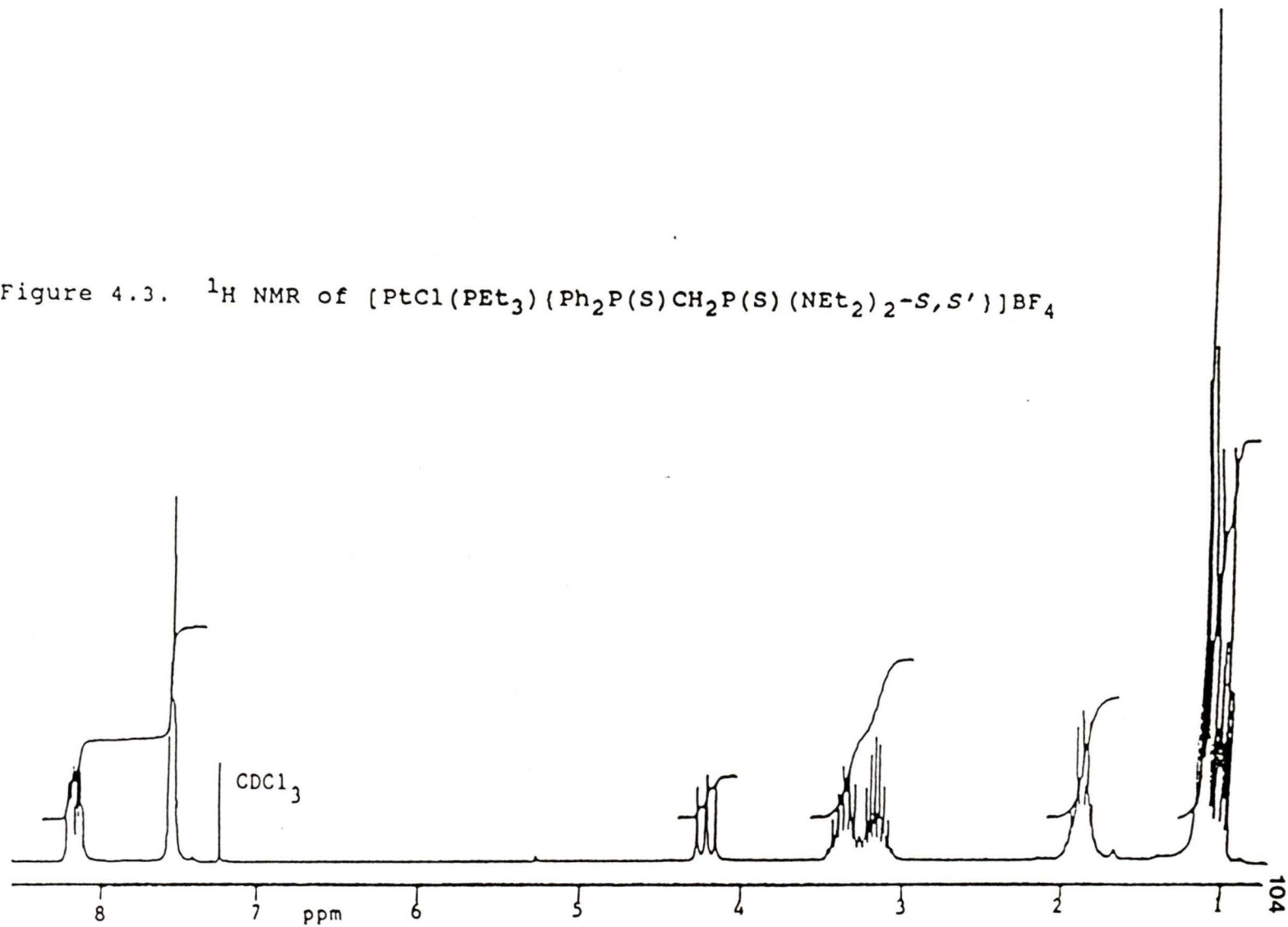


Figure 4.2. $^{31}\text{P}(^1\text{H})$ NMR of $[\text{PtCl}(\text{PET}_3)(\text{Ph}_2\text{P}(\text{S})\text{CH}_2\text{P}(\text{S})(\text{NEt}_2)_2\text{S},\text{S}')]\text{BF}_4$

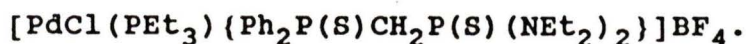
group relative to the triethylphosphine). The *trans*-isomer was similarly verified.

The ^1H NMR (Table 4.4) of all four disulphide products (Pt, Pd, Rh and Ir) looked promising with respect to nitrogen coordination. For example, the ^1H NMR of $[\text{PtCl}(\text{PEt}_3)-\{\text{Ph}_2\text{P}(\text{S})\text{CH}_2\text{P}(\text{S})(\text{NEt}_2)_2\}]\text{BF}_4$ is shown in Figure 4.3. The CH_2 resonance of the diethylamine groups appear as two sets of multiplets between 3.0 and 3.5 ppm. The multiplet arises from $^3\text{J}(\text{P-H})$ and $^3\text{J}(\text{H-H})$ couplings. However, only one set of multiplets would be expected if the amine ethyl groups were chemically equivalent (as in the bisphosphine complexes, see Figure 3.13 for example). That is, no single coupling to the methylene hydrogens can possibly be large enough to double the multiplets. As the same pattern was observed for analogous rhodium and iridium reaction products which can only exist in one isomeric form, the existence of *cis*- and *trans*-isomers cannot be the cause of the two chemically different environments. Therefore, either nitrogen coordination is present or some other process is causing the inequality in chemical environments about the ethyl groups. The only absolute method of analysis was to solve the crystal structure of one of the complexes.⁹⁰

Figure 4.3. ^1H NMR of $[\text{PtCl}(\text{PEt}_3)(\text{Ph}_2\text{P}(\text{S})\text{CH}_2\text{P}(\text{S})(\text{NEt}_2)_2\text{-}S,S')]\text{BF}_4$



4.2.2. Discussion on the X-ray Crystal Structure of



An ORTEP plot of $[\text{PdCl}(\text{PET}_3)\{\text{Ph}_2\text{P}(\text{S})\text{CH}_2\text{P}(\text{S})(\text{NEt}_2)_2\}]\text{BF}_4$ is shown in Figure 4.4 and the pertinent crystallographic data is given in Tables 4.9 to 4.14.

As is seen in the ORTEP plot of $[\text{PdCl}(\text{PET}_3)\{\text{Ph}_2\text{P}(\text{S})\text{CH}_2\text{P}(\text{S})(\text{NEt}_2)_2\}]\text{BF}_4$ the reaction of $[\text{Pd}_2\text{Cl}_2(\mu\text{-Cl})_2(\text{PET}_3)_2]$ with $[\text{Ph}_2\text{P}(\text{S})\text{CH}_2\text{P}(\text{S})(\text{NEt}_2)_2]$ forms an S,S' coordinated complex. The hoped for S,N coordination mode, as predicted from the ^1H NMR, was not formed. There has only been one other S,S' bonded disulphide-bisphosphine crystal structure reported in the literature, that of $[\text{Cu}\{\text{Ph}_2\text{P}(\text{S})\text{CH}_2\text{P}(\text{S})\text{Ph}_2\text{-S,S'}\}\text{Cl}]\text{.Me}_2\text{CO}$.^{80,81} No appreciable difference in the P-S bond distances is observed: 1.978 and 2.018 Å for $[\text{PdCl}(\text{PET}_3)\{\text{Ph}_2\text{P}(\text{S})\text{CH}_2\text{P}(\text{S})(\text{NEt}_2)_2\text{-S,S'}\}]\text{BF}_4$ against 1.970 and 1.974 Å in $[\text{Cu}\{\text{Ph}_2\text{P}(\text{S})\text{CH}_2\text{P}(\text{S})\text{Ph}_2\text{-S,S'}\}\text{Cl}]\text{.Me}_2\text{CO}$.

The P-N bonding distances in $[\text{PdCl}(\text{PET}_3)\{\text{Ph}_2\text{P}(\text{S})\text{CH}_2\text{P}(\text{S})(\text{NEt}_2)_2\text{-S,S'}\}]\text{BF}_4$ are longer than those observed in $[\text{PtCl}(\text{PET}_3)\{\text{Ph}_2\text{PCH}_2\text{P}(\text{NEt}_2)_2\text{-P,P'}\}]\text{BF}_4$ (1.630 and 1.639 Å against 1.580 and 1.584 Å respectively). This may be a consequence of rehybridization of the phosphorus upon oxidation from P(III) to P(V). However, competitive $d_\pi\text{-}p_\pi$ bonding between the sulphur lone-pairs and the nitrogen lone-pairs for the same set of low lying 3d phosphorus orbitals

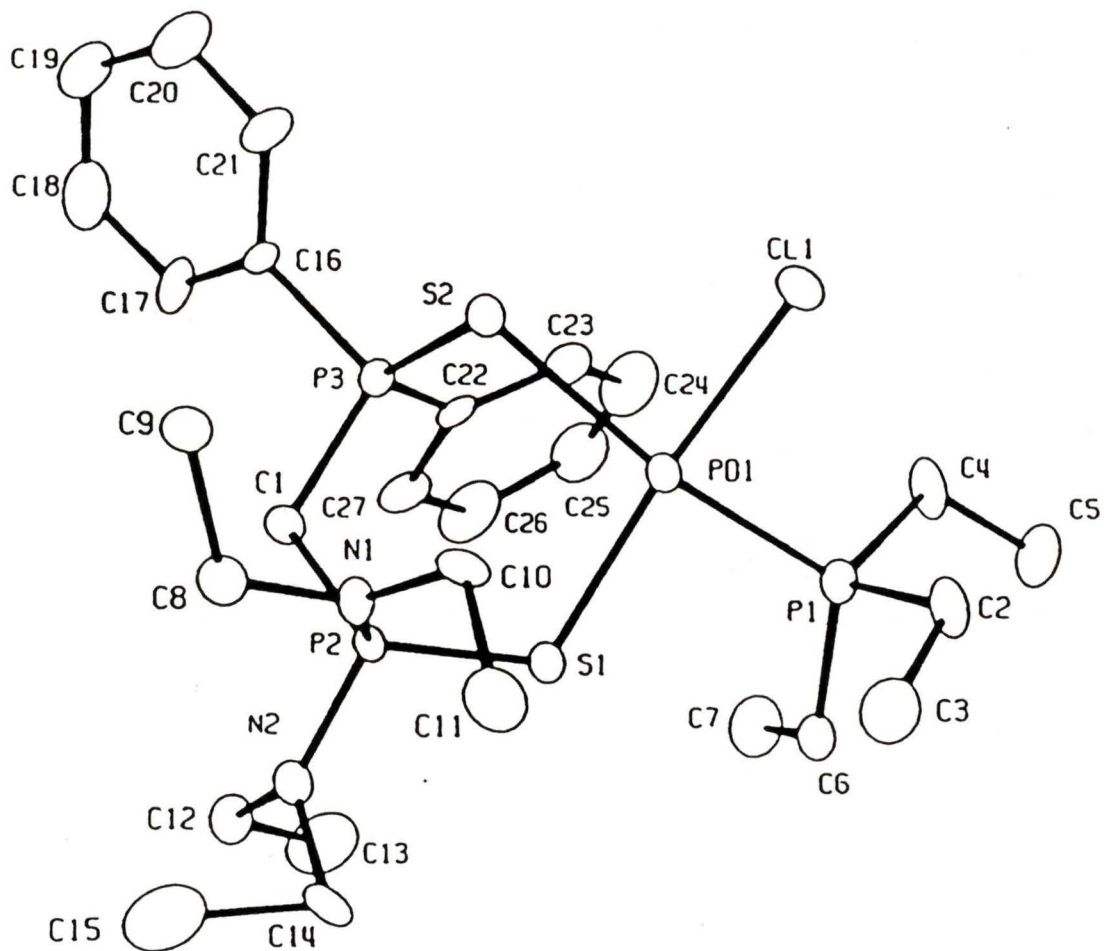
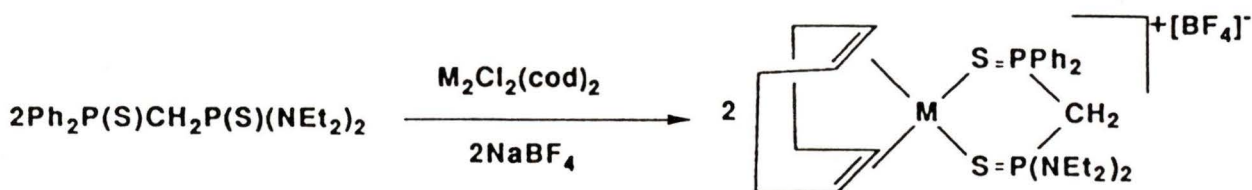


Figure 4.4. ORTEP diagram of *cis*-
 $[\text{PdCl}(\text{PEt}_3)(\text{Ph}_2\text{P}(\text{S})\text{CH}_2\text{P}(\text{S})(\text{NET}_2)_2\text{-S,S}')]\text{BF}_4$

$S, S' \}}]BF_4$ was solved and the lack of nitrogen coordination again rationalized by an extensive $d_{\pi}-p_{\pi}$ interaction. However, nitrogen coordination may be promoted by coordinating a more competitive $d_{\pi}-p_{\pi}$ substituent than sulphur.⁶⁹ That is, an appreciable tendency toward tetrahedral geometry was seen about the nitrogen (N2) competing with the sulphur atom for the same $d_{\pi}-p_{\pi}$ phosphorus d -orbital. The differing extents of $d_{\pi}-p_{\pi}$ interaction between the amino groups and the phosphorus atom, because of the sulphur competing with one of the amine nitrogens for the same phosphorus d -orbitals, accounts for the small but significant difference between the amino groups. A similar argument has been invoked for the multiplet structure of the methyl resonances in the infrared spectra of $PCl_n(NMe_2)_{3-n}$ where $n = 0$ or 1 .⁹¹

In an effort to probe a different transition-metal triad the disulphide complexes of rhodium and iridium were synthesized. Again S, S' coordination was proposed by analogy with the palladium and platinum systems, Scheme 4.4.

Scheme 4.4



M = Rh or Ir

If nitrogen coordination was present, the unique CH₂ resonance in the chelate backbone would show chemically different proton resonances forming an ABXY spin pattern, as seen for the complex [PtCl₂{Ph₂PCH₂P(NEt₂)Ph-P,P'}]; Figure 3.13. However, the hydrogens of the disulphide complexes appear as chemically equivalent A₂XY triplets or a doublet of doublets, the pattern depending on whether ²J(AX) equals ²J(AY) or not; (Figure 4.3).

4.3. The Coordination Chemistry of

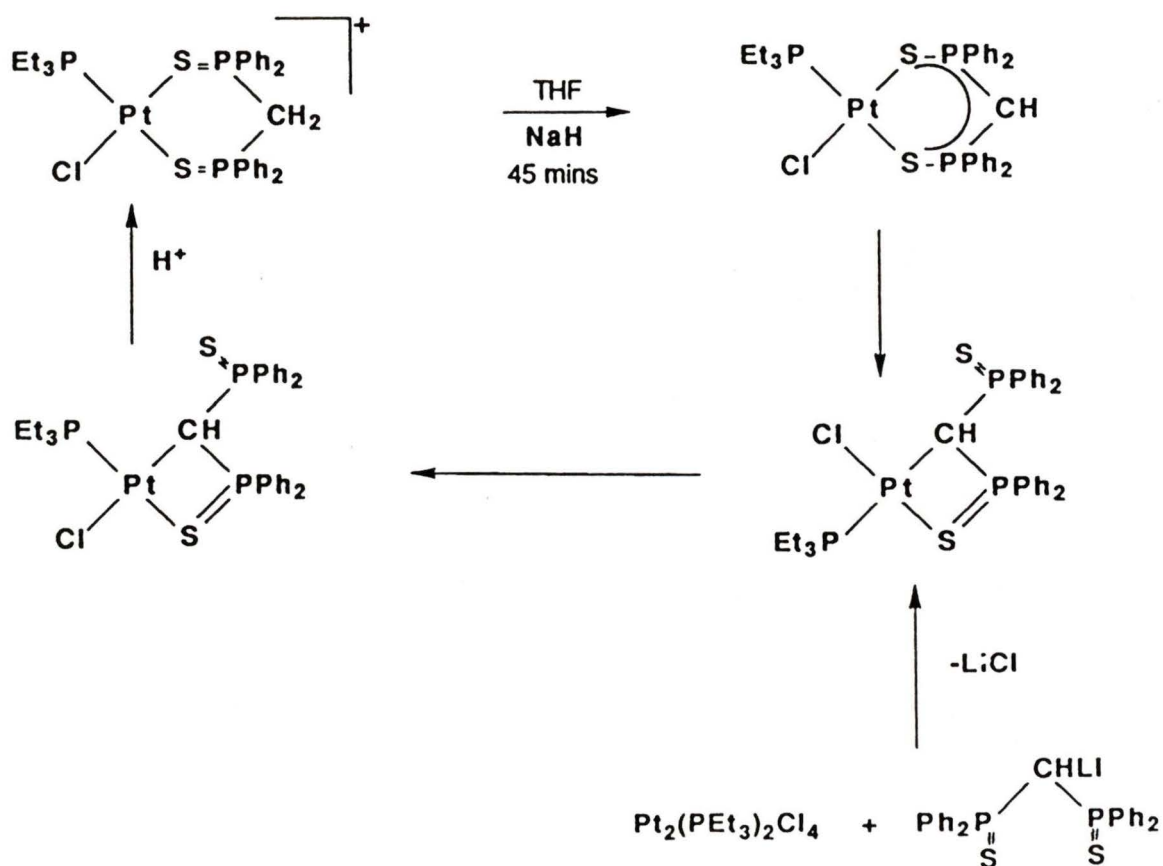
[Ph₂P(S)PCHP(S)(NEt₂)₂]Li with Palladium, Platinum and Rhodium

The coordination chemistry of the ambidentate ligand [R₂P(X)CHP(X)R₂]⁻ has been of interest to our research group for several years. Initial interest stemmed from the ligand being isostructural with the acetylacetonate (acac) ligand, which has a very extensive and well documented coordination chemistry showing both O,O and C bonded complexes. Davison and co-workers have also studied the chemistry of [Ph₂P(X)-CHP(X)R₂]⁻ and the analogous ligand [R₂P(X)NP(X)R₂]⁻. Their

studies focused on the metal ions Fe(II), Co(II) and Ni(II).²⁶ They found that the ligands preferentially coordinate via their chalcogenide atoms (X = S or Se) forming either tetrahedral or square-planar complexes, as deduced from their electronic spectra.

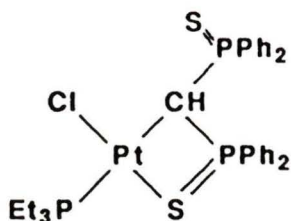
Work carried out in our group⁹² with dimer cleavage reactions, has shown that $[\text{Ph}_2\text{P}(\text{S})\text{CHP}(\text{S})\text{Ph}_2]^-$ can adopt a variety of interesting coordination modes; Scheme 4.5.

Scheme 4.5



Deprotonation of $[\text{PtCl}(\text{PEt}_3)(\text{Ph}_2\text{P}(\text{S})\text{CH}_2\text{P}(\text{S})\text{Ph}_2-S, S')] \text{BF}_4$

with excess sodium hydride generated the *S,S'* coordinated complex $[\text{PtCl}(\text{PET}_3)\{\text{Ph}_2\text{P}(\text{S})\text{CHP}(\text{S})\text{Ph}_2\text{-S,S}'\}]$. This was not reported in the initial publication,⁹² but was observed in later work.²⁵ Over time the *S,S'* coordinated complexes converted to the *S,C* coordinated complex with the carbon *trans* to the triethylphosphine.



Reaction of $[\text{Pt}_2\text{Cl}_2(\mu\text{-Cl})_2(\text{PET}_3)_2]$ with $[\text{Ph}_2\text{P}(\text{S})\text{CH-P}(\text{S})\text{Ph}_2]\text{Li}$ also generated the same *S,C* coordinated complex, which showed a static $^{31}\text{P}\{^1\text{H}\}$ NMR at ambient temperature. During workup, the "static" carbon-bonded metal chelate isomerized to a fluxional *S,C* coordinated complex with the sulphur now *trans* to the triethylphosphine. The observed fluxionality was attributed to the relative *trans*-influence of the various coordinated ligands. A variable-temperature study on the fluxional species was attempted, although satisfactory results could not be obtained as resolution was lost at low temperatures.

The initial four-membered metal chelate was static on the NMR time scale owing to the relatively low *trans*-influence of the chloride ligand. Upon isomerization, however, the strongly *trans*-labilizing triethylphosphine became *trans* to the platinum-coordinated sulphur atom. The triethylphos-

phine was then thought to sufficiently weaken the platinum-sulphur bond to allow for dynamic solution interchange of the sulphur atoms. The process was considered unusual in involving essentially a "bimolecular" reaction controlled by a pivotal motion about a strong metal-ligand bond, as was seen in the crystal structure of $[\text{PtCl}(\text{PEt}_3)\{\text{Ph}_2\text{P}(\text{S})\text{-CHP}(\text{S})\text{Ph}_2\text{-C,S}\}]$ where the dangling sulphur is poised above the coordinated sulphur.⁹²

Work with the ligand $[\text{Ph}_2\text{P}(\text{S})\text{CHP}(\text{S})\text{Ph}_2]^-$ was continued with the transition-metal ions of rhodium and iridium. Deprotonation of the $[\text{Rh}(\text{cod})\{\text{Ph}_2\text{P}(\text{S})\text{CH}_2\text{P}(\text{S})\text{Ph}_2\text{-S,S}'\}]\text{BF}_4$ with sodium hydride, or the anionic ligand cleavage of $[\text{Rh}_2(\mu\text{-Cl})_2(\text{cod})_2]$, were shown by x-ray crystallography and NMR spectroscopy to generate the S,S' coordinated complexes only.²⁵ It was, therefore, a natural extension of earlier $[\text{Ph}_2\text{P}(\text{S})\text{CH}_2\text{P}(\text{S})(\text{NEt}_2)_2]$ chemistry to study the coordination chemistry of $[\text{Ph}_2\text{P}(\text{S})\text{CHP}(\text{S})(\text{NEt}_2)_2]\text{Li}$. It was also of interest to study further the chemistry of the palladium system, which had to-date been unsuccessful owing to its instability. The palladium- $[\text{Ph}_2\text{P}(\text{S})\text{CHP}(\text{S})(\text{NEt}_2)_2]^-$ system would be of greater interest because the lability of palladium complexes makes them more applicable to catalytic processes. Platinum complexes, in general, form compounds which are too stable.

4.3.1. The Coordination Chemistry of

$[\text{Ph}_2\text{P}(\text{S})\text{CHP}(\text{S})(\text{NEt}_2)_2]\text{Li}$ with Rhodium

Reaction of $[\text{Rh}_2(\mu\text{-Cl})_2(\text{cod})_2]$ with two equivalents of $[\text{Ph}_2\text{P}(\text{S})\text{CHP}(\text{S})(\text{NEt}_2)_2]\text{Li}$ generated the same product as that from the sodium hydride deprotonation of $[\text{Rh}(\text{cod})\{\text{Ph}_2\text{P}(\text{S})\text{CH}_2\text{-P}(\text{S})(\text{NEt}_2)_2\}]\text{BF}_4$ as shown by their $^{31}\text{P}\{^1\text{H}\}$ NMR. Therefore

both reactions form the same deprotonated complex, Scheme

4.6. The slight shift to low frequency of the $^{31}\text{P}\{^1\text{H}\}$ NMR resonances ($\delta\text{P}(\text{S})(\text{NEt}_2)_2 = -4.81$ ppm and $\delta\text{P}(\text{S})\text{Ph}_2 = -1.55$ ppm) implies the generation of a six-membered complex in preference to a four-membered C,S coordinated ring complex which would be expected to show a much larger low frequency shift; Figure 4.5.

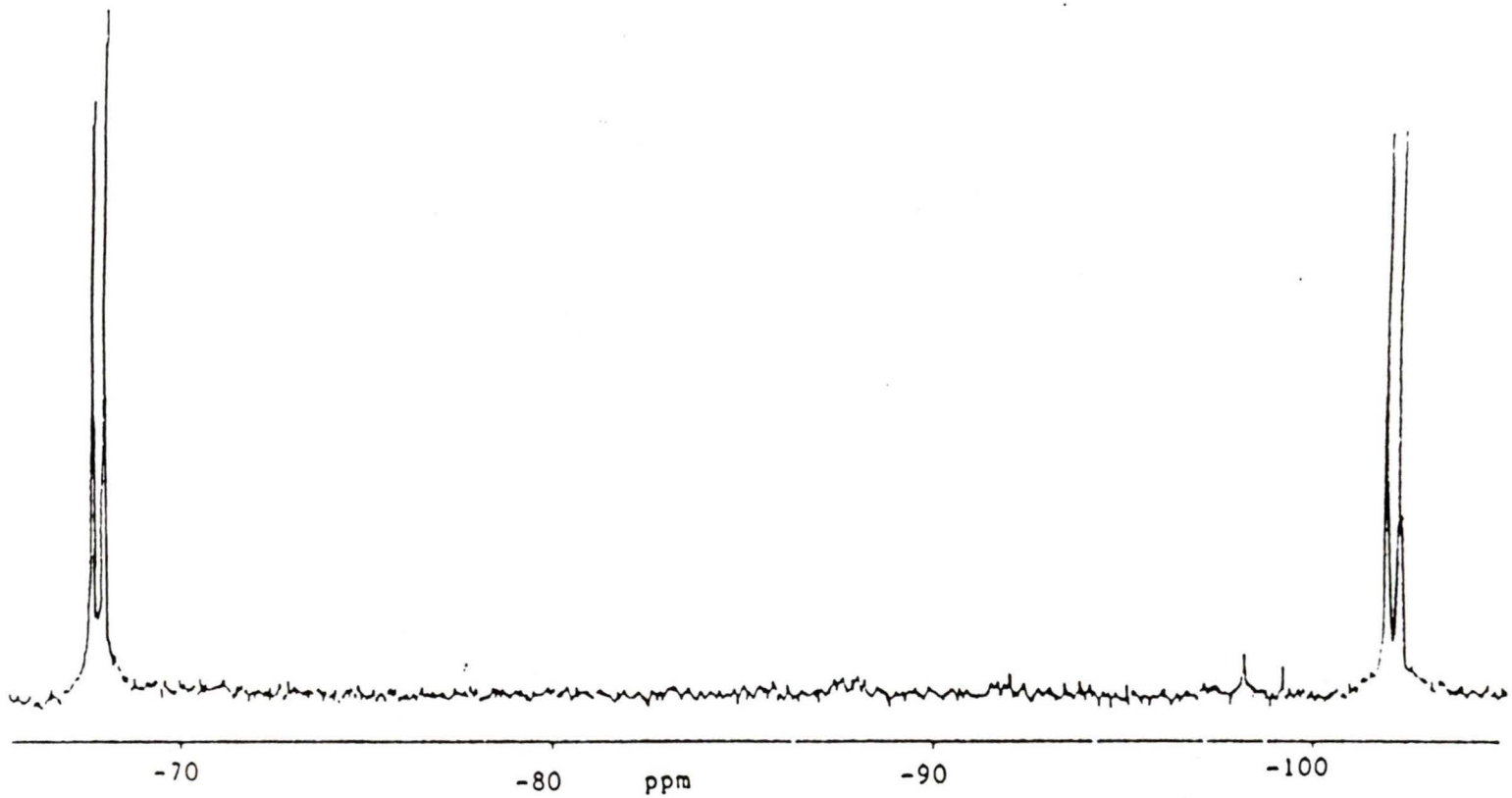
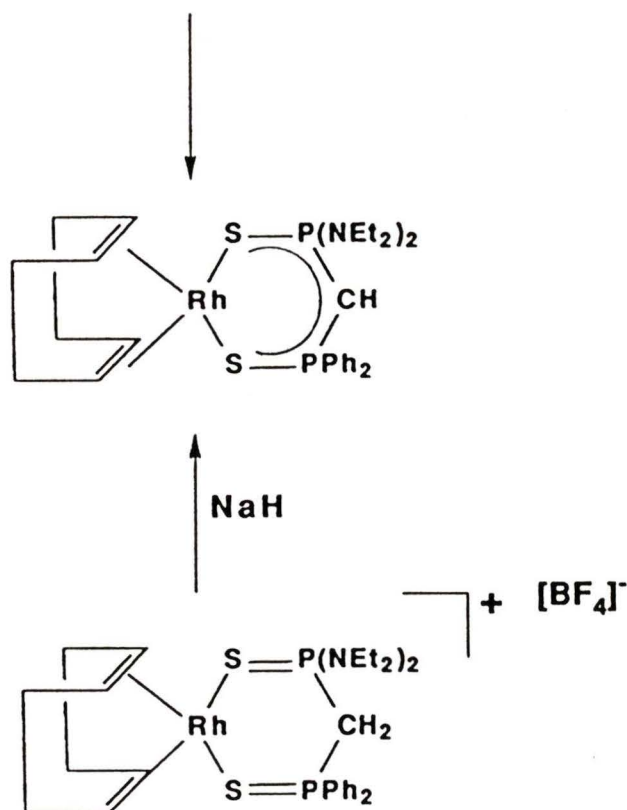


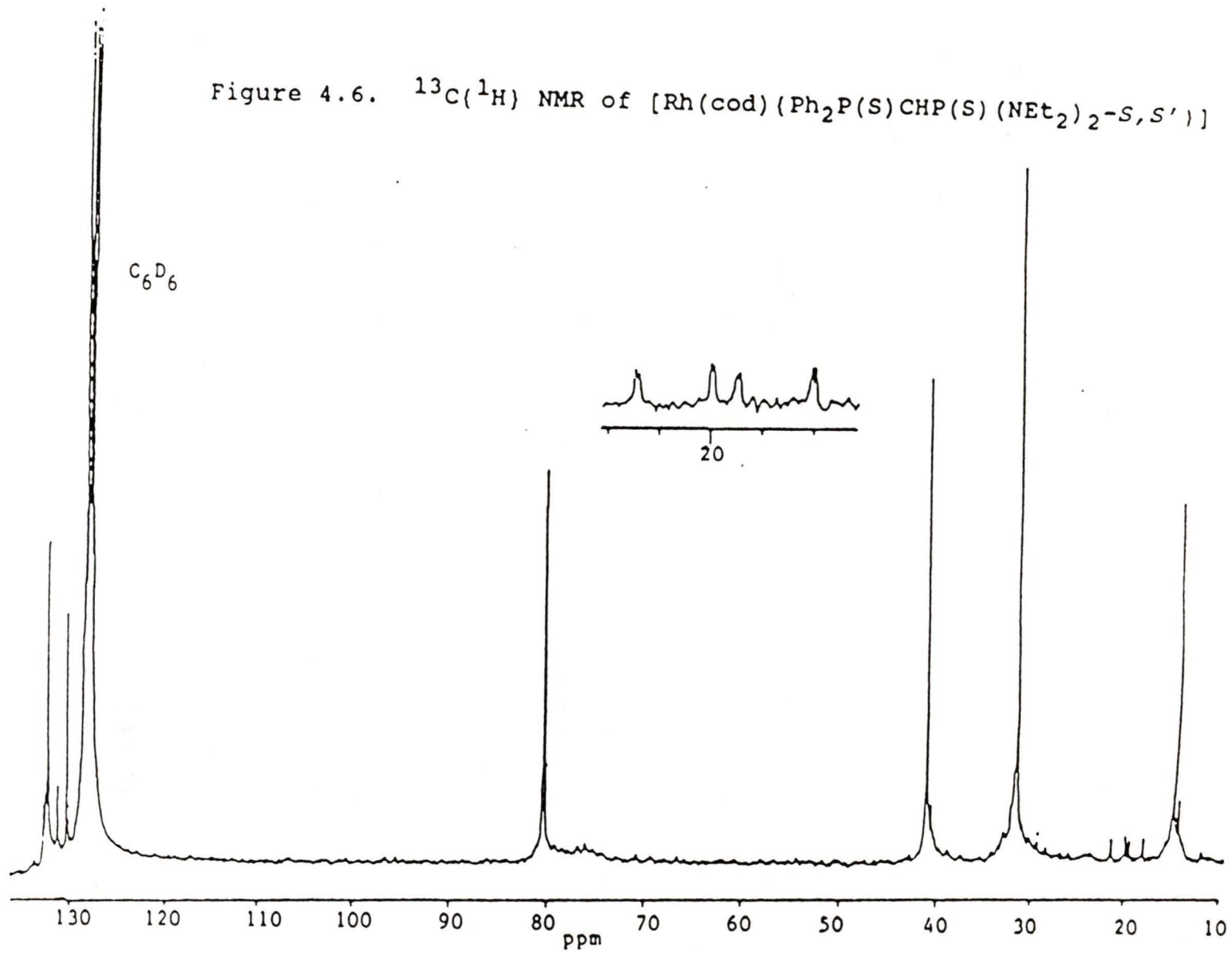
Figure 4.5. ^{31}P (^1H) NMR of $[\text{Rh}(\text{cod})(\text{Ph}_2\text{P}(\text{S})\text{CHP}(\text{S})(\text{NEt}_2)_2\text{-S,S'})]$

Scheme 4.6



Confirmatory evidence was found in the $^{13}\text{C}\{^1\text{H}\}$ NMR of the complex; Figure 4.6. The unique carbon resonance at +19.73 ppm appears as a doublet of doublet of doublets from coupling to the two phosphorus nuclei and the rhodium nucleus. If the ligand was bonded via its central carbon, the single bond phosphorus-carbon couplings would be low, nearing those of the cationic complex (82 and 48 Hz) or the neutral ligand (51 and 82 Hz). This is because coordination to the metal would change the hybridization about the carbon from sp^2 to

Figure 4.6. $^{13}\text{C}(^1\text{H})$ NMR of $[\text{Rh}(\text{cod})(\text{Ph}_2\text{P}(\text{S})\text{CHP}(\text{S})(\text{NEt}_2)_2\text{-S,S}')]$



sp^3 reducing the s -character at the carbon nucleus and so the couplings to it; as described by the Fermi-contact equation. However, $^1J(P-C)$ values were found to be large (92 and 123 Hz) implying sp^2 hybridization and hence no rhodium-carbon bond. These results are also consistent with those for the reaction of $[\text{Ph}_2\text{P(S)CHP(S)Ph}_2]^-$ with $[\text{Ir}_2(\mu\text{-Cl})_2(\text{cod})_2]$ and $[\text{Rh}_2(\mu\text{-Cl})_2(\text{cod})_2]$ described earlier. For example the deprotonation of $[\text{Rh}(\text{cod})\{\text{Ph}_2\text{P(S)CH}_2\text{P(S)Ph}_2\text{-S,S'}\}]\text{BF}_4$ with sodium hydride caused an increase in $^1J(P-C)$ from 48 Hz to 91 Hz.²⁵ More compelling evidence was found in the magnitude of $J(\text{Rh-C})$. If the carbon was directly attached to the metal the rhodium-carbon single bond coupling would be expected to be at least 30 Hz.⁹³ In $[\text{Rh}(\text{cod})\{\text{Ph}_2\text{P(S)CHP(S)(NEt}_2)_2\}]$, $J(\text{Rh-C})$ is found to be about 5 Hz as expected for a three-bond coupling (see expanded insert of $-\text{CH}-$ region in Figure 4.6).

Location of the methyne hydrogen in the ^1H NMR, thus verifying the structural assignment by proton integration, was not possible. It was probably obscured by the ethyl and cod resonances.

An interesting point to note with respect to later discussion is the magnitude of the two-bond phosphorus-phosphorus intrachelate coupling of 28 Hz. It is significantly larger than that found for $[\text{Rh}(\text{cod})\{\text{Ph}_2\text{P(S)CH}_2\text{P(S)(NEt}_2)_2\text{-S,S'}\}]\text{BF}_4$ ($^2J(P-P) = 2$ Hz). Again, this is consistent with the pro-

posed formation of a *S,S'* bonded six-membered ring complex. The increase in *s*-character between the phosphorus nuclei and possible shortening of the phosphorus-carbon bonds by formation of a partially delocalized π electron system, suggests that $^2J(\text{P-P})$ should increase.

Although the ethyl resonances in the proton NMR spectrum appear as two sets of multiplets, the formation of a nitrogen coordinated complex is unlikely based on the results discussed earlier for the cationic complex. Also only one product was observed in the $^{31}\text{P}\{^1\text{H}\}$ NMR from the deprotonation of $[\text{Rh}(\text{cod})\{\text{Ph}_2\text{P}(\text{S})\text{CH}_2\text{P}(\text{S})(\text{NET}_2)_2\text{-S,S}'\}]\text{BF}_4$. If isomerization from the *S,S'* coordinated complex to *N,S* coordinated complex occurred two products would be expected in the $^{31}\text{P}\{^1\text{H}\}$ NMR representing both forms, unless the isomerization was particularly fast.

4.3.2. The Coordination Chemistry of $[\text{Ph}_2\text{P}(\text{S})\text{CHP}(\text{S})(\text{NET}_2)_2]\text{Li}$ with Palladium

A summary of the results of this section is given in Scheme 4.7.

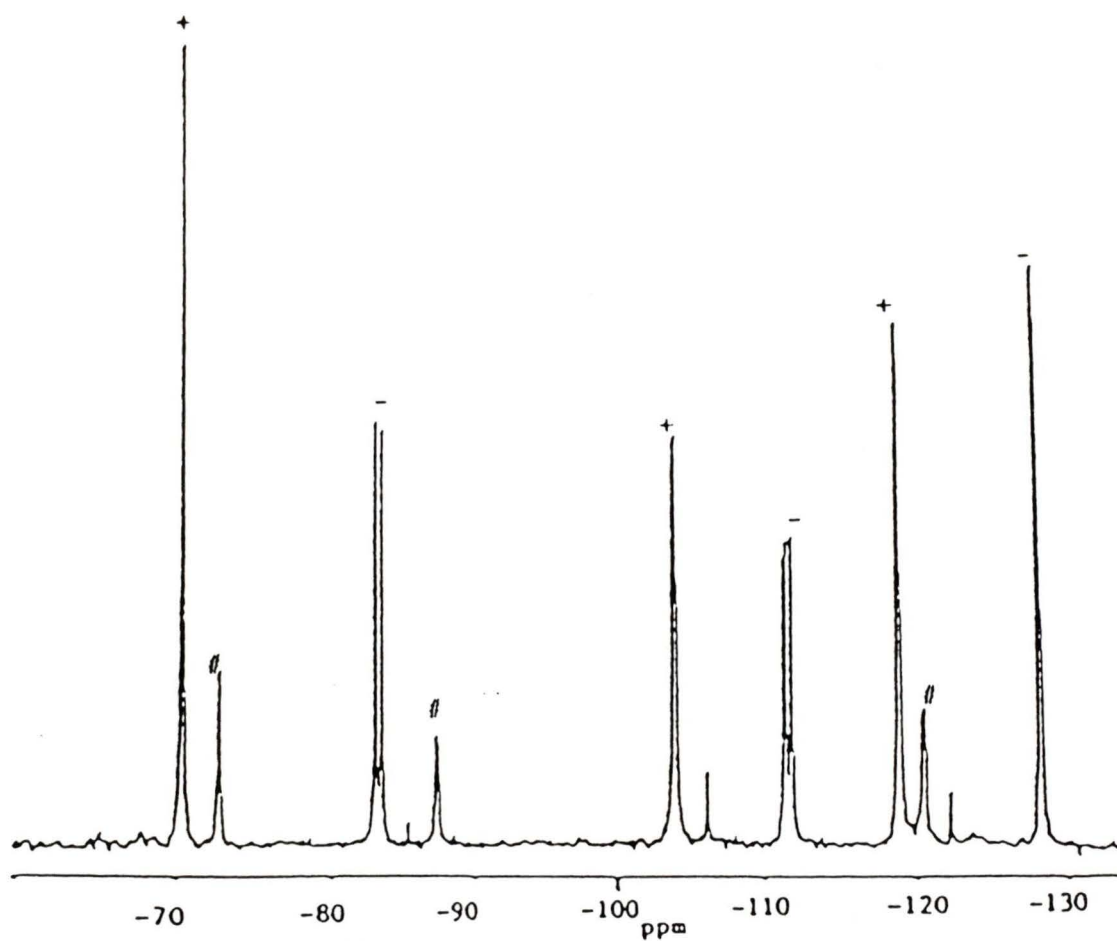


Figure 4.7. $^{31}\text{P}\{^1\text{H}\}$ NMR (-80°C) of an isomeric mixture of S,S' bonded (-) and C,S bonded $[\text{PdCl}(\text{PEt}_3)(\text{Ph}_2\text{P}(\text{S})\text{CH}-\text{P}(\text{S})(\text{NEt}_2)_2)]$ with the carbon *trans* to the chloride and $\text{P}(\text{S})(\text{NEt}_2)_2$ coordinated (+) and $\text{Ph}_2\text{P}(\text{S})$ coordinated (#).

increase in $^2J(\text{P-P})$ of 48 Hz upon deprotonation, is consistent with the trends observed for the deprotonation of $[\text{Rh}(\text{cod})(\text{Ph}_2\text{P}(\text{S})\text{CH}_2\text{P}(\text{S})(\text{NET}_2)_2\text{-S,S}')]\text{BF}_4$. Only one isomeric form of $[\text{PdCl}(\text{PET}_3)(\text{Ph}_2\text{P}(\text{S})\text{CHP}(\text{S})(\text{NET}_2)_2\text{-S,S}')]$ is formed and its geometry, *cis* or *trans*, was unassignable from the data available.

The S,S' coordinated complex, over time, ($t_{1/2} = 20$ min) converted to another "static" species with a significantly different $^{31}\text{P}\{^1\text{H}\}$ NMR. The new complex is assigned to the S,C bonded four-membered ring complex with the carbon *trans* to the triethylphosphine and the bis(diethylamino)phosphino-sulphide *trans* to the chloride.

The collapse to a four-membered ring chelate complex is proposed on coupling information. The largest phosphorus-phosphorus coupling is 16 Hz. This reduction in the magnitude of the intrachelate coupling is consistent with the argument that the unique carbon has changed from sp^2 to sp^3 hybridization upon coordination to the metal. Obtaining the $^{31}\text{P}\{^1\text{H}\}$ NMR at -90°C only improved the resolution of the spectrum, confirming the absence of dynamic sulphur interchange under ambient conditions.

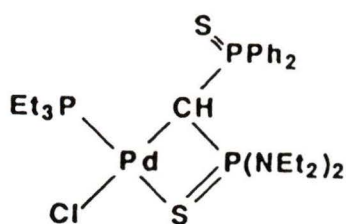
The diphenylphosphinosulphide group (-101.98 ppm) is assumed to be "dangling" as its chemical shift corresponds to that of the "dangling" diphenylphosphinosulphide group in *trans*-

$[\text{PtCl}(\text{PEt}_3)(\text{Ph}_2\text{P}(\text{S})\text{CH}_2\text{P}(\text{S})\text{Ph}_2\text{-C,S})]$ (-100.79 ppm). Its chemical shift is also very close to that for the uncoordinated ligand which resonates at -101.57 ppm. Therefore, the bis(diethylamino)phosphinosulphide group must be coordinated to the palladium (-69.85 ppm). The same S,C coordinated complex was generated by reacting $[\text{Ph}_2\text{P}(\text{S})\text{CHP}(\text{S})(\text{NEt}_2)_2]^-$ with $[\text{Pd}_2\text{Cl}_2(\mu\text{-Cl})_2(\text{PEt}_3)_2]$. This confirmed that the sodium hydride was not reacting further with the complex during deprotonation, for example, by hydride-chloride exchange.

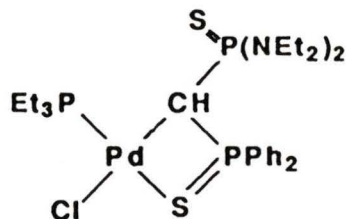
During work-up and over time (ca. 1 h) the S,C coordinated complex isomerized to a complex with three broad $^{31}\text{P}\{^1\text{H}\}$ NMR resonances. Cooling the solution to -80°C resolved the broad resonances into the sharp resonances of two complexes of unequal abundance ($\approx 1:3$). The two complexes each contained three phosphorus atoms with each phosphorus coupled to the other two; Figure 4.7. Again all couplings measured are small, with the largest at 17 Hz, hence an sp^3 hybridized unique-carbon can be inferred. It is proposed that during workup the S,C coordinated complex with the sulphur *trans* to the chloride isomerizes to a S,C coordinated complex with the sulphur now *trans* to the triethylphosphine; similar to the results obtained for the reaction of $[\text{Pt}_2\text{Cl}_2(\mu\text{-Cl})_2(\text{PEt}_3)_2]$ with $[\text{Ph}_2\text{P}(\text{S})\text{CHP}(\text{S})\text{Ph}_2]^-$ discussed in the introduction to this section.

The complexes observed in the $^{31}\text{P}\{^1\text{H}\}$ NMR at -80°C corres-

pond to the complexes with $(\text{NEt}_2)_2\text{P}(\text{S})$ coordinated and $\text{Ph}_2\text{P}(\text{S})$ dangling (major complex) and $\text{Ph}_2\text{P}(\text{S})$ coordinated with $(\text{NEt}_2)_2\text{P}(\text{S})$ dangling (minor complex).



Major



Minor

The assignments (Table 4.5) are based on the diphenylphosphinosulphide chemical shifts, which are backed up by supportive $^{31}\text{P}\{^1\text{H}\}$ NMR data from the $[\text{PtCl}(\text{PEt}_3)\{\text{Ph}_2\text{P}(\text{S})\text{CH}-\text{P}(\text{S})\text{Ph}_2-\text{C},\text{S}\}]$ system. Further assignment evidence is gained by observing which peaks coalesce upon warming (Figure 4.8). The major complex resonance at -100.79 ppm upon warming to ambient temperature coalesces with the resonance at -87.36 ppm to generate the broad resonance at -98 ppm. In the complex $[\text{PtCl}(\text{PEt}_3)\{\text{Ph}_2\text{P}(\text{S})\text{CHP}(\text{S})\text{Ph}_2-\text{C},\text{S}\}]$ the dangling and coordinated diphenylphosphinosulphide groups come at -100.79 and -79.05 ppm respectively. Therefore the resonance at -87.36 ppm is assigned to the coordinated diphenylphosphinosulphide and that at -103.99 ppm to the dangling diphenylphosphinosulphide. This then implies that having the bis-(diethylamino)phosphinosulphide coordinated is the more favorable of the two isomeric possibilities. This agrees with the argument that bis(diethylamino)phosphinosulphide is the more basic sulphide, that is, the electron donating

ability of the amine lone-pair improves the sulphur atom's ability to coordinate to palladium.^{91,94}

The triethylphosphine ligands are assigned to those resonances at low frequency (-118.96 ppm and -120.55 ppm by analogy with many other palladium-triethylphosphine complexes) and the bis(diethylamino)phosphinosulphide to those resonances at high frequency (-70.39 ppm and -72.73 ppm).

Raising the temperature causes coalescence of the respective resonances to give three broad signals at ambient temperature. Thus, upon warming the complex solution, the two isomeric forms undergo a dynamic interchange on the NMR time scale. Employing arguments used for the fully characterized [PtCl(PEt₃)(Ph₂P(S)CHP(S)Ph₂-C,S)] system, the strong *trans*-influencing ability of the triethylphosphine labilizes the palladium sulphur-bond *trans* to it, such that dynamic, intramolecular interchange of coordinated and non-coordinated P=S groups occurs. A dynamic equilibrium was not observed for the sulphur *trans* to the chloride as its *trans* influence is insufficient to labilize the palladium-sulphur bond.

A band shape analysis program (DNMR3), designed by Kleier and Binsch,⁹⁵ was used to extract thermodynamic data for the dynamic equilibrium. The program accepted NMR parameters for the slow exchange spectrum along with the relative populations of the two species estimated from the intensities of

the $^{31}\text{P}\{^1\text{H}\}$ NMR resonances. By varying the rate of spin-spin exchange for the relevant nuclei, simulated spectra for the various temperatures were generated and compared to the actual spectra by eye. Simulated spectra along with their corresponding actual spectra for selected temperatures are shown in Figure 4.8. Spectra were obtained at ten different temperatures between -80°C and 24°C in CD_2Cl_2 and at three temperatures up to $+80^\circ\text{C}$ in DMSO. However, only those spectra recorded in CD_2Cl_2 were analyzed, as it is difficult to account for chemical shift changes with solvent.

Difficulty was encountered simulating the variable-temperature spectra. Owing to the large range of temperatures studied, changes in chemical shift of the various phosphorus nuclei becomes important. This is often found to be a problem in variable-temperature NMR studies, as the changes may go in either direction and at any particular rate (typically $\pm 1\text{-}2$ Hz/deg).⁷⁵ This implies a certain degree of error in the thermodynamic data extracted as it was difficult to account for temperature effects.

Thermodynamic data was obtained by an Eyring plot of $\ln(k_{\text{obs}}/T)$ against $1/T$ (Table 4.7), which gave a good straight line, and when compared with the standard transition-state theory equation,⁹⁶ $\ln(k_{\text{obs}}/T) = -\Delta H^\ddagger/kT + \Delta S^\ddagger/R + \ln(k/h)$, enabled ΔH^\ddagger , ΔS^\ddagger and hence ΔG^\ddagger to be calculated; Table 4.8. Although there is confidence in the value

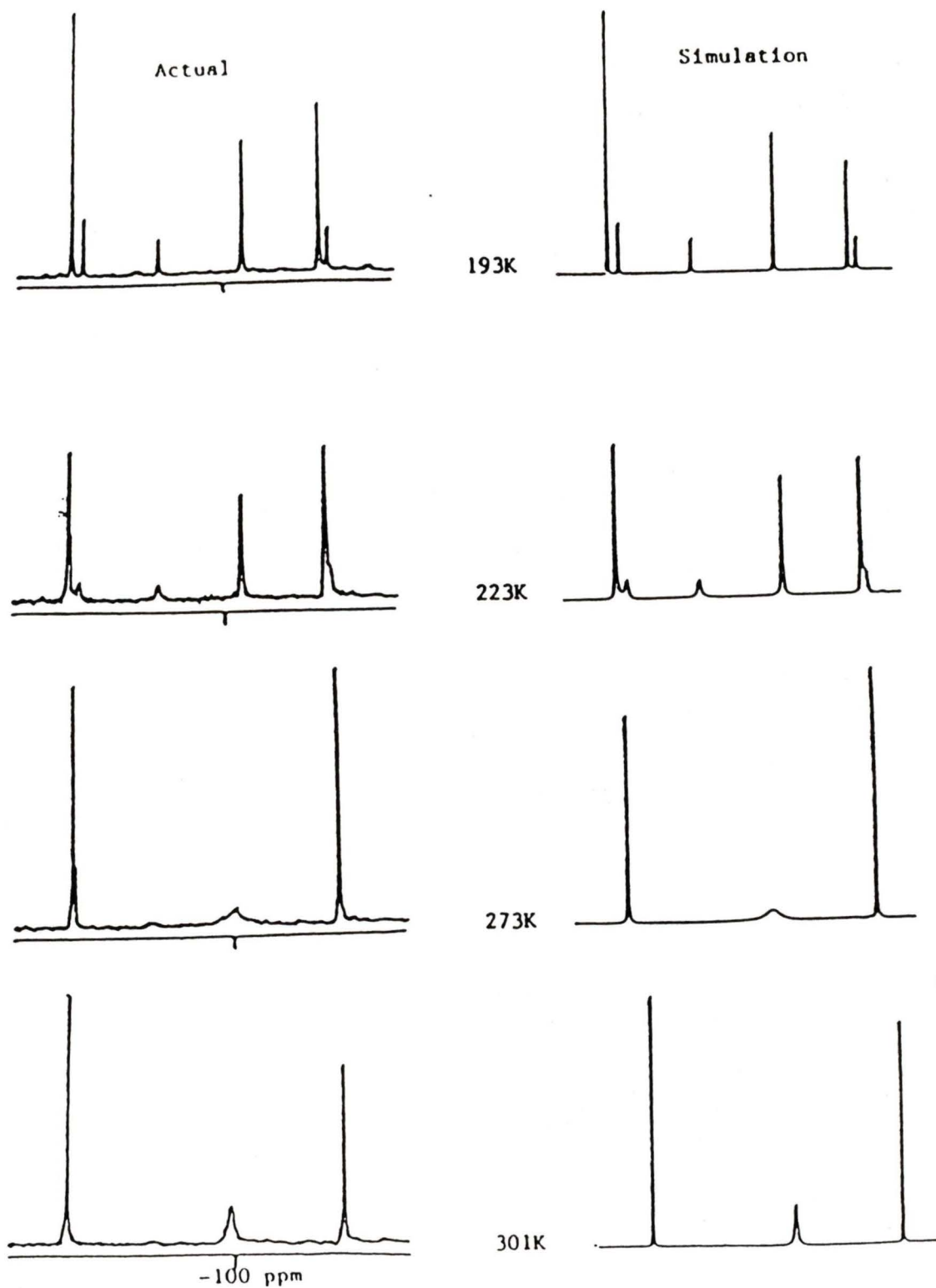


Figure 4.8. Variable-temperature $^{31}\text{P}\{^1\text{H}\}$ NMR of $\text{trans-}[\text{PdCl}(\text{PEt}_3)(\text{Ph}_2\text{P}(\text{S})\text{CHP}(\text{S})(\text{NEt}_2)_2)]$. Both actual and simulated spectra are shown.

of ΔH^\ddagger obtained from the slope of the graph (Figure 4.9), ΔS^\ddagger from the intercept on the logarithmic axis contains an appreciable amount of error. Hence, a weighty discussion on the significance of ΔS^\ddagger is unjustified. A majority of the error arises from not being able to account for chemical shift temperature variations and from comparing the spectra by eye.

The Arrhenius activation energy was obtained by a plot of $\ln(k_{\text{obs}})$ against $1/T$ as in the relationship $\ln(k_{\text{obs}}) = -E_a/RT + \ln A$; $E_a = \Delta H^\ddagger + RT$.

The fact that the dynamic equilibrium was observed on the NMR time scale instantly places the process in a narrow bracket of activation energies. Simulation of the dynamic process was performed mainly to show that the assignment of the resonances and the proposed dynamic process were correct. The results are interesting in that they show the preferential coordinating ability of the bis(diethylamino)-phosphinosulphide group relative to the diphenylphosphino-sulphide group. However, the differences can only be small at about 3 kJ/mol (as estimated from the population ratio in the $^{31}\text{P}\{^1\text{H}\}$ NMR, Figure 4.7).

In an attempt to further verify the proposed collapse of an S,S' coordinated complex to an S,C coordinated complex the $^{13}\text{C}\{^1\text{H}\}$ NMR spectra were recorded at the various stages.

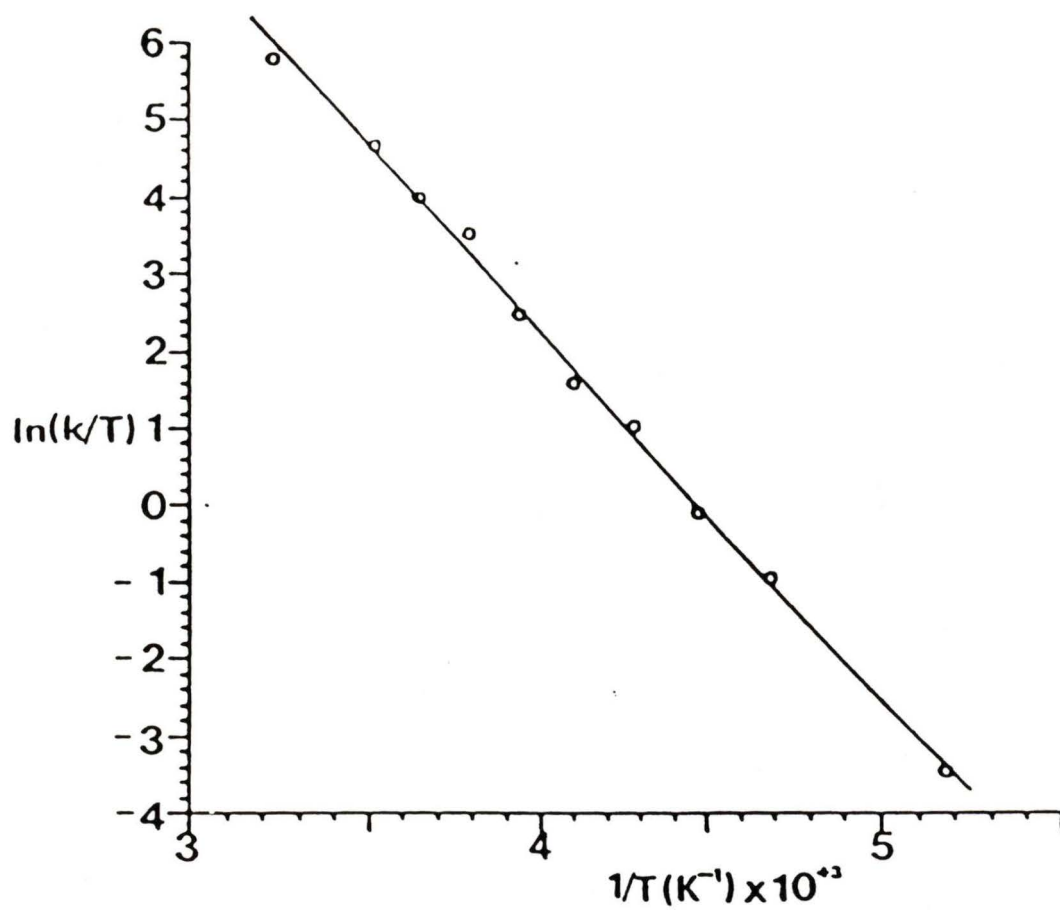


Figure 4.9. Plot of $\ln(k/T)$ vs. $1/T$ with the line of best fit for the dynamic phosphorus interchange in *trans*- $[\text{PdCl}(\text{PET}_3)(\text{Ph}_2\text{P}(\text{S})\text{CHP}(\text{S})(\text{NEt}_2)_2)]$

However, owing to the low intensity of the methyne carbon resonances and the high multiplicity expected, the unique carbon resonance could not be detected. It is thought that it might be buried under the ethyl resonances which also resonate in the region where the CH is expected. Location of the unique carbon using DEPT pulsing sequences was also unsuccessful because of the intensity of the ethyl resonances (i.e. total depression of their intensity was impossible).

In order to "clean" up the low frequency region of the $^{13}\text{C}\{^1\text{H}\}$ NMR, $[\text{PdCl}(\text{PPh}_3)\{\text{Ph}_2\text{P}(\text{S})\text{CH}_2\text{P}(\text{S})\text{Ph}_2\text{-S,S}'\}]\text{BF}_4$ was synthesized via the chloro-bridge cleavage of $[\text{Pd}_2\text{Cl}_2(\mu\text{-Cl})_2(\text{PPh}_3)_2]$ with $[\text{Ph}_2\text{P}(\text{S})\text{CH}_2\text{P}(\text{S})\text{Ph}_2]$. Deprotonation of the complex formed, $[\text{PdCl}(\text{PPh}_3)\{\text{Ph}_2\text{P}(\text{S})\text{CH}_2\text{P}(\text{S})\text{Ph}_2\}]\text{BF}_4$, generated a product with a doublet and a triplet in the $^{31}\text{P}\{^1\text{H}\}$ NMR at -101.91 and -118.65 ppm respectively with $J(\text{P-P}) = 15$ Hz. The spectrum was similar to that for the S,S' coordinated complex $[\text{PtCl}(\text{PEt}_3)\{\text{Ph}_2\text{P}(\text{S})\text{CHP}(\text{S})\text{Ph}_2\text{-S,S}'\}]$. It was concluded that the large phosphorus-phosphorus coupling expected between the chelate phosphorus atoms (≈ 50 Hz) and their most likely close chemical shifts, generates a deceptively simple ABX spin system which appears as an A_2X system. The $^{13}\text{C}\{^1\text{H}\}$ NMR signal of the unique carbon could not be located.

Repeating the deprotonation reaction with $[\text{PdCl}(\text{PEt}_3)\{\text{Ph}_2\text{-}$

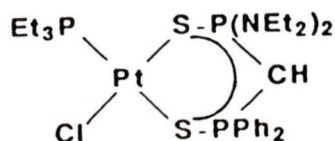
$\text{P}(\text{S})\text{CH}_2\text{P}(\text{S})\text{Ph}_2\text{-S,S'}\text{]BF}_4$ generated a product with a similar $^{31}\text{P}\{^1\text{H}\}$ NMR of a doublet and a triplet at -103.62 and -129.02 ppm representing the diphenylphosphinosulphide group and triethylphosphine respectively ($J(\text{P-P}) = 17$ Hz). The pattern can again be explained as a deceptively simple ABX spin system. Over time the $^{31}\text{P}\{^1\text{H}\}$ NMR degenerated to a complex group of broad resonances which were also obtained by reacting $[\text{Ph}_2\text{P}(\text{S})\text{CHP}(\text{S})\text{Ph}_2]^-$ with $[\text{Pd}_2\text{Cl}_2(\mu\text{-Cl})_2(\text{PET}_3)_2]$. A variable-temperature $^{31}\text{P}\{^1\text{H}\}$ NMR run on the mixture showed a collapse of the broad resonances and emergence of many more peaks. At -90°C , the complex $^{31}\text{P}\{^1\text{H}\}$ NMR was not resolved enough to observe phosphorus-phosphorus coupling, such that identification of the species present was impossible. Again the $^{13}\text{C}\{^1\text{H}\}$ NMR of the unique carbon could not be located.

4.3.3. The Coordination Chemistry of

$[\text{Ph}_2\text{P}(\text{S})\text{CHP}(\text{S})(\text{NET}_2)_2]\text{Li}$ with Platinum

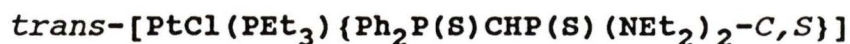
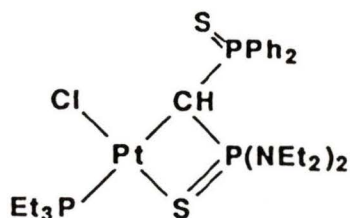
For completion and to provide supporting $^{31}\text{P}\{^1\text{H}\}$ NMR data the chemistry of $[\text{Ph}_2\text{P}(\text{S})\text{CHP}(\text{S})(\text{NET}_2)_2]^-$ with platinum was studied.

Deprotonation of $[\text{PtCl}(\text{PET}_3)\{\text{Ph}_2\text{P}(\text{S})\text{CH}_2\text{P}(\text{S})(\text{NET}_2)_2\}\text{-S,S'}\text{]BF}_4$ generated the S,S' coordinated complex,



as deduced from the magnitude of the intrachelate phosphorus-phosphorus coupling of 54 Hz. *Cis/trans* geometry can not be identified as the two-bond platinum-phosphorus couplings are of similar magnitudes ($^2J(\text{Pt-P}) = 519$ and 477 Hz). Although, if the largest platinum-phosphorus coupling observed for the bis(diethylamino)phosphinosulphide implies that it is *trans* to the chloride ion, then an overall *cis* geometry may be concluded.

Along with the *S,S'* coordinated complex was the *C,S* bonded four-membered metal chelate (5% of total phosphorus) with the carbon coordinated *trans* to the triethylphosphine.



Hence a static $^{31}\text{P}\{^1\text{H}\}$ NMR spectrum was observed. The same *C,S* coordinated complex, along with about 5% of the *S,S'* coordinated complex, was generated by the reaction of $[\text{Pt}_2\text{Cl}_2(\mu\text{-Cl})_2(\text{PEt}_3)_2]$ with $[\text{Ph}_2\text{P}(\text{S})\text{CHP}(\text{S})(\text{NEt}_2)_2]^-$

Assignment of the dangling and coordinated sulphurs of the *C,S* bonded isomer is made simple by the presence of platinum satellites. As was seen with the static palladium *S,C* coordinated complex, $(\text{NEt}_2)_2\text{P}(\text{S})$ is the coordinated sulphide ($\delta = 69.29$ ppm; $^2J(\text{Pt-P}) = 477$ Hz) and $\text{Ph}_2\text{P}(\text{S})$ is the dangling

sulphide ($\delta = -102.43$ ppm; $^2J(\text{Pt-P}) = 93$ Hz). The triethylphosphine is assigned to the resonance at -134.06 ppm because of its large platinum-phosphorus coupling of 2985 Hz. Attempts to observe the CH resonance in the $^{13}\text{C}\{^1\text{H}\}$ NMR were unsuccessful. This is not surprising because the signal would be further coupled with the platinum nucleus.

Isomerization of the static S,C coordinated complex to the fluxional C,S coordinated complex with the coordinated sulphur *trans* to the triethylphosphine ligand was not observed. This is probably owed to the lower lability of platinum complexes relative to palladium complexes and the strong coordinating ability of the $(\text{NET}_2)_2\text{P(S)}$ group.

In summary, the reaction of $[\text{Ph}_2\text{P(S)CHP(S)(NET}_2)_2]^-$ with $[\text{Rh}_2(\mu\text{-Cl})_2(\text{cod})_2]$ formed only the six-membered S,S' coordinated ring complex. The reaction of $[\text{Pd}_2\text{Cl}_2(\mu\text{-Cl})_2(\text{PET}_3)_2]$, however, showed interesting complex formation, which is summarized in Scheme 4.7. The analogous palladium- $[\text{Ph}_2\text{P(S)CHP(S)Ph}_2]^-$ reaction products could not be identified due to the instability of the products and the inability to "freeze" out the apparent dynamic exchange in the $^{31}\text{P}\{^1\text{H}\}$ NMR.

The dynamic equilibrium shown in Scheme 4.7 with reference to the discussion in the thesis introduction (the importance of generating a site of coordination unsaturation in cata-

lytic processes) implies the potential catalytic use of the $[\text{Ph}_2\text{P}(\text{S})\text{CHP}(\text{S})(\text{NEt}_2)_2]^-$ ligand in conjunction with a metal such as palladium.

TABLE 4.1. ^{31}P (^1H) NMR Data for Complexes Containing the Ligand $[\text{Ph}_2\text{P}(\text{S})\text{CH}_2\text{P}(\text{NEt}_2)_2]$

Compound ^a	$\delta\text{P}_A^{\text{b,c}}$	$\delta\text{P}_B^{\text{b,d}}$	$\delta\text{P}_C^{\text{b,e}}$	$^2\text{J}_{(\text{P}_A\text{P}_B)}^{\text{f}}$	$^2\text{J}_{(\text{P}_A\text{P}_C)}^{\text{f}}$	$^2\text{J}_{(\text{P}_B\text{P}_C)}^{\text{f}}$
$[\text{Rh}(\text{cod})\text{PPN}_2\text{S}]^{+\text{g,i}}$	-19.90 (178)	-89.37 (2)	-----	61	---	---
$\text{t}[\text{Pd}(\text{PEt}_3)\text{Cl}(\text{PPN}_2\text{S})]^{+\text{g,i}}$	-38.86	-89.09	-124.73	83	32	581
$\text{t}[\text{Pd}(\text{PEt}_3)\text{Br}(\text{PPN}_2\text{S})]^{+\text{g,i}}$	-40.61	-87.15	-121.42	84	34	581
$[\text{PdBr}_2(\text{PPN}_2\text{S})]^{\text{h}}$	-49.30	-95.73	-----	57	---	---
$\text{t}[\text{Pt}(\text{PEt}_3)\text{Cl}(\text{PPN}_2\text{S})]^{+\text{g,i}}$	-44.47 (2849)	-86.96 (127)	-128.16 (2154)	73	32	500
$\text{t}[\text{Pt}(\text{PEt}_3)\text{Br}(\text{PPN}_2\text{S})]^{+\text{g,i}}$	-44.96 (2850)	-87.71 (j)	-131.68 (2119)	71	30	500
$[\text{PtBr}_2(\text{PPN}_2\text{S})]^{\text{g}}$	-67.35 (4236)	-92.47 (j)	-----	48	---	---

Notes: ^a $\text{PPN}_2\text{S} = \text{Ph}_2\text{P}(\text{S})\text{CH}_2\text{P}(\text{NEt}_2)_2$

^b Chemical shift in ppm relative to TMP.

{ } = coupling to metal in Hz.

^c Bis(diethylamino)phosphine.

^d Diphenylthiophosphino.

^e Triethylphosphine.

^f Coupling between phosphines in Hz.

^g In CDCl_3

^h In CD_2Cl_2

ⁱ $[\text{BF}_4]^-$ counter-ion

^j Too small a coupling to see separately from main peak

TABLE 4.2. $^{31}\text{P}\{^1\text{H}\}$ NMR Data for the Cationic Complexes of the Disulphide Ligand; $[\text{LL}'\text{M}(\text{Ph}_2\text{P}(\text{S})\text{CH}_2\text{P}(\text{S})\text{R}_2-\text{S},\text{S}')]\text{anion}^{\text{a}}$

Compound ^b	$\delta\text{P}_A^{\text{c,d}}$	$\delta\text{P}_B^{\text{c,e}}$	$\delta\text{P}_C^{\text{c,f}}$	$^2\text{J}_{(\text{P}_A\text{P}_B)}^{\text{g}}$	$^2\text{J}_{(\text{P}_A\text{P}_C)}^{\text{g}}$	$^2\text{J}_{(\text{P}_B\text{P}_C)}^{\text{g}}$
t[Pt(PEt ₃)Cl(PPN ₂ S ₂)] ⁺	-82.42 {45}	-108.72 {143}	-129.62 {3236}	2	6	13
c[Pt(PEt ₃)Cl(PPN ₂ S ₂)] ⁺	-84.47 {143}	-106.77 {48}	-129.27 {3310}	2	7	13
t[Pd(PEt ₃)Cl(PPN ₂ S ₂)] ⁺	-78.26	-102.05	-106.36	0	6	12
c[Pd(PEt ₃)Cl(PPN ₂ S ₂)] ⁺	-75.72	-104.19	-105.79	0	10	11
[Rh(cod)(PPN ₂ S ₂)] ⁺	-74.59 {0}	-103.05 {0}	-----	2 ^h	--	--
[Ir(cod)(PPN ₂ S ₂)] ⁺	-78.13	-103.76	-----	5	--	--
[Pd(PEt ₃)Cl(DPPMS ₂)] ⁺ ⁱ	-105.84 ^j	-105.04 ^j	-103.01	9	9	9
[Pd(PPh ₃)Cl(DPPMS ₂)] ⁺	-105.61 ^j	105.61 ^j	-108.22	k	k	k

- Notes: **a** L = PEt₃, PPh₃; L' = Cl or L-L' = cod
b PPN₂S₂ = Ph₂P(S)CH₂P(S)(NEt₂)₂.
 DPPMS₂ = Ph₂P(S)CH₂P(S)Ph₂.
 Counter anion is [BF₄]⁻ unless otherwise noted.
 In CDCl₃.
c Chemical shift in ppm relative to T(OMe)₃.
 {} coupling in Hz to metal when necessary.
d Bis(diethylamino)phosphino when PPN₂S₂.
 Diphenylphosphino when DPPMS₂.
e Diphenylphosphine.
f Either triethylphosphine or triphenylphosphine.
g Coupling between phosphines in Hz.
h Maybe $^2\text{J}_{(\text{P}_A\text{P}_B)}$ or $^2\text{J}_{(\text{RhP}_A)}$.
i Private communication from R. Hilts.
 [ClO₄]⁻ counter anion.
j Cis and trans unidentifiable from data available.
k Unresolved coupling.

TABLE 4.3. $^{13}\text{C}\{^1\text{H}\}$ NMR Data for the Cationic Complexes of the Disulphide Ligand; $[\text{LL}'\text{M}(\text{Ph}_2\text{P}(\text{S})\text{CH}_2\text{P}(\text{S})\text{R}_2-\text{S},\text{S}')]\text{BF}_4^{\text{a}}$

Compound ^{b,c}	$-\text{CH}_2-$	PNCH_2CH_3	PNCH_2CH_3	$\text{PCH}_2\text{CH}_3^{\text{d}}$ or $=\text{C}-\text{H}$	$\text{PCH}_2\text{CH}_3^{\text{e}}$ or $-\text{CH}_2-$	<u>Ph</u>
$[\text{Pt}(\text{PEt}_3)\text{Cl}(\text{PPN}_2\text{S}_2)]^{\text{+}}$	31.29(dd) (82) (32)	13.44(s)	40.29(d) (3)	7.63(s)	ca. 14 ^f	129.3 - 133.7
$[\text{Pd}(\text{PEt}_3)\text{Cl}(\text{PPN}_2\text{S}_2)]^{\text{+}}$	30.94(dd) (86) (48)	13.42(s)	40.26(d) (3)	7.99(d)	15.36(d) (31)	128.8 - 133.8
$[\text{Rh}(\text{cod})(\text{PPN}_2\text{S}_2)]^{\text{+}}$	32.30(dd) (82) (48)	13.68(s)	40.17(d) (3)	84.36(d) (12) 83.66(d) (12)	31.12(s)	128.6 - 133.1
$[\text{Ir}(\text{cod})(\text{PPN}_2\text{S}_2)]^{\text{+}}$	32.51(dd) (80) (46)	13.75(s)	40.35(d) (3)	69.13(s) 68.63(s)	31.63(s)	129.3 - 133.3
$[\text{Pd}(\text{PPh}_3)\text{Cl}(\text{DPPMS}_2)]^{\text{+}}$	31.60(t) (47)	-----	-----	-----	-----	127.2 - 134.9

Notes: ^a L = PEt_3 , PPh_3 , L' = Cl or L-L' = cod.
M = Pd, Pt, Ir or Rh.

() = coupling to phosphorus in Hz.

{ } = coupling to platinum in Hz.

s = singlet, d = doublet, t = triplet,
m = multiplet.

Chemical shift in ppm relative TMS.

^b $\text{PPN}_2\text{S}_2 = \text{Ph}_2\text{P}(\text{S})\text{CH}_2\text{P}(\text{S})(\text{NEt}_2)_2$

$\text{DPPMS}_2 = \text{Ph}_2\text{P}(\text{S})\text{CH}_2\text{P}(\text{S})\text{PPh}_2$.

^c In CDCl_3

^d Either methyl carbon of triethylphosphine or methyne carbon of cod.

^e Either methylene carbon of triethylphosphine or methylene carbon of cod.

^f Other peak of doublet hidden.

TABLE 4.4. ^1H NMR Data for the Cationic Complexes of the Disulphide Ligand; $[\text{LL}'\text{M}(\text{Ph}_2\text{P}(\text{S})\text{CH}_2\text{P}(\text{S})\text{R}_2-\text{S},\text{S}')]\text{BF}_4^{\text{a}}$

Compound ^{b,c}	$-\text{CH}_2-$	PNCH_2CH_3	PNCH_2CH_3	$\text{PCH}_2\text{CH}_3^{\text{d}}$ or $=\text{C}-\text{H}$	$\text{PCH}_2\text{CH}_3^{\text{e}}$ or $-\text{CH}_2-$	Ph
$[\text{Pt}(\text{PEt}_3)\text{Cl}(\text{PPN}_2\text{S}_2)]^{\dagger}$	4.22(dd) (15) (13) 2H	1.14(t) (7) ^f	3.06 - 3.46(m) 8H	1.04(dq) (18) ^f [8]	1.87(dt) (11) [8] 6H	7.51 - 8.22 (m) 10H
$[\text{Pd}(\text{PEt}_3)\text{Cl}(\text{PPN}_2\text{S}_2)]^{\dagger}$	4.15(dd) (15) (13) 2H	g	3.07 - 3.47(m) 8H	g	1.58 - 1.98(m) 6H	7.5 - 8.2 (m) 10H
$[\text{Rh}(\text{cod})(\text{PPN}_2\text{S}_2)]^{\dagger}$	4.02(dd) (15) (13) 2H	1.15(t) (7)	3.01 - 3.5(m) 8H	4.10(bs) 4.22(bs) 4H	1.92(bs) 2.32(bs) 8H	7.6 - 8.1 (m) 10H
$[\text{Ir}(\text{cod})(\text{PPN}_2\text{S}_2)]^{\dagger}$	4.14(dd) (14) (14) 2H	1.13(t) (7)	3.06 - 3.47(m) 8H	3.80(bs) 3.96(bs) 4H	1.66(bs) 2.17(bs) 8H	7.3 - 8.0 (m) 10H
$[\text{Pd}(\text{PPh}_3)\text{Cl}(\text{DPPMS}_2)]^{\dagger}$	4.79(t) (13)					7.2 - 8.0 (m)

Notes: ^a L = PEt_3 , PPh_3 , L' = Cl or L-L' = cod.

M = Pd, Pt, Ir or Rh.

() = coupling to phosphorus in Hz.

s = singlet, d = doublet, t = triplet,

m = multiplet.

Chemical shift in ppm relative TMS.

^b $\text{PPN}_2\text{S}_2 = \text{Ph}_2\text{P}(\text{S})\text{CH}_2\text{P}(\text{S})(\text{NEt}_2)_2$

$\text{DPPMS}_2 = \text{Ph}_2\text{P}(\text{S})\text{CH}_2\text{P}(\text{S})\text{PPh}_2$.

^c In CDCl_3

^d Either methyl hydrogen of triethylphosphine or methyne hydrogen of cod.

^e Either methylene hydrogen of triethylphosphine or methylene hydrogen of cod.

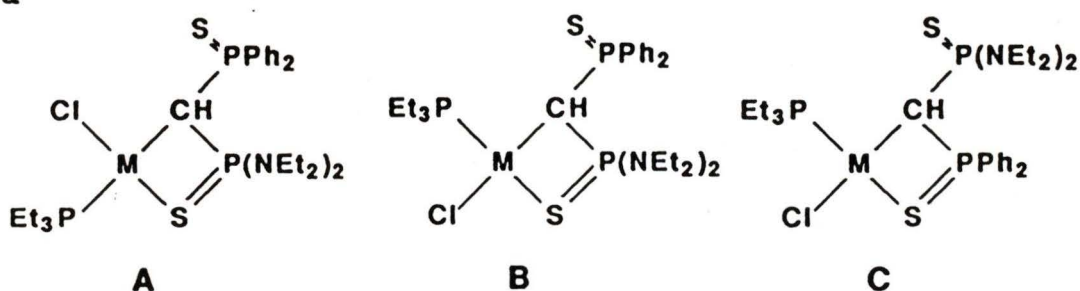
^f Integration of amine methyl and triethylphosphine methyl was 21H.

^g Part of multiplet at 1.01 - 1.23 ppm(21H)

TABLE 4.5. $^{31}\text{P}\{^1\text{H}\}$ NMR Data for
 $[\text{MCl}(\text{PEt}_3)(\text{Ph}_2\text{P}(\text{S})\text{CHP}(\text{S})(\text{NEt}_2)_2\text{-C,S})]$

Compound ^a	$\delta\text{P}_\text{A}^{\text{b,c}}$	$\delta\text{P}_\text{B}^{\text{b,d}}$	$\delta\text{P}_\text{C}^{\text{b,e}}$	$^2\text{J}(\text{P}_\text{A}\text{P}_\text{B})^{\text{f}}$	$^2\text{J}(\text{P}_\text{A}\text{P}_\text{C})^{\text{f}}$	$^2\text{J}(\text{P}_\text{B}\text{P}_\text{C})^{\text{f}}$
M = Pd A	-69.85	-101.98	-120.74	6	5	16
M = Pt A	-69.29 (477)	-102.48 (93)	-134.06 (2985)	7	8	13
M = Pd B	-70.39	-103.99	-118.96	6	5	15
M = Pd C	-72.73	-87.36	-120.55	7	9	17

Notes: ^a



^b Chemical shift in ppm relative to TMP.

{ } = $^2\text{J}(\text{Pt-P})$.

^c Bis(diethylamino)phosphinesulphide.

^d Diphenylphosphinesulphide.

^e Triethylphosphine.

^f Coupling between phosphines in Hz.

TABLE 4.6^a. $^{31}\text{P}\{^1\text{H}\}$ NMR Data for
 $[\text{M}(\text{LL}')\{\text{Ph}_2\text{P}(\text{S})\text{CHP}(\text{S})\text{R}_2-\text{S},\text{S}'\}]$

Compound ^b	δP_A^c	δP_A^c	δP_C^c	$^2\text{J}_{(\text{P}_A\text{P}_B)}^d$	$^2\text{J}_{(\text{P}_A\text{P}_C)}^d$	$^2\text{J}_{(\text{P}_B\text{P}_C)}^d$
$[\text{Pd}(\text{PEt}_3)\text{Cl}(\text{PPN}_2\text{S}_2)]^{e,f}$	-84.43	-113.88	-129.03	51	13	15
$[\text{Pt}(\text{PEt}_3)\text{Cl}(\text{PPN}_2\text{S}_2)]^{e,g}$	-84.51 (519)	-109.91 (477)	-139.84 (3461)	54	10	19
$[\text{Pd}(\text{PEt}_3)\text{Cl}(\text{DPPMS}_2)]^{i,f}$	-103.62	-103.62	-129.02	-f-	17 ^k	17 ^k
$[\text{Pd}(\text{PPh}_3)\text{Cl}(\text{DPPMS}_2)]^{i,g}$	-101.91	-101.91	-118.65	-f-	15 ^k	15 ^k
$[\text{Rh}(\text{cod})(\text{PPN}_2\text{S}_2)]^h$	-67.51 (9)	-103.12 (4)	-----	28	---	---

- Notes: ^a M = Pt, Pt or Rh; L-L' = cod or
L = Cl, L' = PEt₃, PPh₃
^b PPN₂S₂ = [Ph₂P(S)CHP(S)(NEt₂)₂]; DPPMS₂ =
[Ph₂P(S)CHP(S)Ph₂]; P_A = P(S)(NEt₂)₂ for PPN₂S₂
or Ph₂P(S) for DPPMS₂ containing complexes; P_B =
Ph₂P(S); P_C = triethylphosphine.
^c Chemical shift in ppm relative to TMP. {} =
coupling to spin-active metal in Hz.
^d Coupling between phosphines in Hz.
^e Cis or trans configuration unknown.
^f CD₂Cl₂. ^g THF (external C₆D₆). ^h C₆D₆.
ⁱ Deceptively simple ABX spin pattern.
^j A doublet and triplet with directly measured
coupling equal to 1/2(JP_AP_C + JP_BP_C).
^k Unable to determine JP_AP_B.

Table 4.7. Rate Data for the Dynamic Equilibrium of Sulphur Exchange in *trans*-[PdCl(PEt₃)(Ph₂P(S)CHP(S)(NEt₂)₂-C,S)] Derived from the Parameters used in the Band Shape Analysis Simulation of the Variable Temperature ³¹P{¹H} NMR.

T (K)	1/T (K ⁻¹)x10 ³	k _{Obs} (s ⁻¹)	lnk	ln(k/T)
193	5.181	6	1.792	-3.471
213	4.695	80	4.382	-0.979
223	4.484	200	5.298	-0.109
233	4.292	650	6.477	1.026
243	4.115	1200	7.090	1.597
253	3.953	2000	7.601	2.473
263	3.802	9000	9.105	3.533
273	3.663	15000	9.616	4.006
283	3.534	30000	10.309	4.664
301	3.322	100000	11.513	5.783

TABLE 4.8. Rate Plot and Thermodynamic Parameters for
Sulphur Interchange in *trans*-
[PdCl(PEt₃)(Ph₂P(S)CHP(S)(NEt₂)₂-C,S)]

ln k _{obs} vs 1/T	slope	-5075 ± 125
	intercept	28.11 ± 0.52
	correlation	0.9952
ln (k _{obs} /T) vs 1/T	slope	-4853 ± 84
	intercept	21.73 ± 0.35
	correlation	0.9976

$$E_a = 42.2 \text{ kJ/mol}$$

$$\Delta S^\ddagger = -17 \text{ J/K}$$

$$\Delta H^\ddagger = 40.4 \text{ kJ}$$

$$\Delta G^\ddagger = 45.4 \text{ kJ}$$

TABLE 4.9. Crystallographic Parameters for
cis-[PdCl(PEt₃)(Ph₂P(S)CH₂P(S)(NEt₂)₂-S,S')]BF₄

formula	PdClS ₂ P ₃ N ₂ C ₂₇ H ₄₇
fw	785.4
space group	Pna2 ₁
a (Å)	19.673(4)
b (Å)	11.597(3)
c (Å)	15.752(2)
α (degrees)	90
β (degrees)	90
(degrees)	90
volume (Å ³)	3594
Z	4
calculated density (g cm ⁻³)	1.452
crystal size (mm ³)	0.14 x 0.15 x 0.59
F(000) (e)	2352
μ (cm ⁻¹)	8.688960
radiation (Å)	0.71096
temperature (K)	295
scan method	θ/2θ
data collected	0-50 in 2θ
total reflections collected	3335
unique data	2414
parameters refined	367
R	0.0747
R _w	0.0760
largest shift/esd	0.01

TABLE 4.10. Interatomic distances (Å) for



Atoms	Distance	Atoms	Distance
Cl(1) -Pd(1)	2.346(4)	C(7) -C(6)	1.610(35)
S(1) -Pd(1)	2.285(5)	C(9) -C(8)	1.473(31)
S(2) -Pd(1)	2.466(5)	C(11) -C(10)	1.536(28)
P(1) -Pd(1)	2.233(5)	C(13) -C(12)	1.492(41)
P(2) -S(1)	2.018(7)	C(15) -C(14)	1.611(35)
P(3) -S(2)	1.978(6)	C(17) -C(16)	1.347(29)
C(2) -P(1)	1.845(23)	C(21) -C(16)	1.410(28)
C(4) -P(1)	1.824(21)	C(18) -C(17)	1.423(34)
C(6) -P(1)	1.767(22)	C(19) -C(18)	1.391(40)
N(1) -P(2)	1.630(15)	C(20) -C(19)	1.451(35)
N(2) -P(2)	1.639(16)	C(21) -C(20)	1.386(33)
C(1) -P(2)	1.834(17)	C(23) -C(22)	1.390(31)
C(1) -P(3)	1.826(18)	C(27) -C(22)	1.445(33)
C(16) -P(3)	1.819(18)	C(24) -C(23)	1.388(38)
C(22) -P(3)	1.802(23)	C(25) -C(24)	1.350(42)
C(8) -N(1)	1.470(27)	C(26) -C(25)	1.426(41)
C(10) -N(1)	1.483(22)	C(27) -C(26)	1.407(27)
C(12) -N(2)	1.518(24)	F(1) -B(1)	1.245(40)
C(14) -N(2)	1.444(25)	F(2) -B(1)	1.372(35)
C(3) -C(2)	1.510(32)	F(3) -B(1)	1.395(45)
C(5) -C(4)	1.536(31)	F(4) -B(1)	1.270(40)

Estimated standard deviations are given in parentheses.

TABLE 4.11. Bond angles ($^{\circ}$) for

Atoms	Angle	Atoms	Angle
S(1) -Pd(1) -Cl(1)	173.0(2)	C(14) -N(2) -C(12)	111.4(17)
S(2) -Pd(1) -Cl(1)	85.9(2)	P(3) -C(1) -P(2)	112.9(9)
S(2) -Pd(1) -S(1)	98.7(2)	C(3) -C(2) -P(1)	110.3(15)
P(1) -Pd(1) -Cl(1)	86.7(2)	C(5) -C(4) -P(1)	116.8(19)
P(1) -Pd(1) -S(1)	89.4(2)	C(7) -C(6) -P(1)	111.5(17)
P(1) -Pd(1) -S(2)	170.0(2)	C(9) -C(8) -N(1)	116.2(19)
P(2) -S(1) -Pd(1)	111.9(3)	C(11) -C(10) -N(1)	110.9(15)
P(3) -S(2) -Pd(1)	99.4(2)	C(13) -C(12) -N(2)	115.6(18)
C(2) -P(1) -Pd(1)	109.4(7)	C(15) -C(14) -N(2)	107.6(19)
C(4) -P(1) -Pd(1)	111.9(7)	C(17) -C(16) -P(3)	120.8(16)
C(4) -P(1) -C(2)	104.9(9)	C(21) -C(16) -P(3)	118.7(16)
C(6) -P(1) -Pd(1)	117.5(7)	C(21) -C(16) -C(17)	120.3(18)
C(6) -P(1) -C(2)	104.4(11)	C(18) -C(17) -C(16)	123.2(24)
C(6) -P(1) -C(4)	107.8(11)	C(19) -C(18) -C(17)	118.8(27)
N(1) -P(2) -S(1)	112.9(6)	C(20) -C(19) -C(18)	116.8(25)
N(2) -P(2) -S(1)	111.1(6)	C(21) -C(20) -C(19)	123.2(24)
N(2) -P(2) -N(1)	106.3(8)	C(20) -C(21) -C(16)	117.6(22)
C(1) -P(2) -S(1)	111.6(6)	C(23) -C(22) -P(3)	119.8(18)
C(1) -P(2) -N(1)	109.6(8)	C(27) -C(22) -P(3)	119.3(17)
C(1) -P(2) -N(2)	104.9(8)	C(27) -C(22) -C(23)	120.7(22)
C(1) -P(3) -S(2)	113.8(6)	C(24) -C(23) -C(22)	121.9(24)
C(16) -P(3) -S(2)	110.7(7)	C(25) -C(24) -C(23)	118.4(28)
C(16) -P(3) -C(1)	102.9(8)	C(26) -C(25) -C(24)	122.2(26)
C(22) -P(3) -S(2)	112.8(7)	C(27) -C(26) -C(25)	120.7(28)
C(22) -P(3) -C(1)	108.4(9)	C(26) -C(27) -C(22)	115.9(25)
C(22) -P(3) -C(16)	107.6(8)	F(2) -B(1) -F(1)	119.4(39)
C(8) -N(1) -P(2)	118.4(12)	F(3) -B(1) -F(1)	100.0(28)
C(10) -N(1) -P(2)	126.8(14)	F(3) -B(1) -F(2)	97.7(30)
C(10) -N(1) -C(8)	114.5(16)	F(4) -B(1) -F(1)	118.5(30)
C(12) -N(2) -P(2)	122.4(14)	F(4) -B(1) -F(2)	110.1(29)
C(14) -N(2) -P(2)	119.9(14)	F(4) -B(1) -F(3)	107.3(48)

Estimated standard deviations are given in parentheses.

TABLE 4.12. Fractional atomic coordinates and temperature parameters for $[\text{PdCl}(\text{PEt}_3)(\text{Ph}_2\text{P}(\text{S})\text{CH}_2\text{P}(\text{S})(\text{NEt}_2)_2\text{-S,S}')]\text{BF}_4$

Atom	x/a	y/b	z/c	U_{eq}
Pd(1)	5220(0)	14530(0)	17350(0)	321(3)
Cl(1)	1037(3)	111(3)	1809(7)	56(2)
S(1)	-93(3)	2678(3)	1571(5)	43(2)
S(2)	895(3)	1612(3)	3754(4)	39(2)
P(1)	363(3)	1211(3)	-143(5)	42(2)
P(2)	-300(2)	3195(3)	3124(4)	29(1)
P(3)	1179(2)	2817(3)	3722(4)	31(1)
N(1)	-713(7)	2552(9)	3973(13)	34(5)
N(2)	-775(8)	4044(10)	2990(14)	42(6)
C(1)	474(9)	3566(11)	3846(16)	38(5)
C(2)	-248(11)	332(14)	-328(18)	54(8)
C(3)	-946(14)	601(17)	71(27)	82(11)
C(4)	1140(11)	847(14)	-847(17)	49(7)
C(5)	1105(16)	707(19)	-2156(21)	79(11)
C(6)	22(13)	2046(14)	-979(18)	60(8)
C(7)	572(15)	2789(17)	-1183(24)	82(11)
C(8)	-877(13)	2841(13)	5145(19)	57(8)
C(9)	-530(15)	2396(16)	6094(19)	72(10)
C(10)	-892(10)	1654(11)	3735(22)	48(7)
C(11)	-1641(10)	1574(15)	3378(26)	67(9)
C(12)	-478(12)	4918(11)	2768(19)	50(8)
C(13)	-149(15)	5036(17)	1619(31)	95(12)
C(14)	-1455(11)	3972(15)	2529(21)	56(8)
C(15)	-1969(14)	4387(22)	3453(28)	101(14)
C(16)	1698(9)	3069(13)	4974(15)	37(6)
C(17)	1914(11)	3868(15)	5165(19)	55(8)
C(18)	2357(15)	4091(21)	6086(24)	85(13)
C(19)	2559(12)	3463(16)	6857(26)	66(9)
C(20)	2331(13)	2605(19)	6618(21)	76(10)
C(21)	1913(11)	2401(16)	5697(16)	52(8)
C(22)	1665(10)	3084(14)	2455(18)	44(7)
C(23)	1951(10)	2442(14)	1792(25)	49(6)
C(24)	2331(12)	2615(22)	811(25)	78(12)
C(25)	2394(12)	3432(24)	472(24)	78(12)
C(26)	2081(13)	4114(22)	1081(21)	82(12)
C(27)	1704(12)	3959(18)	2091(16)	59(9)
B(1)	345(2)	115(2)	865(4)	9(1)
F(1)	354(1)	194(1)	869(2)	10(1)
F(2)	397(1)	62(1)	892(2)	14(1)
F(3)	346(2)	103(2)	746(2)	22(2)
F(4)	289(1)	86(1)	902(4)	26(3)

Notes for Table 4.12.

Estimated standard deviations are given in parentheses.

Coordinates $\times 10^n$ where $n = 5$ for Pd; 4 for Cl, S, P, N, C; 3 F, B

Temperature parameters $\times 10^n$ where $n = 4$ for Pd; 3 for Cl, S, P, N, C; 2 F, B

U_{eq} = the equivalent isotropic temperature parameter.

$$U_{eq} = 1/3 \sum_i \sum_j U_{ij} a_i^* a_j^* (a_i \cdot a_j)$$

TABLE 4.13. Anisotropic temperature parameters (\AA^2) for
 $[\text{PdCl}(\text{PEt}_3)(\text{Ph}_2\text{P}(\text{S})\text{CH}_2\text{P}(\text{S})(\text{NEt}_2)_2\text{-S,S}')]\text{BF}_4$

Atom	U_{11}	U_{22}	U_{33}	U_{23}	U_{13}	U_{12}
Pd(1)	385(6)	264(6)	315(6)	-21(8)	-19(9)	29(6)
Cl(1)	78(3)	39(2)	50(3)	4(3)	-2(4)	22(2)
S(1)	57(3)	40(2)	33(3)	-6(2)	-5(3)	14(2)
S(2)	47(3)	29(2)	40(3)	0(2)	-6(2)	0(2)
P(1)	56(4)	36(3)	34(3)	-5(2)	-2(2)	5(2)
P(2)	26(2)	27(2)	33(2)	-6(2)	-2(2)	5(2)
P(3)	33(3)	33(2)	28(2)	0(2)	-2(2)	-3(2)
N(1)	38(9)	30(8)	35(8)	-6(7)	1(7)	-6(7)
N(2)	52(11)	32(9)	42(10)	2(7)	-1(8)	4(8)
C(1)	30(9)	34(9)	48(10)	-7(9)	-3(9)	-8(8)
C(2)	59(14)	57(13)	45(12)	-19(11)	17(11)	7(11)
C(3)	67(18)	69(16)	110(24)	-26(18)	2(17)	-21(15)
C(4)	50(12)	58(14)	38(11)	-9(10)	20(10)	-8(11)
C(5)	103(23)	94(21)	40(14)	-3(14)	3(13)	-1(18)
C(6)	89(17)	56(14)	34(11)	-6(10)	-6(12)	21(13)
C(7)	106(22)	79(18)	63(16)	-1(14)	-5(18)	-9(17)
C(8)	76(16)	44(12)	50(13)	17(11)	8(12)	-2(12)
C(9)	110(21)	64(16)	41(13)	8(11)	-14(14)	28(16)
C(10)	32(10)	27(9)	84(15)	-2(11)	-8(11)	9(8)
C(11)	28(11)	65(15)	107(21)	-3(15)	5(12)	-6(11)
C(12)	67(16)	22(9)	61(14)	-5(9)	-12(12)	-1(10)
C(13)	110(22)	77(16)	98(24)	54(20)	-35(23)	-31(16)
C(14)	27(11)	48(13)	93(18)	-28(13)	-14(11)	20(10)
C(15)	59(17)	145(29)	98(24)	36(22)	28(16)	35(18)
C(16)	37(11)	52(13)	23(9)	-6(9)	-11(8)	17(9)
C(17)	52(14)	59(14)	55(14)	-31(12)	-8(11)	-5(11)
C(18)	77(20)	116(26)	64(19)	-31(18)	8(15)	-2(18)
C(19)	68(14)	87(17)	43(13)	6(16)	-14(14)	-15(13)
C(20)	82(16)	119(21)	27(12)	32(16)	15(14)	-1(15)
C(21)	47(13)	78(17)	31(11)	13(12)	-17(10)	-10(11)
C(22)	26(10)	52(13)	54(13)	-2(11)	-29(10)	-9(10)
C(23)	32(8)	72(12)	44(10)	-6(16)	-5(13)	1(8)
C(24)	48(16)	119(27)	68(16)	-15(19)	8(14)	-15(16)
C(25)	38(13)	129(28)	68(17)	-7(19)	5(12)	-10(16)
C(26)	55(17)	145(29)	47(15)	14(16)	26(13)	-39(18)
C(27)	57(15)	89(18)	30(12)	23(10)	2(9)	7(13)
B(1)	9(3)	7(2)	10(3)	4(2)	4(2)	4(2)
F(1)	13(1)	6(1)	13(1)	2(1)	1(1)	-2(1)
F(2)	9(1)	12(1)	20(2)	-1(2)	-2(1)	5(1)
F(3)	43(6)	12(2)	12(2)	0(2)	-3(3)	6(3)
F(4)	13(2)	10(2)	56(7)	6(3)	13(3)	0(1)

Notes for Table 4.13.

Estimated standard deviations are given in parentheses.

U values $\times 10^n$ where $n = 4$ for Pd; 3 for Cl, S, P, N, C; 2 F, B

$$T = \exp -2\pi^2(U_{11}h^2a^{*2} + \dots + 2U_{23}klb^*c^* + \dots)$$

Table 4.14. Selected intermolecular distances (Å) for
 $[\text{PdCl}(\text{PEt}_3)(\text{Ph}_2\text{P}(\text{S})\text{CH}_2\text{P}(\text{S})(\text{NEt}_2)_2\text{-S,S}')]\text{BF}_4$

Atoms	Distance	Sym	T _x	T _y	T _z
C(2) ...Pd(1)	4.449	2	0	0	-1
C(2) ...Cl(1)	3.730	2	0	0	-1
C(3) ...Cl(1)	3.949	2	0	0	-1
C(18) ...Cl(1)	3.643	4	0	0	0
C(19) ...Cl(1)	3.790	4	0	0	0
C(2) ...S(2)	3.484	2	0	0	-1
C(3) ...S(2)	3.807	2	0	0	-1
F(2) ...C(1)	3.410	4	0	-1	0
C(25) ...C(3)	3.634	3	0	0	0
F(4) ...C(4)	3.447	1	0	0	1
C(9) ...C(6)	3.606	1	0	0	1
F(1) ...C(6)	3.346	3	0	0	1
F(3) ...C(8)	3.470	3	0	0	0
F(3) ...C(9)	3.547	3	0	0	0
C(17) ...C(11)	3.586	3	0	0	0
C(22) ...C(11)	3.541	3	0	0	0
C(23) ...C(11)	3.668	3	0	0	0
C(27) ...C(11)	3.678	3	0	0	0
F(2) ...C(12)	3.431	4	0	-1	0
F(2) ...C(17)	3.565	4	0	-1	0
F(4) ...C(17)	3.428	4	0	-1	0
F(1) ...C(24)	3.589	1	0	0	1
F(3) ...C(26)	3.576	4	0	-1	0
F(3) ...C(27)	3.306	4	0	-1	0

Symmetry positions for the second atom are, 1: x, y, z
 2: $-x, -y, \frac{1}{2}+z$
 3: $x+\frac{1}{2}, \frac{1}{2}-y, z$
 4: $\frac{1}{2}-x, \frac{1}{2}+y, \frac{1}{2}+z$

Negative symmetry positions denote inversion and the translations are applied after the symmetry position has been defined.

CHAPTER 5: Experimental Section

Experimental section

Synthetic and Spectroscopic Studies

Data relating to the characterization of the complexes are given in the Tables, the Results and Discussion chapters and the preparative descriptions below. Microanalysis was by the Canadian Microanalytical Services, New Westminster, B.C., Canada. Infrared spectra were recorded on a Perkin-Elmer 283 spectrophotometer and calibrated using the 1601 cm^{-1} absorption of polystyrene. Solids were obtained either as potassium bromide discs or nujol mulls. ^{31}P nuclear magnetic resonance spectra were recorded in appropriate solvents (see tabulated NMR data) at either 24.3 MHz using a Nicolet TT14 Fourier transform spectrometer with a Varian HA60 magnet and an external C_6D_6 lock signal, or at 101.3 MHz using a Brüker WM250 Fourier transform spectrometer locked to the solvent deuterium resonance or to an external C_6D_6 lock signal. ^{13}C , ^1H , ^{195}Pt and ^{15}N spectra were recorded at 62.9, 250.1, 53.5 and 25.35 MHz respectively, in deuterated solvents using the Brüker instrument. For all non-proton nuclei the protons were decoupled by broad band ("noise") irradiation at appropriate frequencies. ^{31}P chemical shifts were measured relative to external $\text{P}(\text{OMe})_3$. ^{13}C , ^1H , ^{195}Pt and ^{15}N are reported in ppm relative to $\text{Si}(\text{Me})_4$, $\text{Si}(\text{Me})_4$, $\Sigma(^{195}\text{Pt}) = 21.4\text{ MHz}^{97}$ and CD_3NO_2 respectively. Positive values are deshielded relative to the

references. Simulated NMR spectra were calculated on an IBM 3031 computer and plotted on a Calcomp 1039 plotter. The programs used were a locally constructed package⁹⁸ based on the UEAITR and NMRPLOT programs from the literature.^{99,100} The band shape analysis program described by Kleier and Binsch⁹⁵ was used to extract thermodynamic data from the variable-temperature $^{31}\text{P}\{^1\text{H}\}$ NMR spectra.

Crystals suitable for study by X-Ray diffraction were photographed with Weissenberg and precession cameras using Cu K α radiation. After the unit cell and the symmetry of the crystals were established, they were transferred to a Picker 4-circle diffractometer using Zr filtered Mo K α radiation. All crystal structures were solved by Dr. J. Browning.

All synthetic operations were carried out at ambient temperature (ca. 25°C; unless otherwise stated) under an atmosphere of dry nitrogen using standard Schlenk tube techniques. Solvents were dried by reflux over appropriate reagents (calcium hydride for dichloromethane, molecular sieves or K₂CO₃ for acetone and potassium/benzophenone for diethyl ether, tetrahydrofuran, benzene and hexane) and were distilled under nitrogen prior to use. Recrystallizations from solvent pairs were by dissolution of the complex in the first solvent (using about double the volume required for complete solution) followed by dropwise addition of sufficient second solvent to cause turbidity at ambient tempera-

ture. Crystallization was then completed by continued very slow dropwise addition of the second solvent.

^{31}P NMR data for the metal complexes used as starting materials were recorded in CD_2Cl_2 solution: $[\text{Pd}_2(\mu\text{-Cl})_2\text{Cl}_2(\text{PEt}_3)_2]$, $\delta(\text{P})$ -91.48 ppm, $[\text{Pt}_2(\mu\text{-Cl})_2\text{Cl}_2(\text{PEt}_3)_2]$, $\delta(\text{P})$ -129.15 ppm, $^1\text{J}_{\text{Pt-P}}$, 3832 Hz.

All starting metal dimers and complexes were prepared by literature methods: $([\text{Pt}_2(\mu\text{-Cl})_2\text{Cl}_2(\text{PEt}_3)_2])$,⁴⁷ $[\text{Pd}_2(\mu\text{-Cl})_2\text{Cl}_2(\text{PEt}_3)_2]$,⁴⁷ $[\text{Rh}(\text{cod})\mu\text{-Cl}]_2$,⁴⁸ $[\text{Ir}(\text{cod})\mu\text{-Cl}]_2$,⁴⁹ $[\text{PtCl}_2(\text{cod})_2]$,¹⁰¹ $[\text{Rh}(\text{cod})\text{Bipyridyl}]\text{BF}_4$ ⁵² and $[\text{Rh}(\text{cod})(\text{MeCN})_2]\text{BF}_4$,¹⁰²

Starting precious metal compounds were obtained from two sources: Aldrich Chemicals Ltd. for $\text{IrCl}_3 \cdot 3\text{H}_2\text{O}$ and $\text{RhCl}_3 \cdot 3\text{H}_2\text{O}$, and Johnson-Matthey Ltd. for PdCl_2 , PtCl_2 and K_2PtCl_4 .

EXPERIMENTAL FOR CHAPTER 2

Preparation of $[\text{P}(\text{NEt}_2)_2\text{Cl}]_2$

A solution of phosphorus trichloride (2.0 mL, 3.1 g, 23.0 mmol) in diethyl ether (10 mL) was added dropwise via a non-pressure equalizing addition funnel to a diethyl ether (100 mL) solution of diethylamine (9.48 mL, 6.70 g, 91.7 mmol) in a round-bottomed flask equipped with an efficient magnetic

stirrer and a condenser, at 0-5°C. After addition the mixture was allowed to warm to ambient temperature over 24 h. The resulting solution was filtered from the white precipitate of amine hydrogenchloride and the solvent removed *in vacuo* to yield $[\text{PCl}(\text{NEt}_2)_2]$ as a pale yellow oil (52%, 2.51 g, 11.9 mmol) which was characterised by $^{31}\text{P}\{^1\text{H}\}$ NMR.

$^{31}\text{P}\{^1\text{H}\}$ NMR: δ (ppm); 12.0 (s).¹⁰³

Preparation of $[\text{PCl}(\text{NMe}_2)_2]$

$[\text{PCl}(\text{NMe}_2)_2]$ was prepared by a similar procedure to that described for the preparation of $[\text{PCl}(\text{NEt}_2)_2]$. The product, a pale yellow oil (50% yield), was characterised by $^{31}\text{P}\{^1\text{H}\}$ NMR.

$^{31}\text{P}\{^1\text{H}\}$ NMR: δ (ppm); 17.4 (s).¹⁰³

Preparation of $[\text{PCl}\{\text{N}(\text{CH}_2\text{CH}_2)_2\text{CH}_2\}_2]$

$[\text{PCl}\{\text{N}(\text{CH}_2\text{CH}_2)_2\text{CH}_2\}_2]$ was prepared by a similar procedure to that described for the preparation of $[\text{PCl}(\text{NEt}_2)_2]$. The product, a pale yellow oil (50% yield), was characterised by $^{31}\text{P}\{^1\text{H}\}$ NMR.

$^{31}\text{P}\{^1\text{H}\}$ NMR: δ (ppm); 8.2 (s).

Preparation of $[\text{PCl}(\text{NEt}_2)\text{Ph}]$

$[\text{PCl}(\text{NEt}_2)\text{Ph}]$ was prepared by a similar procedure to that described for the preparation of $[\text{PCl}(\text{NEt}_2)_2]$. Dichlorophenylphosphine (3.0 mL, 2.3 g, 22.0 mmol); diethylamine

(4.56 mL, 3.22 g, 44.2 mmol). The product, an orange oil (62%, 2.95 g, 13.7 mmol), was characterised by $^{31}\text{P}\{^1\text{H}\}$, ^1H and $^{13}\text{C}\{^1\text{H}\}$ NMR.

$^{31}\text{P}\{^1\text{H}\}$ NMR: δ (ppm); 1.32 (s).¹⁰⁵

^1H NMR: δ (ppm); N-CH₂-CH₃, 1.09 (t, 6H, $^3J_{\text{HH}} = 7$ Hz); N-CH₂-CH₃, 3.10 (m, 4H), Ph, 7.41-7.74 (5H, m)

$^{13}\text{C}\{^1\text{H}\}$ NMR: δ (ppm); N-CH₂-CH₃, 14.04 (d, $^3J_{\text{P-C}} = 6$ Hz), N-CH₂-CH₃, 43.86 (d, $^2J_{\text{P-C}} = 13$ Hz); Ph, 128.31-130.83 (m).

Preparation of $[\text{Ph}_2\text{PCH}_2\text{P}(\text{NET}_2)_2]$

(Method adapted from a procedure by S.O. Grim and J.D. Mitchell).²³

A solution of diphenylmethylphosphine (1.28 mL, 1.38 g, 6.88 mmol), TMEDA (1.54 mL, 1.19 g, 10.2 mmol) and excess *n*-butyllithium (7 mL, 1.6 M in hexanes) in hexane (20 mL) was stirred under nitrogen for 24 h, whereupon $[\text{Ph}_2\text{PCH}_2]\text{-}[\text{Li.TMEDA}]$ precipitated. The supernatant was then extracted and the precipitate washed with 2x20 mL hexane and dried *in vacuo*. $[\text{Ph}_2\text{PCH}_2][\text{Li.TMEDA}]$ (1.23 g, 3.82 mmol, 56%) in THF (5 mL) was then added to a stirred THF (5 mL) solution of $[\text{PCl}(\text{NET}_2)_2]$ (0.805 g, 3.82 mmol). After 1.5 h the solvent was removed *in vacuo* and the oily residue extracted with 2x5 mL diethyl ether and the extracts combined. All volatiles were then removed *in vacuo* for 6 h yielding a pale yellow

oil of $[\text{Ph}_2\text{PCH}_2\text{P}(\text{NEt}_2)_2]$ (1.11 g, 2.97 mmol, 78%) which was characterised by $^{31}\text{P}\{^1\text{H}\}$, $^{13}\text{C}\{^1\text{H}\}$ and $^{15}\text{N}\{^1\text{H}\}$ NMR.

IR, neat, $\nu(\text{cm}^{-1})$: 2965(s), 1433(m), 1370(m), 1190(s), 1185(s), 1020(s), 1010(s), 915(m), 908(m), $\nu_{\text{P-N}}$ 740(s), $\nu_{\text{P-N}}$ 695(s).

$^{15}\text{N}\{^1\text{H}\}$ NMR: δ (ppm): -317.40 (d of d, $^1J_{\text{P-N}} = 75$ Hz, $^3J_{\text{P-N}} = 4$ Hz).

Preparation of $[\text{Ph}_2\text{PCH}_2\text{P}(\text{NMe}_2)_2]$

The title compound was prepared by a similar procedure to that described for $[\text{Ph}_2\text{PCH}_2\text{P}(\text{NEt}_2)_2]$. The product (30% yield) was characterised by $^{31}\text{P}\{^1\text{H}\}$ NMR.

Preparation of $[\text{Ph}_2\text{PCH}_2\text{P}(\text{N}(\text{CH}_2\text{CH}_2)_2\text{CH}_2)_2]$

The title compound was prepared by a similar procedure to that described for $[\text{Ph}_2\text{PCH}_2\text{P}(\text{NEt}_2)_2]$. The product (76% yield) was characterised by $^{31}\text{P}\{^1\text{H}\}$ NMR.

Preparation of $[\text{Ph}_2\text{PCH}_2\text{P}(\text{NEt}_2)\text{Ph}]$

The title compound was prepared by a similar procedure to that described for $[\text{Ph}_2\text{PCH}_2\text{P}(\text{NEt}_2)_2]$. The product (68% yield) was characterised by $^{31}\text{P}\{^1\text{H}\}$ and $^{13}\text{C}\{^1\text{H}\}$ NMR.

Preparation of $[\text{Ph}_2\text{P}(\text{S})\text{CH}_2\text{P}(\text{NEt}_2)_2]$

(Prepared using a method similar to that described by S.O. Grim et al.).²⁴

Methylolithium (7.72 mL, 10.8 mmol, 1.4 M in diethyl ether)

was added dropwise to a stirred solution of Ph_3PS (3.18 g, 10.8 mmol) in THF (10 mL) and diethyl ether (10 mL). A deep red homogeneous solution of $[\text{Ph}_2\text{P}(\text{S})\text{CH}_2]\text{Li}$ was formed after 1 h of stirring. The solution of $[\text{Ph}_2\text{P}(\text{S})\text{CH}_2]\text{Li}$ was then added dropwise to a stirred solution of $[\text{PCl}(\text{NET}_2)_2]$ (2.28 g, 10.8 mmol) in diethyl ether (10 mL). The yellow solution and LiCl precipitate were then stirred for a further 4 h to ensure completion of reaction. Solvents were then removed *in vacuo* and the oily residue extracted with three 10 mL portions of dichloromethane. The extracts were combined and the solvent removed *in vacuo* to yield a pale yellow oil (2.06 g, 5.1 mmol, 47%, ca. 95% pure by $^{31}\text{P}\{^1\text{H}\}$ NMR) which was characterised by $^{31}\text{P}\{^1\text{H}\}$ and $^{13}\text{C}\{^1\text{H}\}$ NMR.

Preparation of $[\text{ClP}(\text{S})(\text{NET}_2)_2]$

A solution of $[\text{ClP}(\text{NET}_2)_2]$ (1.13 g, 5.35 mmol) and sulphur (0.127 g, 5.35 mmol) in benzene (70 mL) was heated under reflux for 0.5 h. The solvent was then removed *in vacuo* to yield the product (1.12 g, 4.26 mmol, 86.4%) as a yellow oil which was characterised by $^{31}\text{P}\{^1\text{H}\}$ and $^{13}\text{C}\{^1\text{H}\}$ NMR.

$^{31}\text{P}\{^1\text{H}\}$ NMR: δ (ppm); -57.15 (s).¹⁰⁵

$^{13}\text{C}\{^1\text{H}\}$ NMR: δ (ppm); $\text{N}-\text{CH}_2-\underline{\text{C}}\text{H}_3$, 13.11 (d, $^3\text{J}_{\text{P}-\text{C}} = 4$ Hz), $\text{N}-\underline{\text{C}}\text{H}_2-\text{CH}_3$, 40.49 (d, $^2\text{J}_{\text{P}-\text{C}} = 4$ Hz)

Reaction of $[\text{ClP}(\text{S})(\text{NET}_2)_2]$ with $[\text{Ph}_2\text{PCH}_2][\text{Li.TMEDA}]$

A solution of $[\text{Ph}_2\text{PCH}_2][\text{Li.TMEDA}]$ ²³ (0.988 g, 3.06 mmol) in

THF (10 mL) was added to a stirred solution of $[\text{ClP}(\text{S})(\text{NET}_2)_2]$ (0.743 g, 3.06 mmol) in THF (5 mL). After 2 h the solvent was removed *in vacuo* and the $^{31}\text{P}\{^1\text{H}\}$ NMR recorded. The $^{31}\text{P}\{^1\text{H}\}$ NMR showed a mixture of compounds, none of which could be identified as $[\text{Ph}_2\text{PCH}_2\text{P}(\text{S})(\text{NET}_2)_2]$.

Reaction of $[\text{ClP}(\text{S})(\text{NET}_2)_2]$ with MeLi

Methyl lithium (3.62 mL, 1.92 mmol, 1.4 M in diethyl ether) was added to a stirred THF (6 mL) solution of $[\text{ClP}(\text{S})(\text{NET}_2)_2]$ (0.465 g, 1.92 mmol). The mixture initially clarified, then turned yellow over 2 h where upon the solvent was removed *in vacuo* and the $^{31}\text{P}\{^1\text{H}\}$ NMR recorded. The $^{31}\text{P}\{^1\text{H}\}$ NMR showed a mixture of unidentifiable compounds.

Preparation of $[\text{Ph}_2\text{PCH}_2\text{P}(\text{O})(\text{NET}_2)_2]$

The title compound was prepared by bubbling air through a stirred dichloromethane (10 mL) solution of $[\text{Ph}_2\text{PCH}_2\text{P}(\text{NET}_2)_2]$ (0.4 g) for 6 h. The solvent was then removed *in vacuo* to yield the product as a viscous cream oil which was characterised by $^{31}\text{P}\{^1\text{H}\}$ NMR.

Preparation of $[\text{Ph}_2\text{P}(\text{S})\text{CH}_2\text{P}(\text{S})(\text{NET}_2)_2]$

Two methods were employed for the synthesis of $[\text{Ph}_2\text{P}(\text{S})\text{CH}_2\text{P}(\text{S})(\text{NET}_2)_2]$. Method A was found to be the most satisfactory.

Method A¹⁰⁶

A solution of sulphur (0.225 g, 7.02 mmol) and $[\text{Ph}_2\text{PCH}_2\text{-P}(\text{NEt}_2)_2]$ (1.31 g, 3.51 mmol) in benzene (100 mL) was heated under reflux for 1 h. The solvent was then removed *in vacuo* to yield a viscous off-white oil of $[\text{Ph}_2\text{P}(\text{S})\text{CH}_2\text{P}(\text{S})(\text{NEt}_2)_2]$ (1.49 g, 3.40 mmol, 97%).

Method B

A solution of sulphur (47 mg, 1.5 mmol) and $[\text{Ph}_2\text{P}(\text{S})\text{CH}_2\text{-P}(\text{NEt}_2)_2]$ (0.598 g, 1.47 mmol) in benzene (70 mL) was heated under reflux for 1 h. The solvent was then removed *in vacuo* to yield the product as an off-white oil. (It was found desirable to add at least 15% less sulphur than required stoichiometrically, as excess was found to be dangerous to future metal-ligand reactions. This also allowed for decomposition of the ligand during reflux). The disulphide was characterised by $^{31}\text{P}\{^1\text{H}\}$ and $^{13}\text{C}\{^1\text{H}\}$ NMR.

IR, neat, $\nu(\text{cm}^{-1})$: 2985(s), 1438(s), 1380(s), 1202(s), 1178(s), 1100(bs), 1020(bs), 940(bs), 800-690(m,bs), 610(s)

Preparation of $[\text{Ph}_2\text{P}(\text{S})\text{CHP}(\text{S})(\text{NEt}_2)_2]\text{Li}^{26}$

n-Butyllithium (0.29 mL, 1.6 M in hexanes) was added to a stirred solution of $[\text{Ph}_2\text{P}(\text{S})\text{CH}_2\text{P}(\text{S})(\text{NEt}_2)_2]$ (0.20 g, 0.46 mmol) in THF (5 mL). The orange solution of $[\text{Ph}_2\text{P}(\text{S})\text{CHP}(\text{S})(\text{NEt}_2)_2]\text{Li}$ was characterised by $^{31}\text{P}\{^1\text{H}\}$ and $^{13}\text{C}\{^1\text{H}\}$ NMR.

EXPERIMENTAL FOR CHAPTER 3**Preparation of $[\text{PtCl}(\text{PET}_3)(\text{Ph}_2\text{PCH}_2\text{P}(\text{NET}_2)_2\text{-P,P}')]\text{BF}_4$**

A solution $[\text{Ph}_2\text{PCH}_2\text{P}(\text{NET}_2)_2]$ (195 mg, 0.52 mmol) in THF (3 mL) was added to a stirred suspension of $[\text{Pt}_2(\mu\text{-Cl})_2\text{Cl}_2(\text{PET}_3)_2]$ (200 mg, 0.26 mmol) and NaBF_4 (57.1 mg, 0.52 mmol) in acetone (5 mL). After 30 min the solvents were removed *in vacuo* yielding an oily pale yellow residue. The residue was then extracted with dichloromethane, the extracts combined, and the solvents removed *in vacuo*. The crude product was then dissolved in a small volume of THF (ca. 0.5 mL) and precipitated by addition of diethyl ether (10 mL). The washing was repeated several times until a solid remained. $^{31}\text{P}\{^1\text{H}\}$ and $^{195}\text{Pt}\{^1\text{H}\}$ NMR indicated a *trans* to *cis* isomer ratio of 9:1. Recrystallization from dichloromethane/hexane afforded colourless crystals of the *cis*-isomer (42 mg, 10%), which were characterised by $^{195}\text{Pt}\{^1\text{H}\}$, $^{31}\text{P}\{^1\text{H}\}$, $^{13}\text{C}\{^1\text{H}\}$, ^1H NMR and x-ray crystallography. Analysis calculated for $\text{C}_{27.5}\text{H}_{48}\text{BCl}_2\text{F}_4\text{N}_2\text{P}_3\text{Pt}$: C, 38.75; H, 5.69; N, 3.29. Found: C, 38.43; H, 5.89; N, 3.63%.

Preparation of $[\text{PdCl}(\text{PET}_3)(\text{Ph}_2\text{PCH}_2\text{P}(\text{NET}_2)_2\text{-P,P}')]\text{BF}_4$

The title compound was prepared by a similar procedure to that described for $[\text{PtCl}(\text{PET}_3)(\text{Ph}_2\text{PCH}_2\text{P}(\text{NET}_2)_2\text{-P,P}')]\text{BF}_4$. The initial product (85% yield) was the *trans*-isomer but on stirring in dichloromethane for 24 h isomerization to the

cis-isomer occurred. Recrystallization from dichloromethane/hexane afforded bright orange crystals which were characterised by $^{13}\text{C}\{^1\text{H}\}$, $^{31}\text{P}\{^1\text{H}\}$ and ^1H NMR. Analysis calculated for $\text{C}_{27}\text{H}_{47}\text{BClF}_4\text{N}_2\text{P}_3\text{Pd}$: C, 44.96; H, 6.57; N, 3.88. Found: C, 44.96; H, 6.43; N, 3.86%.

Preparation of $[\text{PdCl}(\text{PET}_3)\{\text{Ph}_2\text{PCH}_2\text{P}(\text{N}(\text{CH}_2\text{CH}_2)\text{CH}_2)_2\text{-P,P'}\}]\text{BF}_4$

The title compound was prepared by a similar procedure to that described for $[\text{PtCl}(\text{PET}_3)\{\text{Ph}_2\text{PCH}_2\text{P}(\text{NET}_2)_2\text{-P,P'}\}]\text{BF}_4$. The initial product (85% yield) was the *trans*-isomer but on stirring in dichloromethane for 24 h isomerization to the *cis*-isomer occurred, which was characterised by $^{31}\text{P}\{^1\text{H}\}$ NMR.

Reaction of $[\text{Rh}(\text{cod})\mu\text{-Cl}]_2$ with $[\text{Ph}_2\text{PCH}_2\text{P}(\text{NET}_2)_2]$

A solution of $[\text{Ph}_2\text{PCH}_2\text{P}(\text{NET}_2)_2]$ (0.153 g, 0.41 mmol) in acetone (2 mL) was added to a stirred solution of $[\text{Rh}(\text{cod})\mu\text{-Cl}]_2$ (0.1 g, 0.2 mmol) and NaBF_4 (45 mg, 0.41 mmol) in acetone (5 mL). The solution instantly turned from an orange/yellow suspension to an orange/red solution. After 30 min the solvents were removed *in vacuo* and the orange residue extracted with dichloromethane. Removal of the solvent from the combined extracts yielded a brown powder whose $^{31}\text{P}\{^1\text{H}\}$ NMR showed at least two phosphorus containing compounds one of which was $[\text{Rh}(\text{cod})\{\text{Ph}_2\text{PCH}_2\text{P}(\text{NET}_2)_2\text{-P,P'}\}]\text{BF}_4$

Reaction of $[\text{Rh}(\text{cod})(\text{Bipyridyl})]\text{BF}_4$ with $[\text{Ph}_2\text{PCH}_2\text{P}(\text{NET}_2)_2]$

$[\text{Ph}_2\text{PCH}_2\text{P}(\text{NET}_2)_2]$ (0.20 g, 0.53 mmol) in THF (5 mL) was

added to a stirred solution of $[\text{Rh}(\text{cod})(\text{Bipyridyl})]\text{BF}_4$ (0.243 g, 0.53 mmol) in acetone (5 mL). After 30 min the solvents were removed *in vacuo* to yield a dark red/brown powder. $^{31}\text{P}\{^1\text{H}\}$ NMR showed a mixture of at least two products one of which was $[\text{Rh}(\text{Bipyridyl})(\text{Ph}_2\text{PCH}_2\text{P}(\text{NET}_2)_2^{-P,P'})]\text{BF}_4$.

Preparation of $[\text{PtCl}_2(\text{Ph}_2\text{PCH}_2\text{P}(\text{NET}_2)_2^{-P,P'})]$

A solution of $[\text{Ph}_2\text{PCH}_2\text{P}(\text{NET}_2)_2]$ (222 mg, 0.59 mmol) in THF (5 mL) was added to a stirred suspension of $[\text{Pt}(\text{cod})\text{Cl}_2]$ (222 mg, 0.59 mmol) in THF (10 mL). After 2 h the solvent was removed *in vacuo* to yield an oily white residue, which was dissolved in a small volume of dichloromethane (ca. 1 mL) and precipitated as a white powder (351 mg, 0.55 mmol, 93%) by addition of diethyl ether. Recrystallization from dichloromethane/hexane yielded colourless crystals of the title compound which were characterised by $^{31}\text{P}\{^1\text{H}\}$, $^{195}\text{Pt}\{^1\text{H}\}$, $^{13}\text{C}\{^1\text{H}\}$ and ^1H NMR. Analysis calculated for $\text{C}_{12}\text{H}_{32}\text{Cl}_2\text{N}_2\text{P}_2\text{Pt}$: C, 39.38; H, 5.04; N, 4.37; Cl, 11.07. Found: C, 39.41; H, 5.05; N, 4.49; Cl, 11.36%.

Preparation of $[\text{PtCl}_2(\text{Ph}_2\text{PCH}_2\text{P}(\text{NET})\text{Ph}-P,P')]$

The title compound was prepared by a similar procedure to that described for $[\text{PtCl}_2(\text{Ph}_2\text{PCH}_2\text{P}(\text{NET}_2)_2^{-P,P'})]$.

$[\text{PtCl}_2(\text{Ph}_2\text{PCH}_2\text{P}(\text{NET})\text{Ph}-P,P')]$ (yield 94%) was characterised by $^{31}\text{P}\{^1\text{H}\}$, $^{13}\text{C}\{^1\text{H}\}$, $^{195}\text{Pt}\{^1\text{H}\}$ and ^1H NMR. Analysis calculated for $\text{C}_{23}\text{H}_{27}\text{Cl}_2\text{NP}_2\text{Pt}$: C, 42.80; H, 4.22; N, 2.17.

Found: C, 42.15; H, 4.20; N, 2.12%.

Preparation of $[\text{PdCl}_2(\text{Ph}_2\text{PCH}_2\text{P}(\text{NEt}_2)_2\text{-P,P}')]]$

A solution of $[\text{Ph}_2\text{PCH}_2\text{P}(\text{NEt}_2)_2]$ (0.241 g, 0.64 mmol) in THF (3 mL) was added to a stirred suspension of PdCl_2 (0.114 g, 0.64 mmol) in THF (10 mL). After 24 h a yellow suspension in a yellow/orange solution formed. The solvent was then removed *in vacuo* and the residue washed with 3x10 mL hexane (230 mg, 65%). Recrystallization from dichloromethane/hexane afforded colourless crystals which were characterised by $^{31}\text{P}\{^1\text{H}\}$, $^{13}\text{C}\{^1\text{H}\}$ and ^1H NMR. Analysis calculated for $\text{C}_{21}\text{H}_{32}\text{Cl}_2\text{N}_2\text{P}_2\text{Pd}$: C, 45.71; H, 5.85; N, 5.08. Found C, 45.21; H, 5.88; N, 5.05%.

Reaction of $[\text{PtCl}_2(\text{Ph}_2\text{PCH}_2\text{P}(\text{NEt}_2)_2\text{-P,P}')]]$ with $\text{HCl}(\text{g})$

Hydrogen chloride gas was bubbled through a stirred solution of $[\text{PtCl}_2(\text{Ph}_2\text{PCH}_2\text{P}(\text{NEt}_2)_2\text{-P,P}')]]$ (0.1 g) in CDCl_3 (2 mL) for 30 s. The $^{31}\text{P}\{^1\text{H}\}$ NMR was then recorded in approximately 10 min. The HCl reaction was then repeated with the $^{31}\text{P}\{^1\text{H}\}$ NMR recorded after every 30 s of addition.

Reaction of $[\text{PtCl}_2(\text{Ph}_2\text{PCH}_2\text{P}(\text{NEt}_2)\text{Ph-P,P}')]]$ with $\text{HCl}(\text{g})$

Hydrogen chloride gas was bubbled through a stirred solution of $[\text{PtCl}_2(\text{Ph}_2\text{PCH}_2\text{P}(\text{NEt}_2)\text{Ph-P,P}')]]$ (0.1 g) in CDCl_3 (5mL) for 2, 4, 6, 10, 30 and 120 min and the $^{31}\text{P}\{^1\text{H}\}$ recorded between each period of reaction.

Reaction of $[\text{Ph}_2\text{PCH}_2\text{P}(\text{NEt}_2)_2]$ with $\text{HCl}(\text{g})$

Hydrogenchloride gas was bubbled through a stirred solution of $[\text{Ph}_2\text{PCH}_2\text{P}(\text{NEt}_2)_2]$ (400 mg) in diethyl ether (10 mL) for 30 min. A white precipitate immediately formed. The diethyl ether solution was then extracted from the precipitate and the volume reduced *in vacuo*. $^{31}\text{P}\{^1\text{H}\}$ NMR showed a mixture of compounds and the desired product $[\text{Ph}_2\text{PCH}_2\text{P}(\text{Cl})_2]$, which accounted for approximately 60% phosphorus present.

Reaction of $[\text{Pt}(\text{cod})\text{Cl}_2]$ with the product from the $\text{HCl}(\text{g})$ reaction with $[\text{Ph}_2\text{PCH}_2\text{P}(\text{NEt}_2)_2]$

A solution $[\text{PtCl}_2(\text{cod})]$ in dichloromethane (5 mL) was added to the above solution containing $[\text{Ph}_2\text{PCH}_2\text{P}(\text{Cl})_2]$ and stirred for 2 h. The $^{31}\text{P}\{^1\text{H}\}$ NMR showed only decomposed ligand.

Reaction of $[\text{PtCl}_2\{\text{Ph}_2\text{PCH}_2\text{P}(\text{NEt}_2)_2^{-P,P'}\}]$ with $\text{CF}_3\text{CO}_2\text{H}$

(The reaction was carried out following a similar procedure to that described in the literature).⁶⁴

A solution of $\text{CF}_3\text{CO}_2\text{H}$ (0.027 mL, 0.31 mmol) in THF (5 mL) was added to a stirred solution $[\text{PtCl}_2\{\text{Ph}_2\text{PCH}_2\text{P}(\text{NEt}_2)_2^{-P,P'}\}]$ (0.10 g, 0.16 mmol) dichloromethane (10 mL). The $^{31}\text{P}\{^1\text{H}\}$ NMR, after 3 h, showed only the starting complex.

Reaction of $[\text{Ph}_2\text{PCH}_2\text{P}(\text{NEt}_2)_2]$ with $\text{CF}_3\text{CO}_2\text{H}$

A solution of $\text{CF}_3\text{CO}_2\text{H}$ (0.09 mL, 1.0 mmol) in THF (5 mL) was added to a stirred solution of $[\text{Ph}_2\text{PCH}_2\text{P}(\text{NEt}_2)_2]$ (0.192 g, 0.51 mmol) in dichloromethane (10 mL). The initial slightly

cloudy solution instantly cleared. The $^{31}\text{P}\{^1\text{H}\}$ NMR showed only decomposed ligand.

Reaction of $[\text{PtCl}_2(\text{Ph}_2\text{PCH}_2\text{P}(\text{NEt}_2)_2\text{-P,P}')] \text{ with } [\text{Pt}_2(\mu\text{-Cl})_2\text{Cl}_2(\text{PEt}_3)_2]$

A solution of $[\text{PtCl}_2(\text{Ph}_2\text{PCH}_2\text{P}(\text{NEt}_2)_2\text{-P,P}')] \text{ (40 mg, 63.0 } \mu\text{mol)}$ and $[\text{Pt}_2(\mu\text{-Cl})_2\text{Cl}_2(\text{PEt}_3)_2] \text{ (24.1 mg, 31.4 } \mu\text{mol)}$ in THF (10 mL) was heated under gentle reflux for 24 h. The $^{31}\text{P}\{^1\text{H}\}$ NMR showed only unreacted starting precursors.

Preparation of $[\text{PtCl}_2(\text{Ph}_2\text{PCH}_2\text{P}(\text{NEt}_2)_2\text{-P,P}')\{\text{N,N-Rh}(\text{cod})\}]\text{BF}_4$

A solution of $[\text{Rh}(\text{cod})(\text{MeCN})_2]\text{BF}_4 \text{ (21.7 mg, 57.0 } \mu\text{mol)}$ in $\text{CDCl}_3 \text{ (3 mL)}$ was added to a stirred solution of $[\text{PtCl}_2(\text{Ph}_2\text{PCH}_2\text{P}(\text{NEt}_2)_2\text{-P,P}')]$ (36.6 mg, 57 μmol) in $\text{CDCl}_3 \text{ (3 mL)}$. After 1 h the volume was reduced *in vacuo*, and the $^{31}\text{P}\{^1\text{H}\}$, $^{13}\text{C}\{^1\text{H}\}$ and ^1H recorded. The reaction mixture was then reduced to a powder *in vacuo* and washed with 3x5 mL of diethyl ether and dried *in vacuo* for 3 h. The $^{31}\text{P}\{^1\text{H}\}$, $^{13}\text{C}\{^1\text{H}\}$ and ^1H NMR were then recorded. Recrystallization from dichloromethane/hexane afforded bright orange crystals. Analysis calculated for the complex $[\text{PtCl}_2(\text{Ph}_2\text{PCH}_2\text{P}(\text{NEt}_2)_2\text{-P,P}')\{\text{Rh}(\text{cod})\}]\text{BF}_4 \cdot \text{CH}_2\text{Cl}_2$; $\text{C}_{30}\text{H}_{46}\text{BCl}_4\text{F}_4\text{P}_2\text{PtN}_2\text{Rh}$: C, 35.21; H, 4.53; N, 2.74. Found: C 35.56; H, 4.62; N, 2.86%.

^1H NMR: δ (ppm); N-CH₂-CH₃, 1.08 (t, 12H, $^3\text{J}_{\text{HH}} = 7 \text{ Hz}$); N-CH₂-CH₃, 3.09 - 3.36 (m, 8H); P-CH₂-P, 4.53 (t, $^2\text{J}_{\text{PH}} = 13 \text{ Hz}$); -CH₂-(cod), 1.71 - 1.81 (bm); -CH=(cod), 4.20 (bs) and

4.31 (bs); Ph 7.51 - 7.99 (m)

$^{13}\text{C}\{^1\text{H}\}$ NMR: δ (ppm); P- $\underline{\text{C}}\text{H}_2$ -P, 45.85 (dd, $^1J_{\text{PC}} = 35$ Hz, $^1J_{\text{PC}} = 50$ Hz); N- $\underline{\text{C}}\text{H}_2$ - $\underline{\text{C}}\text{H}_3$, 13.82 (s); N- $\underline{\text{C}}\text{H}_2$ - $\underline{\text{C}}\text{H}_3$, 41.00 (d, $^2J_{\text{PC}} = 5$ Hz); $-\underline{\text{C}}\text{H}_2$ -(cod), 30.68 (s) and 30.87 (s); $-\underline{\text{C}}\text{H}=(\text{cod})$, 80.30 (d, $^1J_{\text{RhC}} = 14$ Hz) and 78.67 (d, $^1J_{\text{PC}} = 13$ Hz); Ph, 125.4 - 133.04 (m).

EXPERIMENTAL FOR CHAPTER 4

Preparation of $[\text{Rh}(\text{cod})\{\text{Ph}_2\text{P}(\text{S})\text{CH}_2\text{P}(\text{NEt}_2)_2\text{-S,P}\}]\text{BF}_4$

A solution of $[\text{Ph}_2\text{P}(\text{S})\text{CH}_2\text{P}(\text{NEt}_2)_2]$ (80.1 mg, 197 μmol) in THF (3 mL) was added to a stirred solution of $[\text{Rh}(\text{cod})\mu\text{-Cl}]_2$ (48.6 mg, 98.6 μmol) and NaBF_4 (21.6 mg, 197 μmol) in acetone (5 mL). The initial orange/yellow mixture turned to a dark orange solution over 30 min. The solvent was then removed *in vacuo* to yield an oily orange residue, which was extracted in dichloromethane (3x5 mL), and the combined extracts reduced *in vacuo*. The product was characterised by $^{31}\text{P}\{^1\text{H}\}$ NMR.

Preparation of $[\text{PtCl}(\text{PEt}_3)\{\text{Ph}_2\text{P}(\text{S})\text{CH}_2\text{P}(\text{NEt}_2)_2\text{-S,P}\}]\text{BF}_4$

The title compound was prepared by similar procedure to that described for $[\text{PtCl}(\text{PEt}_3)\{\text{Ph}_2\text{PCH}_2\text{P}(\text{NEt}_2)_2\text{-P,P'}\}]\text{BF}_4$.

$^{31}\text{P}\{^1\text{H}\}$ NMR of the residue showed a *cis-trans* isomer ratio of 10:90.

Reaction of LiBr with $[\text{PtCl}(\text{PET}_3)(\text{Ph}_2\text{P}(\text{S})\text{CH}_2\text{P}(\text{NET}_2)_2\text{-S,P})]\text{BF}_4$

Excess LiBr was added to a stirred solution of $[\text{PtCl}(\text{PET}_3)(\text{Ph}_2\text{P}(\text{S})\text{CH}_2\text{P}(\text{NET}_2)_2\text{-S,P})]\text{BF}_4$ in THF (10 mL). After 5 h the $^{31}\text{P}\{^1\text{H}\}$ NMR showed a 50:50 mixture of *trans*- $[\text{PtCl}(\text{PET}_3)(\text{Ph}_2\text{P}(\text{S})\text{CH}_2\text{P}(\text{NET}_2)_2\text{-S,P})]\text{BF}_4$ and *trans*- $[\text{PtBr}(\text{PET}_3)(\text{Ph}_2\text{P}(\text{S})\text{CH}_2\text{P}(\text{NET}_2)_2\text{-S,P})]\text{BF}_4$. After 24 h the $^{31}\text{P}\{^1\text{H}\}$ NMR showed $[\text{trans-PtBr}(\text{PET}_3)(\text{Ph}_2\text{P}(\text{S})\text{CH}_2\text{P}(\text{NET}_2)_2\text{-S,P})]\text{BF}_4$ and trace amount of $[\text{PtBr}_2(\text{Ph}_2\text{P}(\text{S})\text{CH}_2\text{P}(\text{NET}_2)_2\text{-S,P})]$.

Preparation of $[\text{PdCl}(\text{PET}_3)(\text{Ph}_2\text{P}(\text{S})\text{CH}_2\text{P}(\text{NET}_2)_2\text{-S,P})]\text{BF}_4$

The title compound was prepared by a similar procedure to that described for $[\text{PtCl}(\text{PET}_3)(\text{Ph}_2\text{PCH}_2\text{P}(\text{NET}_2)_2\text{-P,P}')]\text{BF}_4$. The $^{31}\text{P}\{^1\text{H}\}$ NMR showed that only the *trans*-isomer was generated.

Reaction of LiBr with $[\text{trans-PdCl}(\text{PET}_3)(\text{Ph}_2\text{P}(\text{S})\text{CH}_2\text{P}(\text{NET}_2)_2\text{-S,P})]\text{BF}_4$

Excess LiBr was added to stirred solution of $[\text{trans-PdCl}(\text{PET}_3)(\text{Ph}_2\text{P}(\text{S})\text{CH}_2\text{P}(\text{NET}_2)_2\text{-S,P}')]\text{BF}_4$ in THF (10 mL). After 1 h the $^{31}\text{P}\{^1\text{H}\}$ NMR showed a 70:30 mixture of $[\text{trans-PdBr}(\text{PET}_3)(\text{Ph}_2\text{P}(\text{S})\text{CH}_2\text{P}(\text{NET}_2)_2\text{-S,P})]\text{BF}_4$ and $[\text{trans-PdCl}(\text{PET}_3)(\text{Ph}_2\text{P}(\text{S})\text{CH}_2\text{P}(\text{NET}_2)_2\text{-S,P})]\text{BF}_4$. After 24 h the solvent was removed *in vacuo* and the orange residue extracted with dichloromethane. The $^{31}\text{P}\{^1\text{H}\}$ NMR of the extract showed the exclusive formation of $[\text{PdBr}_2(\text{Ph}_2\text{P}(\text{S})\text{CH}_2\text{-}$

$P(\text{NEt}_2)_2\text{-S,P}]$. The solvent was removed *in vacuo* and the solid washed with diethyl ether. Recrystallization from dichloromethane/hexane afforded bright orange crystals of $[\text{PdBr}_2(\text{Ph}_2\text{P(S)CH}_2\text{P(NEt}_2)_2\text{-S,P})]$ which were characterised by $^{31}\text{P}\{^1\text{H}\}$ and $^{13}\text{C}\{^1\text{H}\}$ NMR. Analysis calculated for $\text{C}_{21}\text{H}_{32}\text{Br}_2\text{N}_2\text{P}_2\text{PdS}$: C, 37.49; H, 4.79; N, 4.16. Found: C, 37.42; H, 4.78; N, 4.11%.

$^{13}\text{C}\{^1\text{H}\}$ NMR: δ (ppm). NCH_2CH_3 , 13.78 (d, $^3\text{J(P-C)} = 3$ Hz); NCH_2CH_3 , 43.05 (d, $^2\text{J(P-C)} = 6$ Hz); PCH_2P , 45.91 (dd, $^1\text{J(P-C)} = 27$ Hz, $^1\text{J(P-C)} = 54$ Hz); Ph, 124.7 - 133.6 (m).

Preparation of $[\text{PtCl}(\text{PEt}_3)(\text{Ph}_2\text{P(S)CH}_2\text{P(S)(NEt}_2)_2\text{-S,S'})]\text{BF}_4$

The title compound was prepared by a similar procedure to that described for $[\text{PtCl}(\text{PEt}_3)(\text{Ph}_2\text{PCH}_2\text{P(NEt}_2)_2\text{-P,P'})]\text{BF}_4$. Separation of the *cis* and *trans* isomers could not be affected for solution studies, owing to isomerization in solution giving a *cis-trans* isomer ratio of 1:1. Recrystallization from dichloromethane/hexane afforded yellow crystals which were characterised by $^{31}\text{P}\{^1\text{H}\}$, $^{13}\text{C}\{^1\text{H}\}$, ^1H and $^{195}\text{Pt}\{^1\text{H}\}$ NMR. Analysis calculated for $\text{C}_{27}\text{H}_{47}\text{BClF}_4\text{N}_2\text{P}_3\text{PtS}_2$: C, 37.10; H, 5.42; N, 3.20. Found: C, 37.40; H, 5.43; N, 3.23%.

Preparation of $[\text{PdCl}(\text{PEt}_3)(\text{Ph}_2\text{P(S)CH}_2\text{P(S)(NEt}_2)_2\text{-S,S'})]\text{BF}_4$

The title compound was prepared by a similar procedure to that described for $[\text{PtCl}(\text{PEt}_3)(\text{Ph}_2\text{PCH}_2\text{P(NEt}_2)_2\text{-P,P'})]\text{BF}_4$. Separation of the *cis* and *trans* isomers could not be effec-

ted for solution studies, owing to isomerization in solution. Recrystallization (dichloromethane/hexane) afforded orange crystals which were characterised by $^{31}\text{P}\{^1\text{H}\}$, $^{13}\text{C}\{^1\text{H}\}$ and ^1H NMR. Analysis calculated for $\text{C}_{27}\text{H}_{47}\text{BClF}_4\text{N}_2\text{P}_3\text{PdS}_2$: C, 41.29; H, 6.03; N, 3.57. Found: C, 41.29; H, 6.06; N, 3.58%.

Preparation of $[\text{PdCl}(\text{PPh}_3)\{\text{Ph}_2\text{P}(\text{S})\text{CH}_2\text{P}(\text{S})\text{Ph}_2\text{-S,S'}\}]\text{BF}_4$

The title compound was prepared by a similar procedure to that described for $[\text{PtCl}(\text{PEt}_3)\{\text{Ph}_2\text{PCH}_2\text{P}(\text{NEt}_2)_2\text{-P,P'}\}]\text{BF}_4$ except the dimer $[\text{Pd}_2(\mu\text{-Cl})_2\text{Cl}_2(\text{PPh}_3)_2]$ was employed. Characterization was by $^{31}\text{P}\{^1\text{H}\}$, $^{13}\text{C}\{^1\text{H}\}$ and ^1H NMR. Analysis calculated for $\text{C}_{43}\text{H}_{37}\text{BClF}_4\text{P}_3\text{PdS}_2$: C, 54.98; H, 4.11. Found: C, 53.09; H, 4.11%.

Preparation of $[\text{Rh}(\text{cod})\{\text{Ph}_2\text{P}(\text{S})\text{CH}_2\text{P}(\text{S})(\text{NEt}_2)_2\text{-S,S'}\}]\text{BF}_4$

The title compound was prepared by a similar procedure to that described for $[\text{Rh}(\text{cod})\{\text{Ph}_2\text{P}(\text{S})\text{CH}_2\text{P}(\text{NEt}_2)_2\text{-S,P}\}]\text{BF}_4$. If excess sulphur remained from the ligand synthesis the product yield was reduced by the formation of a brown rhodium-sulphur compound, which from the $^{31}\text{P}\{^1\text{H}\}$ NMR did not contain any phosphorus. Recrystallization from dichloromethane/hexane afforded orange crystals which were characterised by $^{31}\text{P}\{^1\text{H}\}$, $^{13}\text{C}\{^1\text{H}\}$ and ^1H NMR. Analysis calculated for $\text{C}_{29}\text{H}_{44}\text{BF}_4\text{N}_2\text{P}_2\text{RhS}_2$: C, 47.30; H, 6.02; N, 3.80. Found: C, 47.37; H, 6.01; N, 3.83%.

Preparation of $[\text{Ir}(\text{cod})(\text{Ph}_2\text{P}(\text{S})\text{CH}_2\text{P}(\text{S})(\text{NET}_2)_2\text{-S,S}')]\text{BF}_4$

The title compound was prepared by a similar procedure to that described for $[\text{Rh}(\text{cod})(\text{Ph}_2\text{P}(\text{S})\text{CH}_2\text{P}(\text{NET}_2)_2\text{-S,P})]\text{BF}_4$. Recrystallization from dichloromethane/hexane yielded orange crystals which were characterised by $^{31}\text{P}\{^1\text{H}\}$, $^{13}\text{C}\{^1\text{H}\}$ and ^1H NMR. Analysis calculated for $\text{C}_{29}\text{H}_{44}\text{BF}_4\text{IrN}_2\text{P}_2\text{S}_2$: C, 42.18; H, 5.37; N, 3.39. Found: C, 42.47; H, 5.44; N, 3.41%.

Preparation of $[\text{Rh}(\text{cod})(\text{Ph}_2\text{P}(\text{S})\text{CHP}(\text{S})(\text{NET}_2)_2\text{-S,S}')]$

$[\text{Rh}(\text{cod})(\text{Ph}_2\text{P}(\text{S})\text{CHP}(\text{S})(\text{NET}_2)_2)]$ was prepared by two different methods.

Method A

A solution of $[\text{Ph}_2\text{P}(\text{S})\text{CHP}(\text{S})(\text{NET}_2)_2]\text{Li}$ (0.18 g, 0.4 mmol) in THF (5 mL) was added to a stirred solution of $[\text{Rh}(\text{cod})\mu\text{-Cl}]_2$ (0.1 g, 0.2 mmol) in THF (3 mL). The reaction mixture instantly turned from an orange suspension to a deep red solution. The solvent was removed *in vacuo* and the oily residue extracted with hexane (3x5 mL). The product was characterised by $^{31}\text{P}\{^1\text{H}\}$ NMR.

Method B

A solution of $[\text{Rh}(\text{cod})(\text{Ph}_2\text{P}(\text{S})\text{CH}_2\text{P}(\text{S})(\text{NET}_2)_2\text{-S,S}')]\text{BF}_4$ (23.4 mg, 31.7 μmol) in THF (5 mL) was added to stirred suspension of NaH (8 mg, 0.3 mmol). After 45 min the suspension of NaH was allowed to settle and the deep red solution extracted. The solvent was removed *in vacuo* yielding the title compound as a brown powder which was characterised by $^{31}\text{P}\{^1\text{H}\}$,

$^{13}\text{C}\{^1\text{H}\}$ and ^1H NMR.

$^{13}\text{C}\{^1\text{H}\}$ NMR: δ (ppm) NCH_2CH_3 , 14.92 (d, $^3\text{J}(\text{P}-\text{C}) = 3$ Hz); NCH_2CH_3 , 40.95 (d, $^2\text{J}(\text{P}-\text{C}) = 4$ Hz); $\text{cod}(\text{=CH-})$, 80.40 (d, $^1\text{J}(\text{Rh}-\text{C}) = 12$ Hz); $\text{cod}(\text{-CH}_2\text{-})$, 31.51 (s); PCHP , 19.73 (ddd, $^1\text{J}(\text{P}-\text{C}) = 92$ Hz, $^1\text{J}(\text{P}-\text{C}) = 123$ Hz, $^3\text{J}(\text{Rh}-\text{C}) = 5$ Hz); Ph 127.6 - 132.7 (m).

^1H NMR: δ (ppm) NCH_2CH_3 , 1.09 (t, $^3\text{J}(\text{H}-\text{H}) = 7$ Hz); NCH_2CH_3 , 3.02 - 3.45 (m); $\text{cod}(\text{=CH-})$, 4.41 (bs); $\text{cod}(\text{-CH}_2\text{-})$, 2.20 (bs); PCHP not observed; Ph , 7.02 - 8.30 (m).

Reaction of $[\text{Pd}_2(\mu\text{-Cl})_2\text{Cl}_2(\text{PET}_3)_2]$ with $[\text{Ph}_2\text{P}(\text{S})\text{CHP}(\text{S})(\text{NET}_2)_2]\text{Li}$

A solution of $[\text{Ph}_2\text{P}(\text{S})\text{CHP}(\text{S})(\text{NET}_2)_2]\text{Li}$ (57.8 mg, 0.13 mmol) in THF (3 mL) was added to a stirred solution of $[\text{Pd}_2(\mu\text{-Cl})_2\text{Cl}_2(\text{PET}_3)_2]$ (100 mg, 0.13 mmol) in THF (10 mL). The $^{31}\text{P}\{^1\text{H}\}$ and $^{13}\text{C}\{^1\text{H}\}$ NMR were recorded after 15 min. The solvent was then removed *in vacuo* and the oily brown residue redissolved in CD_2Cl_2 . $^{31}\text{P}\{^1\text{H}\}$ NMR was then recorded at -90°C and $+24^\circ\text{C}$. Analysis calculated for $\text{C}_{27}\text{H}_{46}\text{ClN}_2\text{P}_3\text{PdS}_2$: C, 46.49; H, 6.65; N, 4.02. Found: C, 48.2; H, 6.69; N, 3.63 %.

Reaction of $[\text{PdCl}(\text{PET}_3)(\text{Ph}_2\text{P}(\text{S})\text{CH}_2\text{P}(\text{S})(\text{NET}_2)_2\text{-S,S'})]\text{BF}_4$ with NaH

Excess NaH was added to a stirred solution of $[\text{PdCl}(\text{PET}_3)(\text{Ph}_2\text{P}(\text{S})\text{CH}_2\text{P}(\text{S})(\text{NET}_2)_2)]\text{BF}_4$ (0.10 g, 0.13 mmol) in THF (10

mL). The reaction mixture turned from an orange suspension/solution to a deep red solution over 45 min. The NaH was allowed to settle over about 1 h. The reaction solution was then extracted and reduced to about 2 mL *in vacuo*. The $^{31}\text{P}\{^1\text{H}\}$ NMR of the reaction mixture was then recorded. Total removal of the solvent yielded an air sensitive orange/brown powder which was redissolved in CD_2Cl_2 and the $^{31}\text{P}\{^1\text{H}\}$ NMR recorded between -80 and $+35^\circ\text{C}$ and then in DMSO between $+35$ and $+80^\circ\text{C}$.

Reaction of $[\text{Pd}(\mu\text{-Cl})_2\text{Cl}_2(\text{PEt}_3)_2]$ with $[\text{Ph}_2\text{P}(\text{S})\text{CHP}(\text{S})\text{Ph}_2]\text{Li}$

The title reaction was performed under similar conditions to that for the reaction between $[\text{Pd}_2(\mu\text{-Cl})_2\text{Cl}_2(\text{PEt}_3)_2]$ and $[\text{Ph}_2\text{P}(\text{S})\text{CHP}(\text{S})(\text{NET}_2)_2]\text{Li}$. $^{31}\text{P}\{^1\text{H}\}$ and $^{13}\text{C}\{^1\text{H}\}$ NMR were then recorded at $+24$ and -90°C .

Reaction of $[\text{PtCl}(\text{PEt}_3)(\text{Ph}_2\text{P}(\text{S})\text{CH}_2\text{P}(\text{S})(\text{NET}_2)_2\text{-S,S}')]\text{BF}_4$,

$[\text{PdCl}(\text{PEt}_3)(\text{Ph}_2\text{P}(\text{S})\text{CH}_2\text{P}(\text{S})\text{Ph}_2\text{-S,S}')]\text{BF}_4^{25}$ and

$[\text{PdCl}(\text{Ph}_3\text{P})(\text{Ph}_2\text{P}(\text{S})\text{CH}_2\text{P}(\text{S})\text{Ph}_2\text{-S,S}')]\text{BF}_4$ with NaH

Reaction conditions were similar to that described for the analogous palladium reaction above. $^{31}\text{P}\{^1\text{H}\}$ NMR were recorded of respective products.

Reaction of $[\text{Pt}_2(\mu\text{-Cl})_2\text{Cl}_2(\text{PEt}_3)_2]$ with

$[\text{Ph}_2\text{P}(\text{S})\text{CHP}(\text{S})(\text{NET}_2)_2]\text{Li}$

Reaction conditions were similar to that described for the analogous palladium reaction above. $^{31}\text{P}\{^1\text{H}\}$ NMR of the

respective products were recorded.

References

1. Bookham, J. L.; Colquhoun, I. J.; McFarlane, W. *J. Chem. Soc., Dalton Trans.* **1988**, 503-507.
2. Cotton, F. A.; Wilkinson, G. *Basic Inorganic Chemistry*; Wiley: New York, 1976.
3. Melson, G. A. *Coordination Chemistry of Macrocyclic Compound's*; Plenum Press: New York, 1979.
4. Whitcombe, T. *Ph.D. Thesis*, University of Victoria 1988.
5. Vallee, B. L.; Williams, R. J. P. *Chem. Brit.* **1968**, *4*, 397-402.
6. Abutjoglan, A. G.; Harrison, A. M.; Wegman, R. W. *J. Chem. Soc., Chem. Commun.* **1987**, 1891-1892.
7. Puddephatt, R. J. *Chem. Soc. Rev.* **1983**, 99-127.
8. Balch, A. L.; Farr, J. P.; Olmstead, M. M. *J. Am. Chem. Soc.* **1980**, *102*, 6654-6656.
9. Balch, A. L.; Guimerans, R. R.; Wood, F. E. *Inorg. Chem.* **1984**, *23*, 1308-1310.
10. Balch, A. L.; Fossett, L. A.; Olmstead, M. M.; Reedy Jr., P. E. *Organometallics* **1986**, *5*, 1929-1937.
11. Balch, A. L.; Fossett, L. A.; Olmstead, M. M.; Oram, D. E.; Reedy Jr., P. E. *J. Am. Chem. Soc.* **1985**, *107*, 5272-5274.
12. Knowles, W. S.; Sabacky, M.J.; Vineyard, B.D.; Wienkauf, D.J. *J. Am. Chem. Soc.* **1975**, *97*, 2567-2568.
13. Appleton, T. G.; Clark, H. C.; Manzer, L. E. *Coord. Chem. Rev.* **1973**, *10*, 335-432.
14. Pidcock, A.; Richards, R. E.; Venanzi, L. M. *J. Chem. Soc. A* **1966**, 1707-1710.
15. Venanzi, L. M. *Chem. Brit.* **1968**, *4*, 162-167.
16. Allen, F. H.; Sze, S. N. *J. Chem. Soc. A* **1971**, 2054-2056.
17. Allcock, H. R. *Phosphorus-Nitrogen Compounds*; Academic Press: New York, 1972.

18. Kuchen, W.; Fuchs, M.; Peters, W.
Chem. Ber. **1986**, *119*, 1569-1580.
19. Campana, C. F.; Hutchins, L. D.; Light, R. W.; Paine, R. T.
Inorg. Chem. **1980**, *19*, 3597-3604.
20. Emsley, J.; Hall, D.
The Chemistry of Phosphorus; Wiley: New York, 1976.
21. Schmidbaur, H.; Schnatterer, S.
Chem. Ber. **1986**, *119*, 2832-2842.
22. Hutchins, R. O.; Maryanoff, B. G.
J. Org. Chem. **1972**, *37*, 3475-3480.
23. Grim, S. O.; Mitchell, J. D.
Inorg. Chem. **1977**, *16*, 1770-1776.
24. Grim, S. O.; Mitchell, J. D.
Inorg. Chem. **1977**, *16*, 1762-1770.
25. Hilts, R. W. Personal Communication
26. Davison, A.; Reger, D. L.
Inorg. Chem. **1971**, *10*, 1967-1970.
27. McFarlane, H. C. E.; McFarlane, W.; Nash, J. A.
J. Chem. Soc., Dalton Trans. **1980**, 240-244.
28. Falius, H.; Murray, M.
J. Magn. Reson. **1973**, *10*, 127-129.
29. Dixon, K. R.
Multinuclear NMR; Mason, J., Ed.; Plenum Press: New York, 1987, pp. 369.
30. Grim, S. O.; Walton, E. D.
Inorg. Chem. **1980**, *19*, 1982-1987.
31. Colquhoun, I. J.; Grim, S. O.; McFarlane, W.; Smith, P. H.
Inorg. Chem. **1980**, *19*, 3195-3198.
32. Colquhoun, I. J.; McFarlane, W.
J. Chem. Soc., Dalton Trans. **1977**, 1674-1679.
33. Bulloch, F.; Keat, R.; Rycroft, D. S.; Thompson, D. G.
Org. Magn. Reson. **1976**, *12*, 708-712.
34. Keat, R.; Thompson, D. G.
J. Chem. Soc., Dalton Trans. **1978**, 634-638.
35. Cross, R. J.; Green, T. H.; Keat, R.
J. Chem. Soc., Dalton Trans. **1976**, 1424-1428.

36. Grossman, G.; Thomas, B.
J. Magn. Reson. **1979**, *36*, 333-341.
37. Bassett, J. M.; Colquhoun, I. J.; Grim, S. O.;
McFarlane, W. J. *Chem. Soc., Dalton Trans.* **1981**,
1645-1650.
38. Albright, T. A.; Freeman, W. J.; Schwizer, E. E.
J. Org. Chem. **1975**, *40*, 3437-3441.
39. Cremer, S. E.; Gray, G. A.
J. Chem. Soc., Chem. Commun. **1974**, 451-452.
40. Albright, T. A.; Gray, G. A.
J. Am. Chem. Soc. **1976**, *98*, 3857-3861.
41. McFarlane, W. *Proc. Royal Soc. A* **1968**, *306*, 185-199.
42. McFarlane, W. *Quart. Rev.* **1969**, 187-203.
43. Pople, J. A.; Santry, D. P. *Mol. Phys.* **1964**, *8*, 1-18.
44. McFarlane, W.; Wrackmeyer, B.
J. Chem. Soc., Dalton Trans. **1976**, 2351-2355.
45. Cremer, S. E.; Gray, G. A.; Marsi, K. L.
J. Am. Chem. Soc. **1976**, *98*, 2109-2118.
46. Finer, E. G.; Harris, R. K.
Prog. NMR. Spectrosc. **1971**, *6*, 61-0.
47. Hartley, F. R.
*The Chemistry of Platinum and Palladium; Applied
Science: London, 1973.*
48. Crabtree, R. H.; Giordano, G.
Inorg. Synth. **1979**, *19*, 218-220.
49. Herde, J. L.; Lambert, J. C.; Senoff, C. V.
Inorg. Synth. **1974**, *15*, 18-19.
50. Cross, R. J.; Phillips, J. G.
J. Chem. Soc., Dalton Trans. **1981**, 2132-2136.
51. Camus, A.; Cocevar, C.; Mestrani, G.
J. Organomet. Chem. **1972**, *35*, 389-395.
52. Garrau, P. E.; Kunz, R. W.
Chem. Rev. **1981**, *81*, 229-266.
53. Colquhoun, I. J.; Grim, S. O.; McFarlane, W.; Mitchell,
J. D.; Smith, P. H.
Inorg. Chem. **1981**, *20*, 2516-2521.

54. Becker, E. D.
High Resolution NMR - Theory and Applications, 2nd Ed.; Academic Press: New York, 1980.
55. Kunz, R. W.; Pregosin, P. S.
³¹P and ¹³C NMR of Transition-Metal Phosphine Complexes; Springer-Verlag: Berlin-New York, 1979.
56. Pauling, L.
The Nature of the Chemical Bond, 3rd. Ed.; Ithaca: New York, 1960.
57. Corbridge, D. E. C.; Hobbs, E.; Raistrick, B.
Acta Crystallogr. **1953**, *6*, 621-626.
58. Cruickshank, D. W. J.
Acta Crystallogr. **1964**, *17*, 671-672.
59. Corbridge, D. E. C.
The Structural Chemistry of Phosphorus; Elsevier: Amsterdam, 1974.
60. Cruickshank, D. W. J. *J. Chem. Soc.* **1961**, 5486-5504.
61. Hadj-Bagheri, N. *M.Sc. Thesis*, University of Victoria 1984.
62. Fowell, P. A.; Mortimer, C. T.
J. Chem. Soc. **1959**, 2913-2920.
63. Casabianca, F.; Febvay, J.; Riess, J. G.
J. Am. Chem. Soc. **1984**, *106*, 7985-7986.
64. Bouvier, F.; Dupart, J. M.; Riess, J. G.
Inorg. Chem. **1988**, *27*, 427-430.
65. Levy, G. C.; Lichter, R. L.
Nitrogen-15 Nuclear Magnetic Resonance Spectroscopy; Wiley: New York, 1979.
66. Jacobson, R. A.; Kurcher, B. A.; Verkade, J. G.; White, D. W. *J. Am. Chem. Soc.* **1979**, *101*, 4921-4925.
67. Grand, A.; Grec, D.; Hubert-Pfalzgraf, L. G.; Riess, J. G. *J. Am. Chem. Soc.* **1980**, *102*, 7133-7134.
68. Dupart, J. M.; Grand, A.; Pace, S.; Riess, J. G.
J. Am. Chem. Soc. **1982**, *104*, 2316-2318.
69. Goldwhite, H.; Rowsell, D. G.
J. Chem. Soc., Chem. Commun. **1969**, 713-713.
70. Grim, S. O.; Jesson, J. P.; Satek, L. C.; Tolman, C. A.

- Inorg. Chem.* **1975**, *14*, 656-660.
71. Berry, D. E.; Browning, J.; Dixon, K. R.; Hilts, R. W.
Can. J. Chem. **1988**, *66*, 1272-1282.
72. Grove, D. M.; Spek, A. L.; Terheijden, J.;
Van Goten, G.; Vrieze, K.
J. Chem. Soc., Dalton Trans. **1987**, 1359-1366.
73. Kiffen, A. A.; Masters, C.; Visser, J. P.
J. Chem. Soc., Dalton Trans. **1975**, 1311-1315.
74. Cancio, E. M.; Muir, M. M.
Inorg. Chim. Acta **1970**, *4*, 565-567.
75. Balch, A. L.; Hunt, C. T.
Inorg. Chem. **1982**, *21*, 1641-1644.
76. Meek, D. W.; Slinkard, W. E.
J. Chem. Soc., Dalton Trans. **1973**, 1024-1027.
77. Brown, D.; Hill, J.; Pickard, E. F.
Journal of the Less Common Elements **1970**, *20*, 57-65.
78. Ainscough, E. W.; Bergen, H. A.; Brodie, A. M.; Brown,
K. A. *J. Chem. Soc., Dalton Trans.* **1976**, 1649-1656.
79. Hitchcock, P. B.; Haidue, I.; Nixon, J. F.;
Silaghi-Dumitrescu, I.
Inorg. Chim. Acta **1985**, *96*, 77-80.
80. Ainscough, E. W.; Bergen, H. A.; Brodie, A. M.
J. Chem. Soc., Dalton Trans. **1976**, 1649-1656.
81. Ainscough, E. W.; Bergen, H. A.; Brodie, A. M.;
Brown, K. L. *J. Inorg. Nucl. Chem.* **1976**, *38*, 337-338.
82. Ainscough, E. W.; Brodie, A. M.; Brown, K. L.
J. Chem. Soc., Dalton Trans. **1980**, 1042-1047.
83. Ainscough, E. W.; Brodie, A. M.; Mentzer, E.
J. Chem. Soc., Dalton Trans. **1973**, 2167-2171.
84. Ainscough, E. W.; Brodie, A. M.; Furness, A. R.
J. Chem. Soc., Dalton Trans. **1973**, 2360-2363.
85. Camus, A.; Marsich, N.; Pellizer, G.
J. Organomet. Chem. **1983**, *259*, 367-377.
86. Kuhn, W.; Winter, M.
J. Organomet. Chem. **1982**, *239*, C31-C34.
87. Kuhn, N.; Winter, M.
J. Organomet. Chem. **1983**, *246*, C80-C82.

88. Iobana, T. S.; Sharma, K.
Transition Met. Chem. **1982**, *7*, 333-335.
89. Clapp, C. H.; Waldron, R. W.; Wheatland, D. A.
Inorg. Chem. **1972**, *11*, 2340-2344.
90. All crystallography by Dr. J. Browning.
91. Wade, S. R.; Willey, G. R.
J. Inorg. Nucl. Chem. **1981**, *43*, 1465-1468.
92. Browning, J.; Bushnell, G. W.; Dixon, K. R.;
Pidcock, A. *Inorg. Chem.* **1983**, *22*, 2226-2228.
93. Isobe, K.; Maitlis, P. M.; Meanwell, N. J.; Okeya, S.;
Taylor, B. F.; Vazquez de Miguel, A.
J. Chem. Soc., Dalton Trans. **1984**, 1453-1460.
94. Meek, D. W.; Slinkard, W. E.
Inorg. Chem. **1969**, *8*, 1811-1816.
95. Binsch, G.; Kleier, D. A.
Quantum Chemistry Program Exchange Program no. 165;
University of Indiana: Bloomington, IN, 1969.
96. Amdur, I.; Hammes, G. G.
Chemical Kinetics; McGraw Hill: New York, 1966.
97. Kidd, R. G.; Goodfellow, R. J.
NMR and the Periodic Table; Harris, R.K., Mann, B.E.,
Eds.; Academic Press: London, 1978.
98. Dixon, K. R.; Tweedale, A. University of Victoria.
99. Ferreti, J. A.; Harris, R. K.; Johannsen, R. B.
J. Magn. Reson. **1970**, *3*, 84-93.
100. Swalen, J. D.
Computer Programs for Chemistry; vol. 1, Detar, D. F.
Ed.; Benjamin: New York, 1968.
101. McDermott, J. X.; White, J. F.; Whitesides, G. M.
J. Am. Chem. Soc. **1976**, *98*, 6521-6528.
102. Arigos, J.; Oro, C. A.; Sariego, R.; Uson, R.
J. Organomet. Chem. **1979**, *179*, 65-72.
103. Maier, L.; Van Wazer, J. R.
J. Am. Chem. Soc. **1964**, *86*, 811-814.
104. Schmutzler, R. *J. Chem. Soc.* **1965**, 5630-5640.
105. Crutchfield, M.; Dungan, C.; Mark, V.; Van Wazer, J.

Topics in Phosphorus Chemistry, Vol. 5; Wiley:
New York, 1967.

106. Meek, D. W.; Slinkard, W. E.
J. Chem. Soc., Dalton Trans. **1973**, 1024-1027.

VITA

Surname: Phillips

Given Name: Andrew

Place of Birth: Walsall, England

Date of Birth: 31/3/65

Educational Institutions Attended, with Dates of Entering
and Leaving:

University of East Anglia, Norwich, England 1983 to 1986

Degrees, Diplomas, Etc., Awards, with Dates and Names of
Institutions:

BSc. (honors) 1986 University of East Anglia, Norwich

Honors and Awards:

B.C. Government Supplement, 1986/87

University of Victoria Scholarship, 1987/88

Publications:

Browning, J.; Berry, D. E.; Dixon, K. R.; Hilts, R. W.;

Phillips, A. J., *Sulphur Chelation and Metal Carbon Bond*

Formations in Complexes of Bisphosphine Disulphides. Paper

No. 421, **Third Chemical Congress of North America**, June 5 -

10, 1988, Tronto, Ontario, Canada.

PARTIAL COPYRIGHT LICENSE

I hereby grant the right to lend my thesis (the title of which is shown below) to the users of the University of Victoria Library, and to make single copies only for such users or in response to a request from the library of any other university, or similar institution, on its behalf or for one of its users. I further agree that permission for extensive copying of this thesis for scholarly purposes may be granted by me or a member of the University designated by me. It is understood that copying or publication of this thesis for financial gain shall not be allowed without my written permission.

Title of Thesis/Disertation

The Synthesis and Coordination of Amino-substituted
Bisphospines.

Author



(Signature) /

A. J. Phillips
(Name in block letters)

19/ 8/88.
(Date)